University of Szeged
Faculty of Natural Science and Informatics
Doctoral School of Biology

Eötvös Loránd Research Network
Biological Research Centre
Institute of Plant Biology

PhD Thesis

MACRO-ORGANIZATION OF PHOTOSYNTHETIC COMPLEXES DURING SALT STRESS ACCLIMATION OF GREEN MICROALGAE AND IN PLANT CHLOROPLAST ACETYLTRANSFERASE AND SER/THR PROTEIN KINASE MUTANTS

Sai Divya Kanna

Supervisor: Dr. Bettina Ughy

Szeged, 2022

TABLE OF CONTENTS

List of Abbreviations

ACA	aminocaproic acid
ADP	adenosine di-phosphate
ANOVA	analysis of variance
ATP	adenosine triphosphate
BSA	bovine serum albumin
CBB	Coomassie Brilliant Blue
CD	circular dichroism
CDW	cell dry weight
CEF	cyclic electron flow
DAES	decay-associated emission spectrum
Ddx	diadinoxanthin
DDE	diadinoxanthin de-expoxidase
DEP	diatoxanthin epoxidase
Dtx	diatoxanthin
EDTA	ethylene diamine tetra acetic acid
EM	electron microscopy
ETAP	Euglena- tris acetate phosphate
ETC	electron transport chain
ETR	electron transport rate
Fd	ferredoxin
FNR	ferredoxin-NADPH reductase
FQR	ferredoxin plastoquinone reductase
HEPES	2-[4-(2-hydroxyethyl) piperazin-1-yl] ethanesulfonic acid
HPLC	high-performance liquid chromatography
IRF	instrument response function
IT	interthylakoidal
LEF	linear electron flow
LHC	light-harvesting complex
LHCSR3	light-harvesting complex stress related protein-3
NADH	nicotinamine adenine dinucleotide
NADP	nicotinamine adenine dinucleotide
NDH	NADH dehydrogenase
NPQ	non-photochemical quenching
Nx	neoxanthin

OD	optical density
PAGE	polyacrylamide gel electrophoresis
PAM	pulse amplitude modulation
PBS	phycobilisome
PC	plastocyanin
PGR5	proton gradient regulation 5
PGRL1	PGR5-like photosynthetic phenotype-1
PPC	photosynthetic pigment-protein complexes
PQ	plastoquinone
PSI	photosystem I
PSII	photosystem II
RC	reaction centre
RD	repeat distance
ROS	reactive oxygen species
SANS	small-angle neutron scattering
SD	standard deviation
SDS	sodium dodecyl sulphate
SE	standard error
SEM	scanning electron microscopy
TAP	tris-acetate phosphate
TCSPC	time-correlated single photon counting
TEM	transmission electron microscopy
TEMED	N, N, N′, N′-Tetramethylethylenediamine
TM	thylakoid membrane
TRF	time-resolved fluorescence
VAZ	violaxanthin-antheraxanthin-zeaxanthin
VDE	violaxanthin de-epoxidase
Vx	violaxanthin
TAP	tris-acetate phosphate
XC	xanthophyll cycle
ZEP	zeaxanthin epoxidase
Zx	zeaxanthin
β-DM	β-dodecylmaltoside

1. Introduction

1.1. Importance of photosynthesis

Photosynthesis is an important process that supports life on Earth. A wealth of evidence suggests that photosynthetic organisms have evolved some 3.5 billion years ago (Blankenship, 2010). They rely on photosynthesis to produce food from sunlight, water, and carbon dioxide (CO_2) in the atmosphere. Oxygenic photosynthesis is crucial, because it is a source of oxygen (O_2) required for life on earth. This is the best-known form of photosynthesis, which is carried out by cyanobacteria, algae and plants where water is the electron donor with oxygen productions. Photosynthesis provides organic compounds/sugars which are the primary food source for humans and animals along the food chain. The energy stored in all the fossil fuels is obtained through photosynthesis. With a better understanding of photosynthesis, we can enhance crop yields and thus feed the growing human population.

1.2. The photosynthetic apparatus

In plants and eukaryotic algae, photosynthesis occurs in cell organelles called the chloroplasts (Figure 1). Chloroplast is a disk-shaped body composed of double membrane which is a remnant of the incorporation of the free-living cyanobacterium into symbiotic eukaryotes. Photosynthesis is a process during which solar energy is converted into electrical and then chemical energy by using CO_2 as electron acceptor and water as donor, to synthesize carbohydrates and produce O_2 as a side-product. The basic chemical reaction that defines photosynthesis can be represented in the form of an equation.

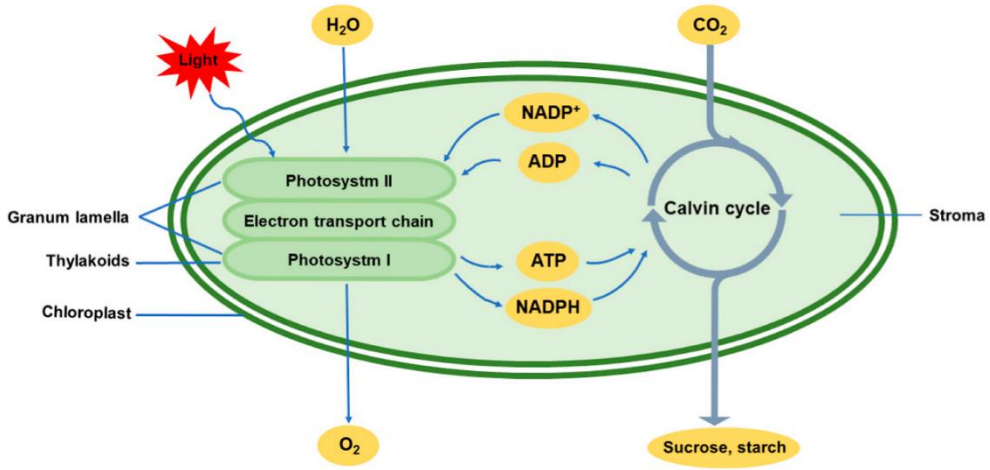

Figure 1. Schematic representation of chloroplasts with thylakoids showing the sites of light and dark reactions (Gan *et al.*, 2019).

Photosynthetic reactions can be divided into two phases:

1) During the light phase the energy of the sunlight is converted into stored chemical energy in the reduced form of $NADP^+$ (NADPH) and ATP as a product of photophosphorylation.
2) While during the dark phase, the products of light phase are used in a series of reducing reactions (the Calvin-Benson cycle) for fixation of CO_2 to produce carbohydrates.

The net equation of photosynthesis:

1.2.1. Organization of the chloroplast thylakoid membranes

Eukaryotic photosynthetic organisms as already mentioned, have specialized organelles called chloroplasts that carry out all photosynthetic reactions. Chloroplasts are semi-autonomous organelles comprised two envelope membranes, an aqueous matrix known as stroma, and internal membranes called thylakoids. A peculiar feature of the thylakoid membrane (TM) is that it consists of two different functional domains: a cylindrical stacked system called grana and interconnecting regions termed stroma lamellae. The helical model of TM can be seen in Figure 2A. The photosynthetic pigment-protein complexes (PPCs) that are involved in the oxygenic photosynthesis are located in the TM. A schematic model showing PPCs in the TM can be seen in Figure 2B. The four major PPCs in the TM include photosystem II (PSII), cytochrome b_6/f (Cyt b_6/f) and photosystem I (PSI) which are electrically connected in series through the electron transport chain (ETC) and ATP synthase (Figure 2B).

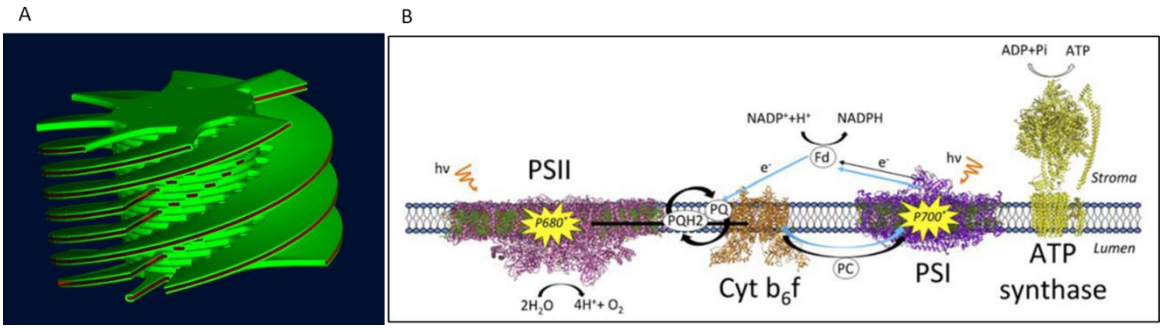

Figure 2. A) 3D computer model of helical arrangement of thylakoid membrane (Mustárdy and Garab, 2003), B) Schematic representation of the major protein complexes PSII, Cyt b_6/f complex, PSI and ATP synthase of thylakoid membrane (Liguori *et al.*, 2020).

PSII is mainly found in the grana thylakoids, whereas PSI and ATP synthase are mostly located in the stroma thylakoids and the outer layers of the grana. The Cyt b_6/f complex is distributed evenly across the TMs. The probable reason for the heterogeneity of the membranes could be the large protruding stroma domains of PSI and ATP synthase, which do not fit into the tightly appressed grana membranes separated by a distance of 3-4 nm (Jensen *et al.*, 2002; Kirchhoff *et al.*, 2011). Because of the separated location of the photosystems, mobile electron carriers are essential for electron transport. Plastoquinone (PQ) shuttles the electrons from PSII to Cyt b_6/f complex and plastocyanin (PC) from the Cyt b_6/f complex to PSI (Figure 2B). All these proteins together use light energy to drive the ETC and generate the products of the light reaction the NADPH and the ATP which are further consumed in CO_2 fixation. The ribulose-1,5-bisphosphate carboxylase oxygenase (RuBisCO) enzyme complex (consisting of 8 large and 8 small subunits) incorporates CO_2 into ribulose-1.5-bisphosphate (RuBP) and finally forming sugar phosphates in the light-independent reaction, completing the Calvin cycle (Hoober, 1989).

1.2.2. Photosynthetic electron transfer pathways

The Calvin cycle demands ATP and NADPH to be delivered in a strict stoichiometry of 3:2 per turnover. To accommodate this requirement the photosynthetic electron transfer must operate in two different modes linear electron flow (LEF) and cyclic electron flow (CEF) both being crucial. LEF provides ATP and NADPH in a 2.6:2 ratio, and CEF mainly drives phosphorylation and thus supplies the remaining ATP. Thus, fine tuning these two electron transfer modes is very important (Takahashi *et al.*, 2013). The electron transfer pathways and the components involved in both LEF and CEF are shown in Figure 3.

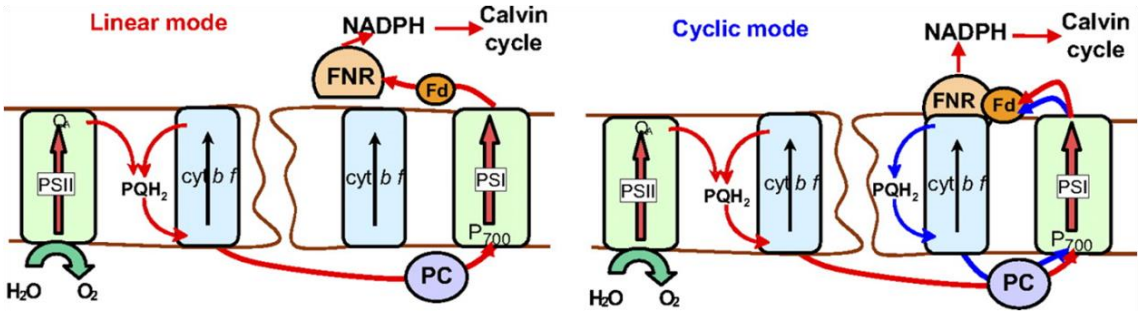

Figure 3. Schematic representation of the linear and cyclic electron flow (LEF and CEF). LEF i.e., Z-scheme of the electron transport from H_2O to $NADP^+$ is shown in red color and CEF is indicated within blue color showing electron transport from FNR to PQ instead of $NADP^+$ as in LEF (Joliot and Johnson, 2011).

LEF pathway involves both the photosystems PSII and PSI that have individual light-harvesting complexes (LHCII, LHCI), whose main function is to capture the sunlight and funnel the excitation energy to their respective photosystems, where stable charge separation occurs across the TM (Nawrocki *et al.*, 2019). This leads to the formation of a strong oxidant on the donor side of PSII (P_{D1}+), which is efficient enough to extract electrons from water along the ETC and transfer them to the PQ pool, and then to the Cyt b_6/f complex and finally to PC and PSI. A second photochemical reaction is required here for the oxidation of PC and for the reduction of ferredoxin, various components of ETC, and finally NADP+. In this phase, ferredoxin-NADPH reductase (FNR) catalyses the formation of NADPH (Lu *et al.*, 2020). Along with the production of reducing power, NADPH, during electron transfer, protons are pumped across the TM from stroma to lumen generating a proton gradient. This energy potential is used by the fourth complex, the ATP synthase to synthesize ATP from ADP and inorganic phosphorous (Pi) (Lapashina and Feniouk, 2018).

Besides this major pathway the so-called Z-scheme, an alternative electron transfer pathway involves some of the electrons from the acceptor side of the PSI return to the PQ pool, resulting in a cyclic electron flow (CEF) around PSI (Figure 2B) (Nixon, 2000; Bukhov and Carpentier, 2004). The CEF pathway is known to be driven by PSI (stroma located), which in energy limiting conditions cycles the electrons back to Cyt b_6/f from PSI thereby generating more energy in the form of ATP only (Avenson *et al.*, 2005). There are two main CEF pathways: (i) the NADH dehydrogenase-like complex-dependent pathway (NDH-CEF); (Yamamoto *et al.*, 2011) and (ii) the ferredoxin plastoquinone reductase pathway (FQR-CEF); (Munekage *et al.*, 2002; DalCorso *et al.*, 2008). In the NDH-CEF pathway, NDH complex accepts electrons from ferredoxin (Fd) on the PSI acceptor side, and transfers them to Cyt b_6/f through PQ reduction (Peltier *et al.*, 2016; Strand *et al.*, 2017). In the FQR-CEF, Cyt b_6/f, PC, PSI, Fd and ferredoxin plastoquinone reductase (FQR) are involved. The essential components required for FQR-CEF in plants and algae include proton gradient regulation 5 (PGR5) and PGR5-like photosynthetic phenotype-1 (PGRL1). PGR5 is a small thylakoid protein with no known motifs that suggest its function (Munekage *et al.*, 2002). PGRL1 is a transmembrane protein with two transmembrane domains and two cysteine residues that are involved in cofactor binding of iron (Hertle *et al.*, 2013). In general, electron transport from Fd to PGRL1 requires the involvement of PGR5 proteins and the loss of any protein would affect CEF (Munekage *et al.*, 2002; DalCorso *et al.*, 2008; Kono *et al.*, 2014; Ma *et al.*, 2021). In the green alga *Chlamydomonas reinhardtii* (*C. reinhardtii*), which lacks NDH-CEF, PGRL1 undergoes conformational changes in a Fe-dependent and redox-induced

manner (Petroutsos *et al.,* 2009) and forms part of a protein super complex that includes PSI and Cyt b_6/f which mediates CEF (Iwai *et al.,* 2010). Both LEF and CEF operation allow the pumping of protons (proton gradient) into the lumen, which is used by ATP synthase for the necessary ATP production that together with NADPH, drives CO_2 fixation via Calvin-Benson cycle. Thus, the generation of NADPH and ATP is essential for the reactions of carbon fixation and cellular metabolism (Nelson and Yocum, 2006).

1.2.3. Photosynthetic pigments

In green algae, sunlight can be captured by pigment molecules and utilized for photosynthesis. Each pigment can respond to only a relatively narrow range of spectrum, there arises a necessity to produce several types of pigments mainly to capture more of sun's energy. Classes of pigments include chlorophylls (Chls) and carotenoids. Chls are green pigments containing a porphyrin ring with a potential to gain or lose electrons easily and provide energized electrons to the other molecules. Majority of the chlorophylls function to absorb the sun light and transfer it to specific Chl molecules in photosystems by resonance energy transfer mechanism. Among various forms of chlorophylls, Chl *a* that is present in plants and in all green algae, is a special form of chlorophyll that serves as a primary electron donor in the ETC. The energy is captured by the pigment molecules of the antenna complex then it is transferred to the reaction centre, in which specific chlorophylls P680 and P700 are localized (Papageorgiou, 2004). Chl *a* absorbs the light mainly at 400-450 nm and at 650-700 nm wavelengths. Chl *b* mainly involved in light harvesting can be found in land plants, occurs in green algae, and it absorbs in between 450-500 nm and 600-650 nm. Usually, Chls are primarily bound to proteins and some proteins are not functional or stably folded in the absence of pigments. The binding of pigments to proteins organizes them and influences their spectroscopic properties, favoring pigment-pigment interactions and modulating their energy levels and absorption properties.

Carotenoids (Cars) are orange, yellow pigments found in photosynthetic organisms. They cannot directly transfer the captured sunlight to the photosynthetic pathway, instead they must pass the absorbed energy to the Chls and therefore called as accessory pigments. They are primarily found in the photosynthetic complexes. There are more than 600 known Cars which can be classified into 2 types namely xanthophylls (contain oxygen) and carotenes (do not contain oxygen and are pure hydrocarbons). Xanthophylls include lutein and zeaxanthin or violaxanthin, while carotenes include α-carotene and β-carotene. Their quantity and composition can vary in different organisms. Their absorption range is typically around 400–500 nm.

Primarily in pigment-protein complexes along with Chls, Cars increase the absorption spectrum of the photosystems and transfer their excitation energy to Chl. In addition to absorbing the light energy essential for photosynthesis, Cars are able to protect the photosynthetic apparatus from photodamage caused by excessive light absorption. β-carotene in the PSII RC plays a photoprotective role of preventing oxidative damage often attributed to reactive oxygen species (ROS) by quenching Chl triplet state and singlet oxygen (Polívka and Frank, 2010).

1.2.4. Regulation of photosynthetic reactions

Photosynthesis is an exclusive process of converting light energy into usable chemical forms and involves the generation of highly reactive intermediates, which must be controlled to avoid cell damage in most cases. Perturbing environmental conditions such as stress conditions, the availability of light, CO_2, H_2O, and nutrients results in considerable changes in ATP, NADPH and products of carbon fixation. Photosynthetic apparatus can regulate the light reactions of photosynthesis by responding to these changing environmental conditions. When available light energy exceeds the capacity of photosynthetic machinery, excess energy is dissipated as heat through a process called non-photochemical quenching (NPQ) (Demmig-Adams and Adams, 1992; Szabó *et al.*, 2005; Ruban, 2016). NPQ is the most effective photoprotective response in plants and algae. NPQ consists of three different components (Muller *et al.*, 2001), the fast component is energy dependent quenching (qE), intermediate one is the state-transition related quenching (qT), and the slow component is photoinhibition related quenching (qI). Most studied component in higher plants and algae is qE. In general, qE is activated by three essential factors which include xanthophyll cycle, the pH gradient and some proteins of LHC superfamily. During qE-NPQ, LHCII senses the state of light energy balance directly through ΔpH changes across the membrane and responds through structural changes (Papageorgiou, 2014). The TM of plants and green algae contain proteins able to sense the lumenal pH, such as PsbS protein and LHC stress-related 3 (LHCSR3) protein (only in algae). These proteins are known to play a key role in the activation of NPQ in plants and *C. reinhardtii*. In vascular plants, PsbS is necessary for qE by inducing the formation of quenching sites either in LHCs (Ruban, 2018) or at the interface of LHCs and PsbS (Barros *et al.*, 2009). LHCSR proteins are known for regulating qE in algae (Bag, 2021). It has been described in *C. reinhardtii*, that PsbS is responsible for NPQ activation by promoting the conformational changes necessary to induce the LHCSR3 dependent quenching in PSII antenna (Correa-Galvis *et al.*, 2016). In addition, xanthophyll cycle (XC) is known to partially mediate qE-NPQ. Violaxanthin-antheraxanthin-zeaxanthin

(VAZ) cycle is the XC in higher plants and green algae (Yamamoto *et al.*, 1999; Wilhelm *et al.*, 2006). During VAZ cycle, pH dependent conversion of Violaxanthin (Vx) to Zeaxanthin (Zx), through Antheraxanthin (Ax) occurs (Szabó *et al.*, 2005). This cycle is catalyzed by the enzymes Vx de-epoxidase (VDE) and Zx epoxidase (ZEP) as shown in the Figure 4. VDE is located on the lumen side; it is optimally active at about pH 5-6. ZEP is located on the stroma side, with an optimum pH of approximately 7.5 (Yamamoto *et al.*, 1999). For the enzymatic activity, VDE needs the acidic form of ascorbate and ZEP requires NADPH, H^+ and O_2 as co-factors. Due to the build-up of transthylakoid proton gradient during stress conditions; pH of lumen and stroma change, thereby activating VDE. As a result, de-epoxidation becomes dominant and accumulation of Zx occurs. When the light intensity decreases, epoxidation of Zx occurs forming Vx which is catalyzed by ZEP. Therefore, VAZ cycle causing the accumulation of xanthophylls depends on the activity of the enzymes which in turn depends on the light intensity and pH change. VAZ cycle is replaced by diadinoxanthin (Ddx) cycle in some algae like diatoms (Lavaud and Kroth, 2006; Lavaud, 2007), where de-epoxidation of Ddx to diatoxanthin (Dtx) is catalyzed by Ddx de-epoxidase (DDE). Dtx gets epoxidized to Ddx through Dtx epoxidase (DEP). Ddx cycle is also known to play a photoprotective role in *Euglena* species (Tamaki *et al.*, 2021). The comparison of VAZ and Ddx cycle is shown in Figure 4.

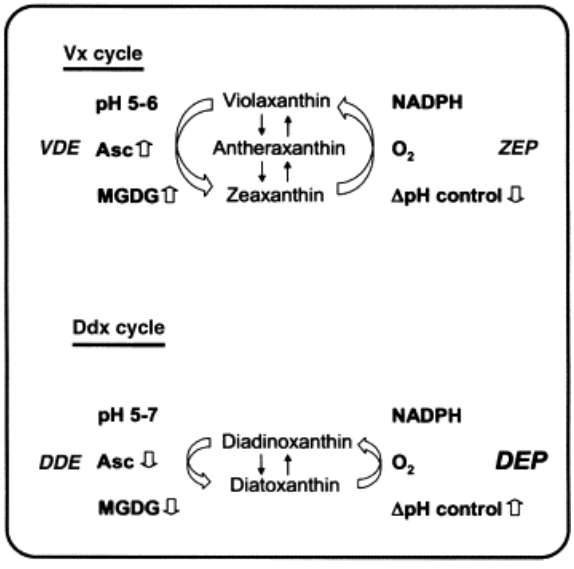

Figure 4. Comparison of VAZ and Ddx cycle (Wilhelm *et al.*, 2006)

Balancing the excitation energy absorption between PSII and PSI during unfavourable conditions also can help to maintain the chloroplast redox poise under fluctuating light or stress conditions in plants and algae (Bhatti *et al.*, 2020; Wood and Johnson, 2020). Photosynthetic organisms operate this mechanism of adjusting the flow of

energy to the photosystems to meet the cell's demand for ATP under changing environmental conditions (Cardol *et al.*, 2009). It is well-known that changes in the quality or quantity of light for any of the reasons can alter the equilibrium of the system. This leads to the over-excitation of PSII compared to the PSI, PQ pool gets reduced to PQH_2 and binds to Qo site of Cyt b_6/f, which further activates a kinase called Stt7/STN7 (serine/threonine protein kinase) for *C. reinhardtii* and *Arabidopsis thaliana* respectively, phosphorylating a portion of LHCII (Bennett, 1979; Murata, 2009). Phosphorylation weakens the tendency of LHCII to associate with PSII, thereby detaches and migrates with increasing affinity towards PSI. This shifts the system into the so-called State-2. This process can be reversed i.e., transition from state-2 to state-1 occurs when the PQ pool is oxidized. During this transition, kinase gets inactivated and dephosphorylation of LHCII occurs by chloroplast protein phosphatase 1 (PPH1/TAP38) (Shapiguzov *et al.*, 2010; Cariti *et al.*, 2020). Then the dephosphorylated LHCII returns to PSII from PSI which corresponds to State-1. (Allen, 2003; Pribil *et al.*, 2010). This alteration in the relative antenna sizes of PSI and PSII balances the excitation energy and ensures the redox homeostasis of the ETC (Wood and Johnson, 2020). Thus, changes in the redox state of PQ pool can be sensed by LHCII through a complex signalling network composed of Cyt b_6/f, protein kinase and phosphatase all of which work collectively to restore the redox poise of the electron carriers to maintain the photosynthetic efficiency. A schematic representation of switching between states that is called state transitions is visualized in Figure 5.

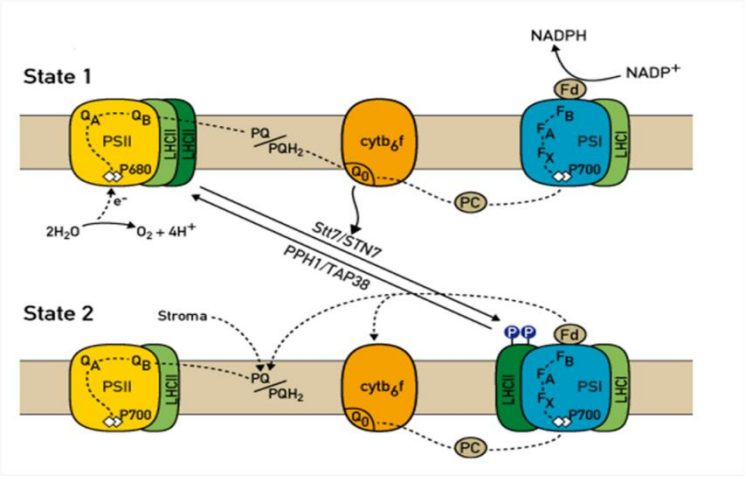

Figure 5. Mechanism of state transitions showing the movement of phosphorylated LHCII from PSII to PSI and back (Rochaix, 2014).

One important role of state transitions in both plants and algae is to maintain the redox poise of the PQ pool and respond to metabolic needs (Fernyhough et al., 1983).

1.2.5. Dynamic macroorganization of the thylakoid membranes

In each chloroplast, the thylakoids form a physically continuous, three-dimensional network that encloses a single, aqueous space called the thylakoid lumen. Models of three-dimensional membrane organization have reported the highly dynamic nature of TM architecture, focusing on membrane stacking and unstacking (Arvidsson and Sundby, 1999; Mustárdy and Garab, 2003). The most striking effect of membrane stacking is the physical separation of most PSII to stacked grana membranes, and of most PSI to unstacked stroma membranes (Staehelin and van der Staay, 1996). An extraordinary lateral heterogeneity was observed, due to an uneven distribution of photosynthetic complexes (Shimoni *et al.*, 2005). A major difference between the TM of microalgae and higher plants is that microalgae generally have loosely arranged membrane systems. In most green algae, lateral heterogeneity is much less pronounced than in vascular plants, but their chloroplasts contain both stacked and unstacked TMs (Goodenough and Staehelin, 1971). For example, the chloroplast of the green alga *C. reinhardtii*, which is closely related to the chloroplasts of higher plant leaves, contains stacked and unstacked membranes but no fully developed grana (Bellafiore *et al.*, 2005).

The TM can undergo highly variable structural rearrangements under different conditions. It remains to be clarified whether only one or several factors are involved in the regulation of induced membrane rearrangements. The TMs of photosynthetic organisms respond to changing environmental conditions with systematic modulations in both the light-harvesting antennae of the photosystems and the amounts of electron transport components and ATP synthase. These changes are consistent with the membrane organization. Lateral heterogeneity and functional sub-compartmentalization of the TM into stacked grana and nonstacked stroma membranes has been proposed to facilitate many purposes, including increasing light-harvesting efficiency, balancing electron flow between PSII and PSI, or preventing spillover of excitation energy from PSII to PSI (Anderson, 1981; Trissl and Wilhelm, 1993), fine-tuning photosynthesis under variable light conditions (Chow *et al.*, 2005), or to shift from linear to cyclic electron flow (Chow, 1984). Depending on the environmental conditions, the average repeat distances (RD) between the TM layers might change in different photosynthetic organisms. Shade plants are characterized by much broader grana with more stacked thylakoids per granum compared to sun plants (Lichtenthaler *et al.*, 1981). During acclimation of photosynthetic organisms to different light environments, changes in the degree of membrane stacking can be observed *in vivo* (Anderson et al., 1988) often within a few minutes. These movements include reversible

phosphorylation of a part of LHCII and its subsequent migration from the edges of the grana stacks to stromal thylakoids. The state transitions, apparently require major reorganizations in the TM (Tikkanen *et al.*, 2012; Minagawa, 2013).

Current knowledge of the structural organization and ultrastructure of TMs has been based mainly on electron microscopy (EM) studies for about four decades (Menke, 1960; Wehrmeyer, 1964; Staehelin, 2003). Scanning electron microscopy (SEM) and transmission electron microscopy (TEM) studies were used to determine the localization of thylakoid membrane proteins which contribute to grana stacking in *Arabidopsis thaliana* (Armbruster *et al.*, 2013). EM studies showed that in the stacks of grana, the inter-thylakoidal (IT) space is smaller than the lumenal space which is 3.2 nm and 4.5 nm, respectively (Daum and Kühlbrandt, 2011). However, small-angle neutron scattering (SANS) studies have shown that the IT space and lumenal space are 4 and 4.5 nm, which is comparable (Ünnep *et al.*, 2014a). Repeat distance (RD) values measured by SANS are generally comparable to those obtained with electron microscopy (Shimoni *et al.*, 2005; Wood *et al.*, 2018). Early in, the basic correlation between the RD of TMs, derived from TEM and calculated from the Bragg peak of the SANS profile of thylakoid membranes isolated from *Euglena gracilis* and spinach, was established by Sadler and Worcester (Sadler and Worcester, 1982). Further, this correlation has been extended to cyanobacteria and algae, as well (Nagy *et al.*, 2011; Posselt *et al.*, 2012; Liberton *et al.*, 2013a; Liberton *et al.*, 2013b). Previous reports have shown that there is significant change in membrane ultra-structure, when whole leaves were exposed to different environmental conditions leading to state transitions (Chuartzman *et al.*, 2008; Dietzel *et al.*, 2011) or when exposed to severe light stress (Kirchhoff *et al.*, 2011; Herbstová *et al.*, 2012; Kouřil *et al.*, 2013). Rapid small but distinct light-induced changes in membrane organization and RD were observed in cyanobacteria (Nagy *et al.*, 2011; Stingaciu *et al.*, 2016), green algae (Nagy *et al.*, 2014), diatom cells (Nagy *et al.*, 2011; Nagy *et al.*, 2012; Nagy *et al.*, 2013), and intact leaves of various species (Ünnep *et al.*, 2014b). It should be noted that RD of TM increased (i.e., swelled) in cyanobacteria and diatoms when illuminated, whereas the data in plants TM showed shrinkage or reduction (Nagy *et al.*, 2011). The cause of this discrepancy is unclear and highlights the complex nature of membrane dynamics (Lambrev and Akhtar, 2019).

CD spectroscopy is a sensitive, non-invasive tool for monitoring changes in the structure and/or arrangement of pigment-protein complexes. The visible CD spectra contain information about the excitonic pigment-pigment interactions and pigment-protein interactions as well as the macro-organization of the protein complexes. CD is the difference in the absorption of left-handed circularly polarized light and right-handed circularly

polarized light and occurs (i) when a molecule contains one or more chiral chromophores (light-absorbing groups) (intrinsic CD – for Chl(s) and Car(s) this CD is very weak and can be neglected here), (ii) when there is short-range, excitonic interaction between chromophores (excitonic CD) – excitonic signals, split bands dominate the CD spectra in the Soret (between about 430 and 480 nm) and around 650 nm (iii) when the chromophores (and/or the pigment-protein complexes) are assembled in chirally organized 3D macroarrays (psi-type CD; psi, polymer or salt-induced) – the large, anomalously shaped intense psi-type bands with long tails, peaking at around (+)510 and (+)690 nm originate from long-range chiral array of the protein complexes of PSII and LHCII, and at (-)675 nm, which is sensitive to the stacking of membranes (Garab and van Amerongen, 2009). In chloroplasts, the Chl molecules are bound to different pigment-protein complexes, in which the distances between the pigment molecules and their mutual orientations are well-defined; differences in the distances and mutual orientation, e.g., upon monomerization of trimeric complexes or degradation of the complexes, may lead to the changes in the excitonic CD spectra, while rearrangements of the protein complexes may result in changes in the psi-type CD bands. Earlier study on the membrane organization of isolated TM showed changes in the psi-type CD upon illumination (Garab *et al.*, 1988). In the thylakoid membranes, psi-type CD is tightly correlated with the occurrence of grana (Fulda *et al.*, 2006). Upon unstacking by removing the ions from the medium, psi-type CD of chloroplasts of wild-type plants is shown to be destroyed and in case of Chl-*b*-less mutants, psi-type CD is rather decreased (Garab *et al.*, 1991). Psi-type CD exists even in some algae like diatoms which lack typical granal organization (Szabó *et al.*, 2008). Like the grana TM of higher plants, the cells of diatoms also exhibit large psi-type CD signals, indicating the presence of higher ordered complexes (Szabó *et al.*, 2008). In the case of *Phaeodactylum tricornutum*, the light-induced changes in the membrane RD were closely correlated with psi-type CD (Szabó *et al.*, 2008) further illustrating the high structural flexibility of TM. Comparison of CD spectra of *Phaeodactylum tricornutum* cells with SANS spectra showed that the loss of CD amplitude under heat treatment was accompanied by an increase in membrane RD, suggesting that the psi-type CD signal may not only originates from the lateral macroorganization, but vertical appression of TM also contributes to it (Nagy *et al.*, 2012). Phosphorylation of LHCII leads to an increase in the TM flexibility – enhanced heat- and light-induced reorganizations in TM upon phosphorylation *in vitro* were detected by CD spectroscopy (Várkonyi *et al.*, 2009). The changes in macroorganization of membrane and RD (stacking) during state transitions in *C. reinhardtii* has been revealed by both CD spectroscopy and SANS measurements (Nagy *et al.*, 2014).

1.3. *Arabidopsis thaliana* as a model organism

Arabidopsis thaliana (*A. thaliana*) is an annual flowering plant belonging to the family of Brassicaceae in the dicotyledonous group of angiosperms (Krämer, 2015). It is small plant consisting of a rosette of leaves (Figure 6) and the main shoot holds the inflorescence; produces approximately 10000–30000 seeds (Masson, 2001).

Figure 6. A) Image of 4-week-old *Arabidopsis thaliana* WT (columbia-0) plant B) Image of 4-week-old *Arabidopsis thaliana gnat2* plant.

It can be cultivated well in laboratory conditions with a limited quantity of light on the shelves at room temperature. It has a short generation time of about 6 weeks (Krämer, 2015). It usually reproduces through self-pollination although it could carry out cross-pollination. Its nuclear genome is small sized (125 Mb) and has been fully sequenced (Masson, 2001). It is a widely used model organism for studying growth and development processes, most used for research in plant molecular genetics, physiology, and biochemistry. Among the plants, it is a reference organism for the study of metabolism of chloroplasts and photosynthesis, especially often used for studying abiotic stress physiology (Taylor *et al.*, 2009).

1.4. Microalgae as model organisms

Microalgae are the fastest growing photosynthetic organisms that can rapidly generate biomass using solar energy. Microalgae can be classified as unicellular algae that include prokaryotic (cyanobacteria) and eukaryotic microorganisms. Eukaryotic microalgae evolved from endosymbiosis events. In primary endosymbiosis, a eukaryotic cell engulfed a cyanobacterium and gained the advantage of photosynthesis. In secondary endosymbiosis event, eukaryotes (euglenophytes, cryptophytes, chloroarachniophytes, chromophytes and apicomplexans) engulfed other photosynthetic eukaryotes such as chlorophytes, rhodophytes

and glaucocystophytes (Keeling, 2009). They can grow in a variety of environments including freshwater, marine water and soil (Round, 1984). They require simple inorganic nutrients, as well as water, CO_2 and light for growth. On the other hand, some algae can be grown under heterotrophic or mixotrophic growth conditions (Liang *et al.*, 2009; Drexler and Yeh, 2014). They are highly efficient biological organisms to convert CO_2 and nutrients into biomass. Microalgal biomass and algae-derived compounds have a very wide range of potential applications, from animal feed to human nutrition and health products (Borowitzka et al., 1980; Pignolet et al., 2013; Lu et al., 2016). They provide food sources available in the form of carbohydrates, proteins, pigments, fatty acids, and triglycerides. Studies show that microalgae like *Chlorella*, *Dunaliella*, *Chlamydomonas, Scenedesmus* and *Spirulina* contain a large amount (>50% of the dry weight) of starch and/ or glycogen, that can serve as starting materials for ethanol production (Rodjaroen et al., 2007; Ho et al., 2013). Some microalgae strains can produce hydrogen gas or other useful secondary metabolites (Benemann, 2000). Microalgae biomass can have better quality proteins than vegetables and crops but not better than the animal proteins regarding their essential amino acid content and based on their protein usability (Rizwan *et al.*, 2018; Wang *et al.*, 2021). Several microalgae species might be suitable for lipid (oil) production, since they can produce neutral lipids (triacylglycerides) through photosynthesis (Meng et al., 2009; Vicente et al., 2009; Bellou et al., 2012; Devi and Mohan, 2012; Campos et al., 2014; Drexler and Yeh, 2014) and they can produce about 80% oil in terms of dry biomass weight (Khan et al., 2009; Abou-Shanab et al., 2014).

Microalgal species are capable of producing different kinds of antioxidant, carotenoid, enzyme polymer, lipid, natural dye, poly-unsaturated fatty acid, peptide, toxin and sterols, which are used in several industrial products (Moreno-Garcia *et al.*, 2017). In addition, microalgae are medicinal sources for treating diseases such as high cholesterol, atherosclerosis, and cancer. Microalgae can be considered as sources of medicines (Raja *et al.*, 2007; Raja *et al.*, 2018). *Euglena gracilis* is known to accumulate large quantities of the reserve polysaccharide paramylon, a β-1,3-glucan, which is known to exhibit antidiabetic and hepatoprotective activities and lower cholesterol levels; furthermore, used for the treatment of cancers (Ooi and Liu, 2000; Barsanti *et al.*, 2011). Feed enriched with a small amount of microalgal biomass helped to boost the immunity of animals, provide resistance to diseases, increase antiviral and antibacterial protection and contribute immensely to weight gain (Madeira *et al.*, 2017). Some cyanobacterial species produce sugars like sucrose which is of biotechnological interest as a sweetener in food industry as well as a feedstock for the cultivation of heterotrophic microorganisms (Ducat et al., 2012; Du et al., 2013; Kirsch et al.,

2018). Moreover, microalgae are used for feeding in aquaculture. For example, astaxanthin, which is extracted from microalgae strains such as *Haematococcus pluvialis*, *Chlorella zofingiensis*, *Scenedesmus obliquus* improves the colour and appearance of fish and shrimp as an additive in aquaculture feed in the industry (Lu *et al.*, 2021). The addition of astaxanthin has been found to increase the growth rate and lifespan of larvae in aquaculture (Lim *et al.*, 2018). *Chlorella vulgaris* has been commonly used as feed in aquaculture due to its potential medicinal and immunomodulatory properties (Ahmad *et al.*, 2020). Furthermore, microalgal systems can be used in the wastewater treatment (Abdel-Raouf *et al.*, 2012; Li *et al.*, 2019).

Eukaryotic algae have a striking plasticity and adaptability to the majority of abiotic stresses. They are relatively easy to maintain and grow in a confined space, when required nutrients are supplied. They have become a significant source of genetic and chemical diversity. In addition, they are biotechnologically very important. Besides their biotechnological importance, they are excellent model systems for studying and improving photosynthesis under stress conditions.

1.4.1. *Chlamydomonas reinhardtii*

Chlamydomonas reinhardtii (*C. reinhardtii*) is a unicellular biflagellate green alga with cell size around 10 μm in diameter. The species is commonly found in soil and freshwater. The cells have hydroxyproline-rich glycoproteins containing cell wall and the chloroplast occupies up to 40% of the volume of the cell, Furthermore, within the cells there are several mitochondria, a large pyrenoid, an eyespot that aids in light perception, a nucleus and all other compartments that exist in a eukaryotic system. (Figure 7).

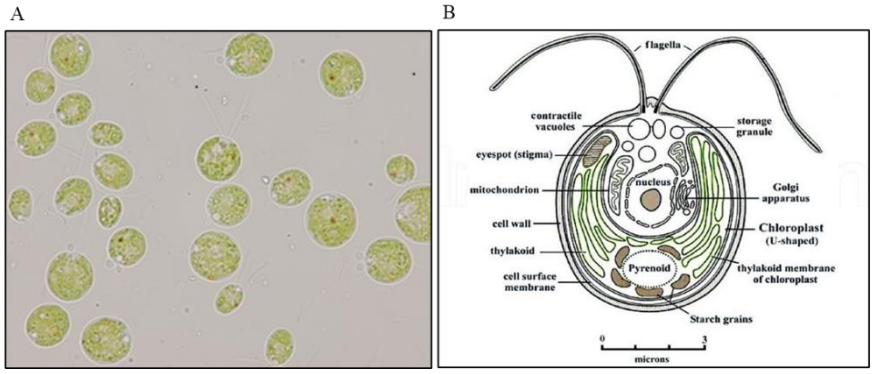

Figure 7. A) *C. reinhardtii* cells observed under microscope (own picture), B) Diagrammatic representation of *C. reinhardtii* cell showing all the organelles (Kukwa and Chetty, 2021).

It can be grown phototrophically in the light, heterotrophically with acetate in the dark, or mixotrophically on acetate in the light. Their optimal temperature is 25°C, while the

optimal pH for growth is 7.0. Within the green plant lineage, it is a reference organism for the study of chloroplast metabolism and photosynthesis and in particular it is often used as model organism for the study of abiotic stress (Hoober, 1989). *C. reinhardtii* as a model organism has the advantages of a short generation time, complete availability of the genome sequence and the similarity of its photosynthetic machinery to that of higher plants. *C. reinhardtii* is used in photosynthesis research for industrial applications such as bioethanol or biohydrogen production (Torzillo *et al.*, 2015; de Farias Silva and Bertucco, 2016).

1.4.2. *Euglena gracilis*

Euglena gracilis (*E. gracilis*) is a freshwater species of unicellular eukaryotic algae. *E. gracilis* is a mixotrophic species that can feed either by phagocytosis or by photosynthesis. It can be grown autotrophically, mixotrophically or heterotrophically (Wang *et al.*, 2018b). The cells are usually thin and spindle-shaped with a size of up to 100 µm but sometimes change into ovoid spheres of about 20 µm. The cells have a single emergent flagellum, while the second is hidden in a reservoir - an invagination at the front end of the cell (Adl *et al.*, 2012) Under stress conditions, cells can develop inactive, dormant cysts by forming a protective wall to survive periods of unfavourable environmental conditions (Strauch *et al.*, 2018). The cells under normal conditions have no cell wall but are surrounded by pellicle consisting of a protein layer. The cells have an organelle called eyespot which consists of carotenoid pigment granules (Figure 8).

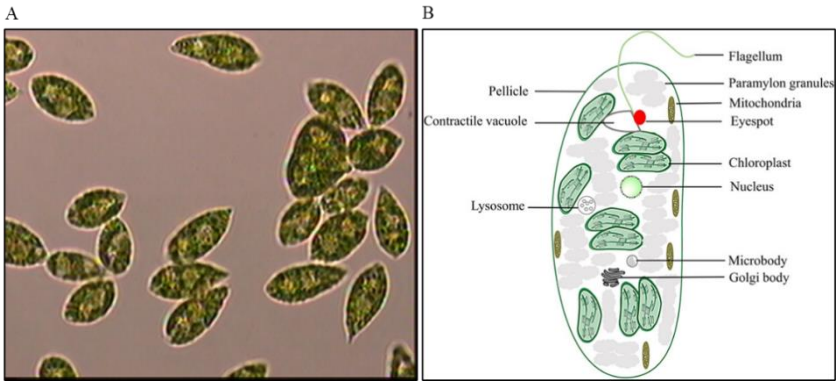

Figure 8. A) *E. gracilis* cells observed under microscope (own picture) B) Diagrammatic representation of *E. gracilis* cell showing all the organelles (Khatiwada *et al.*, 2020).

Their plastids are acquired by secondary endosymbiosis (Lefort-Tran *et al.*, 1980) which allows them to feed autotrophically like plants. Their optimal temperature is 25°C, and the optimal pH for growth is 7.0. Chloroplasts are surrounded by three membranes, similar to dinoflagellates (Gibbs, 1960) unlike green algae and higher plants whose chloroplasts have

two membranes. Importantly, both photosystems of *E. gracilis* appear to use a common antenna system that includes both LHCI and LHCII proteins, which can participate in the spillover of excitation energy from PSII to PSI contrary to that of other microalgae and higher plants (Doege *et al.*, 2000). In addition, the pigment composition of *E. gracilis* differs from that of plants and green algae. *E. gracilis* contains β-carotene and xanthophylls such as neoxanthin (Nx) and Ddx, but pigments of the classical violaxanthin cycle i.e., Vx and Zx are not present (Doege *et al.*, 2000). However, diadinoxanthin functions as a component of diadinoxanthin cycle in chloroplasts. The diadinoxanthin cycle plays a similar role as the xanthophyll cycle, which dissipates excess light energy under elevated light intensities and helps protect against photooxidative stress during photosynthesis in *E. gracilis*. (Goss and Jakob, 2010; Kato *et al.*, 2017). It has been suggested that in *E. gracilis* the presence of Ddx stabilizes the LHCs, similar to lutein in higher plants (Brandt and Wilhelm, 1990). Chloroplasts of *E. gracilis* contain pyrenoids that are used to synthesize complex carbohydrate, paramylon, which can serve as an energy source during periods of light deficiency. There is great interest in biotechnology for paramylon due to their immunostimulatory and antimicrobial bioactivities (Barsanti *et al.*, 2001; Russo *et al.*, 2017; Gissibl *et al.*, 2018). *E. gracilis* is a perfect source of numerous other valuable compounds (O'neill *et al.*, 2015), such as wax esters (Inui *et al.*, 1982; Zimorski *et al.*, 2017), polyunsaturated fatty acids, α-tocopherol (vitamin E), biotin (vitamin B_7), and proteins (Gissibl *et al.*, 2019).

1.5. Salt stress adaptation of photosynthetic organisms

Photosynthetic organisms regularly face adverse conditions that retard growth and development, reduce productivity, and in extreme cases even leads to death. They are often exposed to a range of stressful conditions such as high light, low temperature, salt, drought, heat, oxidative stress, heavy metal toxicity etc. Due to these abiotic stresses, the agricultural industry suffers great losses in the form of crop productivity. Acclimation to environmental conditions is essential for plants and algae; therefore, they employ different strategies when exposed to stress. Acclimation depends on the activation of cascades of molecular networks involved in stress perception, signal transduction, and adaptations. Under adverse conditions, photosynthetic organisms have evolved to adapt to environmental conditions to maintain photosynthetic efficiency (Horton *et al.*, 1994).

Salinity is one of the most important abiotic factors limiting productivity in many arid and semi-arid areas around the world (Msanne *et al.*, 2011). It is one of the major threats to

the agricultural sector. Salinity affects 20% of the world's cultivated land, and about 50% of irrigated land (Rhoades, 1990). Photosynthetic organisms can trigger different physiological and biochemical mechanisms to deal with salt stress, which include: changes in morphology, photosynthesis, ion distribution, and biochemical adaptation (Ashraf and Harris, 2013). Several studies on salt stress have reported morphological changes in some green algal species. Salinity causes both ionic and osmotic stress as primary effects (Mager and Siderius, 2002). This can lead to secondary effects such as oxidative damage leading to membrane disorganisation, decreased enzyme activity, attenuated nutrient uptake, inhibition of photosynthesis, and finally resulting cell death (Hasanuzzaman *et al.*, 2013). The cation transport system accelerates the elimination of sodium, and osmotic regulation via osmolyte synthesis as one means of reducing the harmful effects of salt stress (Yancey, 2005). It has been reported that in *C. reinhardtii*, salt stress impairs cell division and causes the formation of multicellular aggregates called palmelloids in which the cell size is reduced, and the cell motility is lost (Neelam and Subramanyam, 2013; Khona et al., 2016; Shetty et al., 2019). NaCl can cause disruption in pigment-protein-lipid complexes resulting in a reduction of pigments in the stress condition (Turan *et al.*, 2009). Decrease in Chl *a* and Chl *b* pigments by NaCl treatment was reported in several plants such as *Zea mays*, *Paulownia imperiallis*, *Carthamus tinctorius*, etc., mainly due to increase in the chlorophyll destroying enzyme called chlorophyllase (Parvaneh *et al.*, 2012). In contrast, *Dunaliella salina* a salt-tolerant microalga in response to a spike in salt concentration, increases Chl *a* content to raise the photosynthetic activity (Talebi *et al.*, 2013). Salt stress inhibited PSII activity in higher plants, salt-tolerant plants such as mangroves (Tiwari et al., 1998), and the red alga *Porphyra perforate* (Satoh et al., 1983). Reduced PSII activity due to salt stress has been associated with state-2 transition in the green algae *Dunaliella tertiolecta* (Gilmour et al., 1982) and *C. reinhardtii* (Endo *et al.*, 1995). It has been demonstrated that the inhibition of electron transport on the donor and acceptor sides of PSII causes damage to the phycobilisome, that is the light harvesting antennae of cyanobacteria and some red algae, and the shift in the distribution of excitation energy in favour of PSI in *Arthrospira* (*Spirulina*) *platensis* is due to salt stress (Lu and Vonshak, 2002). LHCs of PSI and proteins of PSII involved in O_2 evolution are damaged by ROS at high salt concentrations in *C. reinhardtii* (Subramanyam *et al.*, 2010; Neelam and Subramanyam, 2013). Reportedly the protein turnover of D1 protein of PSII was reduced in both plants and cyanobacteria under salt stress (Allakhverdiev *et al.*, 2000a). It is well known that CEF is an essential alternative pathway to meet the requirement of ATP under abiotic stress conditions. Earlier studies demonstrated the impact of salt stress

on the CEF activity of the photosynthetic organisms. It has been described that salt stress induced higher CEF activity in higher plants such as cucumber (Wu *et al.*, 2019), salt tolerant soybean (He *et al.*, 2015) and salt tolerant *Chlamydomonas* sp. UWO 241 (Kalra *et al.*, 2020; Stahl-Rommel *et al.*, 2022).

Water relations and the capacity for osmotic adjustment are important for plant growth response which are particularly affected under salt stress (Ozturk *et al.*, 2004). Photosynthetic organisms have evolved complex mechanisms to adapt to osmotic and ionic stress caused by high salinity (Meloni *et al.*, 2004). Although the molecular basis of the mechanisms involved in salt tolerance in many organisms is not fully understood, some concepts have emerged. These mechanisms include (i) Inhibition of Na^+ influx and preventing intracellular Na^+ accumulation, which leads to greater salt tolerance (Apte and Thomas, 1986; Apte *et al.*, 1987; Apte and Bhagwat, 1989) (ii) osmotic adjustment, which usually occurs through the uptake of inorganic ions, such as K^+ ; (Miller *et al.*, 1976; Thomas and Apte, 1984; Reed and Stewart, 1985; Apte and Bhagwat, 1989; Meloni *et al.*, 2004). High concentrations of NaCl inactivate Na^+/H^+ antiporters in cyanobacterial cells (Allakhverdiev *et al.*, 2000a; Allakhverdiev *et al.*, 2000b). They have also evolved a variety of protective mechanisms against adverse salt-stress conditions based on the role of Na^+/H^+ antiporters (Allakhverdiev *et al.*, 2000a; Nishiyama *et al.*, 2001), water and ion channels (Allakhverdiev *et al.*, 2000a; Allakhverdiev *et al.*, 2000b).

Accumulation of compatible solutes (osmoprotectants), such as glucopyranosyl-glycerol (Borowitzka *et al.*, 1980), sucrose (Blumwald *et al.*, 1983), trehalose, or glycine betaine (Reed *et al.*, 1984; Hayashi *et al.*, 1998; Chen and Murata, 2002) and salt stress-induced proteins (Apte and Bhagwat, 1989; Hagemann *et al.*, 1990; Hagemann *et al.*, 1991; Allakhverdiev and Murata, 2008) in the cells subjected to salinity stress have been reported. The expression of genes involved in the biosynthesis of compatible solutes is enhanced under salt stress (Fulda *et al.*, 2006), and the levels of accumulated compatible solutes are correlated with the extent of tolerance to salt stress (Zhu, 2002; Allakhverdiev and Murata, 2008). In the mangrove plant *Bruguiera parviflora*, a subsequent decrease in starch content and an increase in the content of reducing and non-reducing sugars and in the level of polyphenols due to salt stress has been reported (Parida *et al.*, 2002). In plants and cyanobacteria, glycine betaine acts as a compatible solute by stabilizing the quaternary structures of proteins, cell membranes, and the oxygen-evolving complex of PSII during salt stress (Papageorgiou and Murata, 1995). In *C. reinhardtii*, increased accumulation of glycerol content was recorded with increasing salinity (León and Galván, 1994). Salt-stressed *Dunaliella* cells accumulate

huge amounts of glycerol, and it was found that the content of intracellular glycerol is proportional and osmotically equivalent to the external salt concentration (Ben-Amotz and Avron, 1973). Proline is another osmoregulatory solute whose concentration in higher plants and algae increases linearly with increasing salinity (Brown and Hellebust, 1978; Liu and Zhu, 1997). It has been shown that high-salt stress leads to increased production of trehalose in *Chlamydomonas* (Wang et al., 2018a), *Chlorella* and *Scytonema* (del Pilar Bremauntz et al., 2011). Trehalose was observed to reduce the negative effects of high salt-stress as an osmoprotectant in maize (Zeid, 2009). High-salt stress can negatively affect photosynthetic performance of *E. gracilis* cells and trehalose accumulation has been observed under osmotic stress (González-Moreno et al., 1997; Takenaka et al., 1997; Porchia et al., 1999). In *Phaseolus vulgaris*, a decrease in the total protein content was observed under salt stress (Beltagi *et al.*, 2006). Since *Dunaliella* has no cell wall, the cells can rapidly alter volume during severe salt stress by changing the internal ion and glycerol content restoring the osmotic pressure of cells (Ben-Amotz and Avron, 1973; Kaçka and Dönmez, 2008). In contrast, *Chlorella* cells have a rigid cell wall thereby limiting its ability to change the cell volume. However, cells maintain osmotic homeostasis under salinity through production of compatible solutes and inorganic ion accumulation (Ahmad and Hellebust, 1984). Accumulation of lipids occurs in most green algae, when subjected to salt stress. *Chlamydomonas* sp. JSC4 is a salt-tolerant strain from a marine environment that exhibits significant lipid accumulation under extreme salt stress (Ho *et al.*, 2014). Salt stress enhanced production of β-carotene in response to salt stress in *D. salina* (Pisal and Lele, 2005; Ye *et al.*, 2008). Under moderate salt stress (0.05 M - 0.15 M), *C. reinhardtii* and *Chlorella vulgaris* also show high carotenoid production (Annamalai *et al.*, 2016).

Because the methods used by cells to tolerate salt could have significant marketable functions, many biotechnologists, physiologists, microbial biochemists, and ecologists are interested in studying salinity as a major environmental factor (Galinski and Trüper, 1994).

Studying the saline stress responses of green algae can help us better understand the acclimation processes of photosynthetic organisms. Over four decades of research findings demonstrate the way microalgae respond physiologically while adapting to salt stress (Shetty *et al.*, 2019). However, different algal species use specific strategies to overcome the effects of this challenging stress. Moreover, freshwater algal species need to develop mechanisms to deal with salinity to which they are not accustomed. Salt-induced changes in the physiology of some of the microalgal species have not yet been fully characterized. More importantly, the role of membrane reorganization in the adaptation mechanisms of photosynthetic

organisms has not been explored in detail. Extensive characterization of the responses of photosynthetic apparatus to salinity stress can help improve the agricultural productivity. Therefore, studies from the structural to the functional level, i.e., from the supramolecular organization of TM to the photosynthetic energy transfer processes, provide a holistic approach to gain insight into the acclimatory responses of algae to salt stress.

2. Aims of the study

The major aim of the presented project was to better understand the dynamics of photosynthetic complexes and membrane organization in the cases of salt stress in biotechnologically important microalgal strains revealing the relation to their stress tolerance and in *Arabidopsis thaliana* chloroplast mutants.

To gain a better insight into salt stress response of microalgae we studied:

1. The changes in the structure and function of photosynthetic apparatus under salinity stress in *C. reinhardtii*.
2. The acclimation responses of *E. gracilis* to moderate salt stress by investigating the morphological and pigment composition changes in addition to the macro-organization of photosynthetic apparatus.

Understanding the acclimation responses of algae to salinity stress is essential to advance basic research in algal biology and biotechnology.

3. In addition, we studied the macro-organisation of the photosynthetic complexes in thylakoid membrane of *A. thaliana* chloroplasts in the cases of chloroplast acetyltransferase *gnat2* and Ser/Thr kinase *stn7* mutants. The *gnat2* mutant exhibiting reduced lysine acetylation of specific thylakoid proteins. The STN7 kinase regulates the organization and dynamics of thylakoid structure through phosphorylation.

A thorough characterization of the responses of photosynthetic apparatus to salt stress could be important for increasing agricultural productivity and the plant mutants help understanding the dynamics of thylakoid membrane.

3. Materials and Methods

3.1. Plant material, propagation, and growth conditions

A. thaliana plants were grown under a photon flux density of 120 µmol m^{-2} s in an 8 h light/16 h dark regime at 23 °C and in a relative humidity of 50%. We used ecotype Columbia-0 (WT), the *gnat2* (nsi-1, SALK_033944; (Koskela *et al.*, 2018) and *stn7* (SALK_073254) mutant strains of *A. thaliana*. In the *stn7* mutant, the gene encoding the serine-threonine protein kinase (STN7 protein kinase) associated with the thylakoid membranes required for the phosphorylation of LHCII is inactivated (Pesaresi *et al.*, 2010). The *gnat2* mutant, the gene encoding for first chloroplast lysine/N-terminal acetyl transferase (GNAT2 acetyl transferase) associated with the regulation of photosynthetic light reactions (Koskela *et al.*, 2018).

3.2. Cell culture and growth conditions

C. reinhardtii cultures were grown mixotrophically in Tris-acetate-phosphate (TAP) medium (composition below) on a rotatory shaker at 120 rpm, 25 °C under cool fluorescent light 50 µmol photons m^{-2} s^{-1} with continuous illumination. We used mutants *pgrl1* (obtained from Prof. Gilles Peltier CEA - CNRS - Aix Marseille Université, France), *stt7* (kind gift from Prof. Yuchiro Takahashi, Okayama University, Japan) and wild type (CC-125, 137AH) strains of *C. reinhardtii*. In the *stt7* (CC-4178 stt7 mt+) mutant, the gene encoding the serine-threonine protein kinase associated with the thylakoid membranes that is an ortholog of *Arabidopsis* STN7 is inactivated (Depège *et al.*, 2003). The *stt7* is defective in state transition between PSII and PSI. The *pgrl1* mutant (AH137 pgrl1 mt+) is defective in CEF around PSI, because the *pgrl1* gene encoding the proton gradient regulator like 1 protein that is involved in CEF is inactivated (Tolleter *et al.*, 2011). Subcultures were inoculated by setting the OD to 0.2 at 750 nm. The culture usually reached stationary phase in 5-6 days.

E. gracilis cells were grown mixotrophically in ETAP medium (composition below). Cultures were grown on a rotary shaker with gentle shaking at 110 rpm under 16 h of illumination (40 µmol photons m^{-2} s^{-1}) and 8 h of darkness at 24 °C. Subcultures were inoculated by adjusting OD to 0.2 at 750 nm. The culture usually reached stationary phase within 4-5 days.

3.2.1. Preparation of TAP medium

Table 1. Composition of TAP medium

Compound	**per L**
TRIS	2.42 g
TAP salts	25 mL
Phosphate buffer	0.375 mL
Glacial acetic acid	1 mL
Hutner's trace elements	1 mL

TAP salts: 7 mM NH_4Cl, 0.83 mM $MgSO_4 \cdot 7H_2O$, 0.45 mM $CaCl_2 \cdot 2H_2O$

Hutner's trace elements: 134 µM $Na_2EDTA \cdot 2H_2O$, 136 µM $ZnSO_4 \cdot 7H_2O$, 184 µM H_3BO_3, 40 µM $MnCl_2 \cdot 4H_2O$, 32.9 µM $FeSO_4 \cdot 7H_2O$, 12.3 µM $CoCl_2 \cdot 6H_2O$, 10 µM $CuSO_4 \cdot 5H_2O$, 4.44 µM $(NH_4)_6Mo_7O_2 \cdot 4H_2O$

Preparation: 50 g of EDTA (disodium ethylenediamine tetraacetate) is added to 750 mL of distilled water. EDTA is dissolved by adding 40% or 5 N NaOH until pH ~6.0 at which EDTA should all go into the solution. 22.0 g $ZnSO_4 \cdot 7H_2O$ is slowly added to heated solution. When the solution starts to boil $ZnSO_4$ gets dissolved. Each of the salts are added in the proper quantities and in the given order. After the second salt is added EDTA falls back out of solution because the pH is lowered by the addition of the acidic salts. The solution is mildly heated and sufficient base (KOH or NaOH) is added to dissolve the EDTA again. EDTA and salts are dissolved by adjusting the pH to be ~6–7. The final volume is made up to 1 L. Solution is let to stand for two weeks at room temperature and stirred once a day until its colour turns purple then filtered through paper and stored in fridge.

3.2.2. Preparation of Euglena-TAP medium

Table 2. Composition of E-TAP medium

Compound	**per L**
$NaNO_3$	1 g
Beef extract	1 g
Bacto-tryptone	2 g
Yeast extract	2 g
Hutner's Trace elements solution (see above)	1 mL

3.3. Salt treatment

The cells of *C. reinhardtii* were grown in TAP media containing different salt concentrations (50 mM, 100 mM and 150 mM NaCl). Usually, control cells reached mid-log phase i.e., approximately $3x10^6$ cells/ml in about four days with an optical density (OD 750 nm ~1). The experiments were performed with four-day old cultures.

The cells of *E. gracilis* were grown in ETAP media with various concentrations of NaCl (50 mM, 100 mM and 150 mM). Experiments were conducted for four days with daily sampling.

3.4. Measurement of optical density

Measurements of optical density of the cells were performed by a Shimadzu UV-1601 spectrophotometer. The optical density of the *C. reinhardtii* and *E. gracilis* cultures was measured at 750 nm (OD_{750}).

3.5. Pigment analysis

3.5.1. Spectrophotometric analysis of pigments

Pigments in *C. reinhardtii* were extracted by adding 1 mL of 100% methanol to the cell pellet (1 mL), vortexing it for 2 minutes and dark adapted for 5 minutes (3–4 repetitions). Resuspended samples are centrifuged at 10000 g for 5 minutes. The absorbance of the methanol extracts (supernatant) was measured at 652 nm and 665 nm. The average value of different repetitions was calculated and the Chl content was determined spectrophotometrically using molar absorption coefficients with the following equations (Porra *et al.*, 1989).

Chl *a* (mg/mL) = $(16.29 \cdot A_{665} - 8.54 \cdot A_{652}) \cdot$ dilution factor

Chl *b* (mg/mL) = $(30.66 \cdot A_{652} - 13.58 \cdot A_{665}) \cdot$ dilution factor

Chl *a*+*b* (mg/mL) = $(22.12 \cdot A_{652} + 2.71 \cdot A_{665}) \cdot$ dilution factor

Chl concentration in *E. gracilis* cells was measured by adding 1ml of 90% methanol to the cell pellet, vortexing it for 2 minutes and dark adapted for 5 minutes (3–4 repetitions). Resuspended samples were centrifuged at 10000 g for 10 minutes as described previously by Devars *et al.* (1992). The absorbance of the methanol extracts was measured at 653 nm and 666 nm. The mean value of all the repetitions was calculated and the Chl content was determined spectrophotometrically using molar absorption coefficients with the following equations as described by Lichtenthaler and Wellburn (1983):

Chl *a* (mg/mL) = (15.65 · A_{666} – 7.34 · A_{653}) · dilution factor

Chl *b* (mg/ml) = (27.05 · A_{653} – 11.21 · A_{666}) · dilution factor

Chl *a*+*b* (mg/mL) = (4.44 · A_{666} + 19.71 · A_{653}) · dilution factor

Chl concentration of isolated TM (as described in section 3.6) of *A. thaliana* was estimated by resuspending 2 µL of TM in 80% acetone and vortexing it for 2 minutes followed by dark incubation for 5 minutes. Then the resuspension was centrifuged at 10000 g for 5 minutes. The absorbance of the acetone extracts was measured at 646.6 nm and 663.6 nm. Average values of the repetitions was calculated and the Chl content was determined spectrophotometrically using molar absorption coefficients with the following equations (Porra *et al.*, 1989).

Chl *a* (mg/mL) = (12.25 · $A_{663.6}$ – 2.55 · $A_{646.6}$) · dilution factor

Chl *b* (mg/mL) = (20.31 · $A_{646.6}$ – 4.91 · $A_{663.6}$) · dilution factor

Chl *a*+*b* (mg/mL) = (7.34 · $A_{663.6}$ + 17.76 · $A_{646.6}$) · dilution factor

3.5.2. Pigment analysis by High-performance liquid chromatography (HPLC)

For pigment determination, 1.5 mL of *E. gracilis* cell suspensions harvested from day 0 to day 4 were pelleted by centrifugation at 3000 g for 3 min and snap frozen in liquid nitrogen and stored at -80 °C until use. The pigments were extracted by resuspending the cells in ice-cold 100% acetone followed by 30 minutes dark incubation with continuous shaking at 1000 rpm. The samples were centrifuged at 11500 g for 10 minutes at 4 ºC and the supernatant was passed through a PTFE 0.2 µm pore size syringe filter. The pigment composition of the cells was determined as described by Zsiros and co-workers (Zsiros *et al.*, 2020).

Quantification of carotenoids was performed by high-performance liquid chromatography (HPLC), using a Shimadzu Prominence HPLC system (Shimadzu, Kyoto, Japan) consisting of two LC-20AD pumps, a DGU-20A degasser, a SIL-20AC automatic sample injector, CTO-20AC column thermostat and a Nexera X2 SPD-M30A photodiode-array detector. Chromatographic separations were carried out on a Phenomenex Synergi Hydro-RP 250 x 4.6 mm column with a particle size of 4 µm and a pore size of 80 Å. 20 µL aliquots of acetonic extract was injected to the column and the pigments were eluted by a linear gradient from solvent A (acetonitrile, water, triethylamine, in a ratio of 9:1:0.01) to solvent B (ethylacetate). The gradient from solvent A to solvent B was run from 0 to 25 min at a flow rate of 1 mL/min. The column temperature was set to 25 °C. Eluates were monitored in a wavelength range of 260 nm to 750 nm at a sampling frequency of 1.5625 Hz. Pigments

were identified according to their retention times and absorption spectra and quantified by integrated chromatographic peak area recorded at the wavelength of maximum absorbance for each kind of pigments using the corresponding molar decadic absorption coefficient (Wright *et al.*, 2005).

3.6. Isolation of thylakoid membranes

Thylakoid membranes of *A. thaliana* were isolated according to Lambrev and co-workers. (Lambrev *et al.*, 2007). *Arabidopsis* wild type and mutant plants were grown in a green house. Chloroplast thylakoid membranes were isolated from leaves of two-week-old seedlings.

Buffers:

B1: 50 mM Tricine, 0.4 M Sorbitol, 5 mM $MgCl_2$, 5 mM KCl, pH 7.5.

B2: 50 mM Tricine, 5 mM $MgCl_2$, 5 mM KCl, pH 7.5.

B3: 50 mM Tricine, 0.8 M Sorbitol, 5 mM MgCl2, 5 mM KCl, pH 7.5.

Procedure:

Leaves were homogenized in ice-cold B1 buffer. The homogenate was then filtered through four-layered cheese cloth and the remaining debris was centrifuged at 500 g for 2 minutes. Then the supernatant was centrifuged at 6500 g for 5 minutes. Pellet was resuspended in ice-cold B2 buffer and then immediately resuspended in B3 buffer. The suspension was then centrifuged at 7000 g for 5 minutes. The pelleted thylakoid membranes were resuspended in buffer B3 to a final Chl concentration of 1–2 mg/mL and stored on ice.

Thylakoid membranes of *E. gracilis* cells were prepared from four-day-old cells using the method described in (Block and Albrieux, 2018) with slight modifications. The Precellys Evolution homogenizer (Bertin Technologies, France) was used to break up the cells before isolation.

Buffers:

B1: 300 mM sorbitol, 50 mM HEPES-KOH, 2 mM Na_2EDTA, 1 mM $MgCl_2$, 1% w/w BSA, pH 7.5.

B2: 50 mM HEPES-KOH, 330 mM sorbitol

B3: 25 mM Bis tris/HCl, 20% w/v glycerol

Three-step Percoll gradients of 65%, 45% and 20% with B2 were prepared.

Procedure:

Cell pellet was washed in ice-cold buffer B1 for 2 minutes at 500 g. Then the pellet was resuspended in 1.5 mL of B1 buffer and transferred into bead beating tubes containing

1:1 0.1 mm/0.5 mm beads for lysis at 8000 rpm with 4 cycles of about 30 seconds at 4 °C. Lysed cells were centrifuged at 120 g for one minute at 4 °C and the cell debris was removed. Then the supernatant was centrifuged at 6500 g for 5 minutes at 4 °C. Then the pellet was resuspended in 0.5 mL of ice-cold B1 buffer before loading onto the gradient. Gradients were centrifuged at 2990 g for 40 minutes at 4 °C. Thylakoid fraction was then collected from the interface of the 20% and 45% gradient. Thylakoid fraction was washed with ice-cold B2 buffer and centrifuged at 10000 g for 5 minutes. Pellet was then resuspended in ice-cold buffer B3, and chlorophyll content was measured. Then the thylakoids were dissolved with 2% β-DM for 30 minutes at 4 °C and centrifuged at 18000 g for 20 minutes. Finally, solubilized thylakoids (supernatant) were collected.

3.7. Small-angle neutron scattering (SANS)

The experiments were performed on the SANS II small-angle neutron scattering instrument at the Paul Scherrer Institute (PSI, Villigen, Switzerland). The applied settings for the measurements of the samples were: SD, 3 m; collimation, 3 m; λ, 5.52 Å. (SD, sample-to-detector distance; λ, neutron wavelength). As a subtractable sample background, we measured the D_2O-based culture medium, which was used as a suspension buffer for the algal cells during the measurements. The instrumental background was recorded with the beam blocked by a cadmium plate. All experimental data were corrected for detector efficiency obtained from measurements performed on Cd plate, cuvette and H_2O in a quartz cuvette with 1 mm path length, with instrument setting of SD, 1.5 m; collimation, 2 m; and λ, 5.52 Å. For data treatment the "Graphical Reduction and Analysis SANS Program" package (GRASP) (developed by C. Dewhurst, ILL) was used. The observed 2D scattering patterns did not reveal significant anisotropy; therefore, further analyses were performed on 360° radially-averaged scattering curves. The scattering curves exhibited two characteristic peaks – around 0.035 $Å^{-1}$ and 0.06 $Å^{-1}$. In order to quantify any structural changes observed with SANS, the 1D scattering curves were fitted with a sum of constant, a power function and two Gaussian functions, similar to the method described earlier (Nagy *et al.*, 2013). The fitting range was 0.0204 – 0.0856 $Å^{-1}$ (Kanna *et al.*, 2021).

3.8. Scanning Electron Microscopy

For scanning electron microscopy (SEM), *E. gracilis* cells were fixed in phosphate buffer containing 2.5% glutaraldehyde (Sigma-Aldrich) for 3 hours, then filtered and washed on poly-L-lysine–coated polycarbonate filters. Following post-fixation in 1% OsO_4 for one

hour the samples were dehydrated in aqueous solutions of increasing ethanol concentrations, critical-point dried, covered with 15 nm gold by a Quorum Q150T ES sputter and visualized in a JEOL JSM-7100F/LV scanning electron microscope using 5 kV accelerating voltage under different magnifications (Kanna *et al.*, 2021).

3.9. Transmission Electron Microscopy

For transmission electron microscopy (TEM) of *C. reinhardtii* cells, approximately 0.5 mL of control and salt-treated cell samples from all groups (n = 2/group) of both WT and *stt7* mutant were immersed into a modified Karnovsky fixative solution (Karnovsky, 1965) (pH 7.4), which contained 2% paraformaldehyde (Sigma-Aldrich; St. Louis, MO, USA) and 2.5% glutaraldehyde (Polysciences; Warrington PA, USA) in phosphate buffer. Samples were fixed overnight at 4 °C, then briefly rinsed in distilled water (pH 7.4) for 10 min and fixed further in 2% osmium tetroxide (Sigma-Aldrich, St. Louis, MO, USA) in distilled water (pH 7.4) for 2 h. After osmification, samples were briefly rinsed in distilled water for 10 min, then dehydrated using a graded series of ethanol (Molar Chemicals; Halasztelek, Hungary), from 50 to 100% for 30 min in each concentration. Afterwards, cells were proceeded through propylene oxide (Molar Chemicals), then embedded in an epoxy-based resin (Durcupan ACM; Sigma-Aldrich). After polymerization for 48 h at 56°C, resin blocks were etched and 50 nm thick ultrathin sections were cut using an Ultracut UCT ultramicrotome (Leica; Wetzlar, Germany). Sections were mounted on a single-hole, formvar-coated copper grid (Electron Microscopy Sciences; Hatfield, PA, USA), and the contrast of the samples was enhanced by staining with 2% uranyl acetate in 50% ethanol (Molar Chemicals, Electron Microscopy Sciences) and 2% lead citrate in distilled water (Electron Microscopy Sciences) (Reynolds, 1963; Hayat and Giaquinta, 1970).

Ultrathin sections from the cells were screened at 3000× magnification on a JEM-1400Flash transmission electron microscope (JEOL; Tokyo, Japan) until 25–30 granum cross-sections were identified from each sample (n = 2/group). For quantitative measurements of the RD, images of thylakoid membrane structures were recorded at 50000× magnification using a 2 k × 2 k Matataki Flash scientific complementary metal-oxide-semiconductor camera (JEOL). Finally, quantitative analysis of the membrane repeat distances were performed using the built-in measurement module of the microscope. RDs were measured from both the control and salt (100 mM NaCl) treated cells of WT and *stt7* in two sets (biological repetitions). A number of 40 repeat distances were measured from each group by choosing 10 cells (4 measurements) from each group. All the repeat distances were

averaged, and the average of the biological repetitions was averaged.

For transmission electron microscopy (TEM), *E. gracilis* cells were fixed in 2.5% (v/v) glutaraldehyde for 2 days and suspended in 2.5% tepid agar. After solidification, small cubes were cut from the samples and post-fixed in 1% (w/v) OsO_4 for 1 hour. Fixatives were buffered with 0.07 M Na_2HPO_4-KH_2PO_4 (pH 7.2). Following dehydration in aqueous solutions of increasing ethanol concentrations, samples were embedded in Durcupan ACM resin (Fluka, Switzerland). Ultra-thin sections were cut by a Reichert Jung Ultracut M microtome (Reichert-Jung Ltd., Austria), mounted on copper grids, then contrasted with 5% uranyl acetate and Reynold's lead citrate solution and observed by a Hitachi 7100 (Hitachi Ltd., Japan) and JEOL JEM 1011 (Jeol Ltd., Japan) transmission electron microscopes. To determine the repeat distance of thylakoid membranes from TEM images we used ImageJ software. On the micrographs made with 80x magnification, sharp regions were selected where the thylakoid membranes appeared to be sliced perpendicularly to their membrane planes (Ünnep *et al.*, 2014b). We applied fast Fourier transformation (FFT) analysis on the selected region, which provided values on the periodicity (RD) of the thylakoids. This RD incorporates the widths of the two aqueous phases (the lumen and the IT aqueous phase), and twice the width of the membrane. Each average RD was calculated from more than 160 data of stacked thylakoids, which were measured on images of chloroplasts from 18–19 cells (Kanna *et al.*, 2021).

3.10. Circular dichroism spectroscopy

Circular dichroism (CD) spectra of cells from *C. reinhardtii* (control and salt grown) WT, *stt7*, *pgrl1* strains; from control (WT) and mutant (*stn7* and *gnat2*) leaves and thylakoids of *A. thaliana*; and from control and salt-stressed cells of *E. gracilis* were recorded using JASCO-815 spectropolarimeter at room temperature in the spectral range of 400-800 nm with 3 nm spectral resolution using a J815 spectropolarimeter (Jasco, Japan). Measurements were carried out in standard glass cuvettes with optical path length of 1 cm in the case of liquid samples. Three individual scans were accumulated at a scan speed of 100 nm/min with data being collected at every nanometer with integration time of 2 seconds. Chl concentration of the cell sample was set to 15 µg mL^{-1} in *C. reinhardtii* and the cells were diluted to Chl concentration of 20 µg mL^{-1} for each sample in *E. gracilis*. Chl concentration of freshly isolated thylakoid membranes of *A. thaliana* was adjusted to 20 µg mL^{-1} and measured. Intact leaves supported by a flat cell were placed perpendicularly to the optical path. Before the measurements, leaves were infiltrated with distilled water to improve the signal to noise ratio.

For baseline correction, respective culture media were used in *C. reinhardtii* and *E. gracilis*. For baseline correction in case of *A. thaliana*, empty baseline was used for leaves; resuspension buffer was used for thylakoids. The CD spectra were normalized to the Chl Q_y absorption band with a reference wavelength at 750 nm. Multiple independent CD scans were recorded and averaged. Difference of the amplitudes of (+)690 nm and (−)676 nm psi-type CD bands in *C. reinhardtii*; (+)690 nm and (−)674 nm psi-type CD bands in *E. gracilis* respectively were calculated to compare the effect of salt treatment on the psi-type CD in the red spectral region. Amplitudes of (+)690 nm and (−)674 nm and (+)506 nm psi-type CD bands were calculated to compare the difference between psi-type CD in the red and blue spectral region of leaves and thylakoids in *A. thaliana*.

For analysing the circular dichroism spectral data, the MATLAB programming interface and Spectr-O-Matic Toolbox and Origin pro 8 program were used.

3.11. OJIP Chl *a* fluorescence induction kinetics

OJIP Chl *a* fluorescence transients from control and salt-stressed *E. gracilis* cells were measured using Aqua Pen AP-C 100 fluorometer (PSI, Czech Republic). Prior to measurements, cultures were dark adapted for 20 minutes. Measurements were carried out at room temperature. Cell suspension containing a total of 1 µg Chl was pipetted into a cuvette. Illumination (650 nm) was provided by an LED array which was focused on the sample to provide uniform irradiance. Fluorescence measurements were carried out with 5 seconds flash of 3000 µmol photons m^{-2} s^{-1}. The first reliably measured point of the fluorescence transient is at 20 µs, which was taken as F_0. Fluorescence transients were recorded from three biological repetitions (Kanna *et al.*, 2021). The OJIP-test (Strasser 2000) was used to analyze the Chl *a* fluorescence transient, and the following original data were acquired: O (F_0) initial fluorescence level (measured at 50 µs), P (F_m) maximal fluorescence intensity, as well as the J (at about 2 ms) and the I (at about 30 ms) intermediate fluorescence levels. From these specific fluorescence features the following parameters of photosynthetic efficiency were calculated: Maximal PSII quantum yield, F_v/F_m; The ratio of variable fluorescence to initial fluorescence, F_v/F_0 where $F_v = F_m - F_o$; Probability of electron transport out of Q_A**,** $(1 - V_j)/V_j$ where $V_j = (F_{2ms} - F_0)/F_v$.

3.12. Simultaneous measurements of PSII and PSI yield using Dual-PAM

The Chl *a* fluorescence and light-induced absorbance changes at 820 nm of intact cells were measured using a Dual-PAM-100 chlorophyll fluorometer (Heinz Walz GmbH,

Germany). The cells were dark-adapted for 20 min prior to measurements. Cell suspension equivalent to 40 µg Chl was filtered onto a Whatman glass microfibre filter (GF/C) of 25 mm diameter, which was placed in between two microscope cover slips separated by a spacer. The minimum and maximum fluorescence yield levels, F_o and F_m, respectively, were determined on the dark-adapted state. The intensity of the saturating pulses was 3000 µmol photons m^{-2} s^{-1} and F_m in the light-adapted state was determined with a saturating pulse. Actinic red light with increasing intensity was applied consecutively in the range of 10 – 664 µmol photons m^{-2} s^{-1} for 2 min which was enough to achieve steady-state fluorescence level. Electron transport rate and redox changes of P700 were determined from the light response curves. P700 reduction was followed by measuring the absorbance change of P700. Rate of re-reduction of P700 was obtained by fitting the decay kinetics of $P700^+$ reduction by using one-component exponential analysis. PSI yield (ϕ_I) and PSII yield (ϕ_{II}) were calculated according to Kramer and co-workers (Kramer *et al.*, 2004) and Klughammer and Schreiber (Klughammer and Schreiber, 1994) respectively.

3.13. Measurement of NPQ of the chlorophyll fluorescence using Dual-PAM

The protocol of (Genty *et al.*, 1989) was used to measure the NPQ of Chl fluorescence. Measurements were done using a Dual-PAM-100 chlorophyll fluorometer. Dark-adapted cells were first exposed to a weak modulated beam of 2 µmol photons m^{-2} s^{-1} followed by a saturating flash of 8000 µmol photons m^{-2} s^{-1} for a duration of 800 ms. After 20 seconds, cells were exposed for 15 min to a continuous actinic light of 660 µmol photons m^{-2} s^{-1}. Thereafter, the cells were exposed to a saturating pulse of 8000 µmol photons m^{-2} s^{-1} for 800 ms. Continuous actinic light was turned off after 10 seconds, followed by 5 min of dark adaptation (to determine the recovery of fluorescence).

3.14. Low temperature fluorescence spectroscopy

In *C. reinhardtii* WT, *stt7*, *pgrl1* strains and *E. gracilis*, low-temperature fluorescence emission spectra of cells (control and salt grown) were recorded with a Fluorolog 3 double-monochromator spectrofluorometer (Horiba Jobin-Yvon, USA). The cell suspension with equal Chl concentration (control and salt treated samples of 5 µg/mL) were loaded on Whatmann glass filber (GF/B) discs and immersed in liquid nitrogen. Frozen filters were transferred into a Dewar vessel filled with liquid nitrogen that was placed into the measurement chamber of the spectrofluorometer. Measurements were performed with 1 nm increment and 1 second integration time. The samples were excited at 436 nm and the

emission spectra were recorded between 650 and 800 nm, with 3 nm excitation and emission bandwidths in *C. reinhardtii*. Emission spectra from 650 to 800 nm were recorded with excitation wavelengths of 436 nm and 480 nm while the excitation and emission bandwidths were set to 3 and 5 nm respectively in *E. gracilis*. The emission spectra were normalized to the fluorescence maxima in the range of 690 to 720 nm and 700 to 730 nm in all the *C. reinhardtii* strains and *E. gracilis* respectively. The result was an average of three independent repetitions of each sample. For analysing the emission spectral data, the MATLAB programming interface and Spectr-O-Matic Toolbox, and Origin Pro 8 programs were used.

3.15. Time-resolved fluorescence spectroscopy

Time-resolved fluorescence measurements of *C. reinhardtii* cells (control and salt grown) WT, *stt7, pgrl1* strains were performed at room temperature as described by (Akhtar *et al.*, 2016). Briefly, we used time-correlated single photon counting (TCSPC) system of a Fluotime 200 spectrometer (PicoQuant, Germany) equipped with a microchannel plate detector (Hamamatsu, Japan) and a PicoHarp 300 TCSPC system (PicoQuant). Excitation pulses at 633 nm with 6 ps temporal width, 0.1 pJ pulse energy and 20 MHz repetition rate were generated by a White Micro supercontinuum laser (Fianium, UK). Fluorescence emission was detected through a monochromator at wavelengths between 670 and 750 nm and binned in 4 ps time channels. The sample was continuously circulated through a flow cell with 1.5 mm path length. The optical density at the excitation wavelength was 0.03. The total instrument response (IRF) width was 40 ps, measured using 5% Ludox as scattering solution. Fluorescence decays collected at different detection wavelengths were analyzed by a global lifetime fitting routine using a kinetic model and convolution with the measured IRF. The fitting algorithm, written in MATLAB, minimized the squared sum of residuals weighted by the Poisson distribution. The method of variable projection was employed, wherein rate constants (lifetimes) were global nonlinear fit parameters and amplitudes (spectra) were wavelength-dependent linear least-squares fit parameters (Stokkum, et al., 2004).

3.16. Blue native polyacrylamide gel (BN-PAGE) electrophoresis

The solubilized complexes of the isolated thylakoid membranes of *E. gracilis* were separated on a 5–13% (w/v) gradient and 4% stacking gel (as described in Table 3) of 1 mm thickness with 10 wells. The composition of the gradient gel of Blue-native polyacrylamide gradient electrophoresis (BN-PAGE) is as given in the table after (Schagger *et al.*, 1994).

Table 3. Composition of gradient gel

Component	**5%**	**13%**	**4%**
100% glycerol (g)	-	0.7	-
Milli-Q (MQ) water (mL)	2.65	1.36	1.44
6X Gel buffer (mL)	0.63	0.63	0.33
Acrylamide/bisacrylamide (37.5%: 40%) (mL)	0.48	1.24	0.2
TEMED (µL)	4	3	3
10% APS (µL)	20	14	20
Total volume (mL)	**3.8**	**3.8**	**2**

The gel buffer consists of 0.5 M ACA (aminocaproic acid) and 50 mM Bis Tris/HCl. The loading buffer contains 750 mM ACA and 5% Coomassie Brilliant Blue (CBB) G-250. The anode buffer consists of 0.5 M Bis-Tris/HCl. The cathode buffer consists of 0.5 M Tricine, 150 mM Bis-Tris/HCl, and 0.2% CBB G-250. All buffers were adjusted to a pH of 7.8 mg Chl-containing control and salt-treated (50, 100, and 150 mM NaCl) samples were loaded onto the lanes indicated in the figure legend, and Blue-native gel electrophoresis was performed at 4 °C. First, the gel was run at 8 mA (milliamps) for 15 minutes and then at 15 mA for 30 minutes. Then, the cathode buffer was replaced with the buffer without CBB G-250 staining. Finally, the gel was run at 300 V for 60 minutes. CBB G-250 was used to stain the BN gel.

3.17. Extraction of paramylon

Paramylon from *E. gracilis* cells was extracted and purified following the protocol of (Barsanti *et al.*, 2001) with minor modifications. Cells, both control as well as NaCl-treated, on day 4 were pelleted by centrifugation of 20 mL of culture and kept frozen for at least 4 hours. Then, the pelleted cells were resuspended in medium containing 1% SDS and 5% Na_2EDTA and incubated at 37 °C for 30 minutes. After incubation, the suspension was centrifuged at 1000 g for 10 minutes to extract the paramylon granules. The treatment was repeated, and the extract was washed twice with hot distilled water (70 °C). After washing, the suspension was applied to pre-weighed Whatman glass microfiber filters (GF/C) and dried overnight at 90 °C. The dried filters were weighed to determine the paramylon content. The amount of paramylon per mg dry weight was calculated for all sample types. The dry weight was determined gravimetrically.

3.18. Statistical analyses

Origin Pro 8 program was used for statistical analyses. All measurements were performed with at least 3 independent biological experiments. Data are presented as mean ± standard error (SE). Significance levels were tested using the one-way method ANOVA at $p < 0.05$. Multiple comparisons of means to determine trends and distribution patterns of the data were performed using the Tukey post-hoc test.

4. Results and discussion

4.1. Effect of salt stress on membrane organization of *C. reinhardtii*

4.1.1. Effect on growth rate and chlorophyll content

In *C. reinhardtii* cells, salt stress had a direct effect on the growth rate. *C. reinhardtii* cells subjected to severe salt stress have a lower growth rate compared to control cells. Untreated (control) cells reached an optical density (OD) of 1 at 750 nm in four days, while it took five days for the 150 mM NaCl treated cells (Subramanyam *et al.*, 2010). We observed a great reduction of Chl content with increasing salt concentration in WT, *stt7* and *pgrl1*, especially, in the case of 100 and 150 mM NaCl (Figure 9). In case of WT cells, 50 mM NaCl treatment also led to decreased Chl content relative to the control. The effect of moderate salt stress on the Chl content seems more robust in WT than in *stt7* and *pgrl1* mutant cells. However, magnitude of salt effect is similar in case of all the strains based on statistical analysis. This indicated that *C. reinhardtii* is sensitive to salt stress in agreement with the previous observations (Subramanyam *et al.*, 2010; Neelam and Subramanyam, 2013). Similar results were reported in other algae e.g. *Chlorella vulgaris* when treated with higher salt (0.3-0.4 M NaCl) concentrations (Hiremath and Mathad, 2010). Earlier studies indicated that culture with high salt levels had lower chlorophyll content in *Spirulina platensis* (Vonshak *et al.*, 1996). The decrease in chlorophyll content to higher salinities was correlated to reduced photosynthesis because of osmotic and ionic stress (Moradi and Ismail, 2007). Chlorophyll was also reported to be the primary target for salt toxicity that limits net assimilation rate reducing photosynthesis and growth (Kumar Rai, 1990; Rai and Abraham, 1993). Conversely, Chl levels have been reported to increase in order to increase the photosynthetic activity under salt stress in *Dunaliella salina*, which tolerates NaCl in contrast to freshwater algal species (Talebi *et al.*, 2013) . This is coherent with another study on *Dunaliella salina* where Chl *a*/*b* ratio increased slightly as the salt concentration increased (3 M NaCl) (Mishra *et al.*, 2008). However, increased photosynthetic activity of salt-tolerant strains at moderately higher salinities is probably a regulatory response, as these strains often need to deal with fluctuating saline levels. Therefore, it can be understood that the effect of salt stress varies with algal species, which indicates the varying mechanisms of algae acclimatizing to the salt stress. However, in case of *C. reinhardtii*, it has been suggested that loss of chlorophyll due to salt stress caused the reduction in LHCII protein content and thereby impairment of energy transfer from LHCII to PSII core (Neelam and Subramanyam, 2013). Moreover, it has also been suggested the salt-induced damage on the photosynthetic

activity of the cells is due to the oxidative stress (Subramanyam *et al.*, 2010; Liu *et al.*, 2012). Hence, our observations of decreased Chl content can suggest the possible effect of salinity on the photosynthetic activity of the cells.

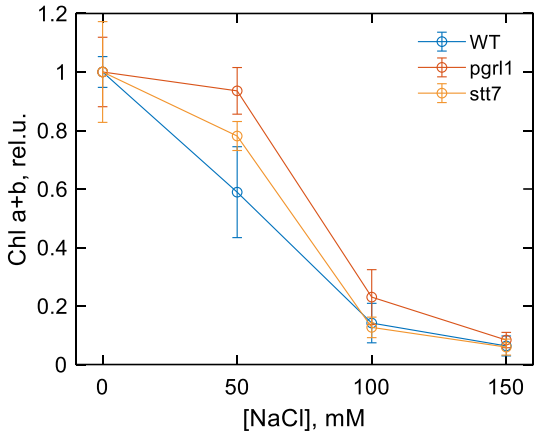

Figure 9. Changes in total Chl content (calculated in µg/mL) of *C. reinhardtii* wild type (WT) and *pgrl1* and *stt7* mutant cells grown under different concentrations of salt (50, 100 and 150 mM NaCl), relative to the control (0 mM NaCl) (Devadasu *et al*. in preparation).

4.1.2. Ultrastructural changes upon salt stress

TEM can be used to study the ultrastructure of photosynthetic membranes; in particular, the arrangement of stacks of grana thylakoids.

Transmission electron micrographs of *C. reinhardtii* cells showed that the typical stacked granal thylakoid membrane ultrastructure was retained in salt-grown cells (100 mM NaCl). However, grana margins change significantly in the cells grown in 100 mM NaCl compared to the untreated ones (Figure 10). We observed thickening or swelling of the grana thylakoids in the cells exposed to salt stress. We found that in the WT strain of *C. reinhardtii*, the RDs between thylakoid membrane layers increased by approximately 2 nm in cells treated with 100 mM NaCl (Table 4). Similar results were observed in *A. thaliana* under state transition conditions (light-induced), where the connection of grana to stroma was altered and the grana stacks were loosened due to phosphorylation of LHCII (Chuartzman *et al.*, 2008). Therefore, our results can suggest that the salt stress may induce phosphorylation of LHCII and as a consequence the grana margins are loosened. Correspondingly, the changes in the repeat distance of the thylakoid membranes in the cells of the *stt7* mutant upon salt stress are very slight. This clearly implies the role of state transitions in the thylakoid membrane reorganization of the cells subjected to salt stress. Thus, it can be interpreted that phosphorylated LHCII (P-LHCII) could induce a change in the connections between the grana stacks causing them to destabilize in case of 100 mM NaCl treated WT cells. This is in

agreement with the previous reports showing that thylakoid stacking is loosened in state-2 compared to state-1 in *C. reinhardtii* (Iwai *et al.*, 2008).

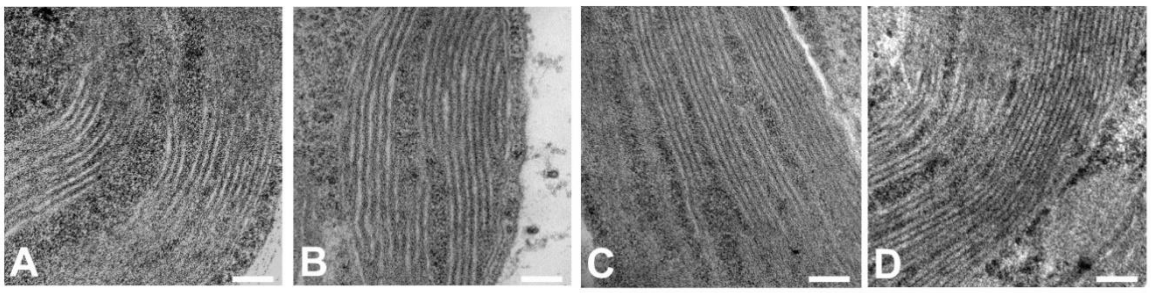

Figure 10. Transmission electron micrograph images of *C. reinhardtii* strains: (A) control wild type (WT) cells, (B) WT cells grown in 100 mM NaCl containing media, (C) control *stt7* cells, (D) *stt7* cells grown in 100 mM NaCl containing media. Bar: 0.1 μm or 100 nm (Devadasu *et al*. in preparation).

Table 4. Thylakoid repeat distances (nm) of control and salt (100 mM NaCl) grown cells of wild type and *stt7* cells measured on transmission electron micrographs.

Repeat distance (nm)			
WT control	**WT salt**	***stt7* control**	***stt7* salt**
21.885 ± 0.33	23.7 ± 0.59	20.375 ± 0.31	20.725 ± 0.42

4.1.3. Structural changes in the macroorganization of pigment-protein complexes

Decrease in the Chl content of the cells might indicate alterations in the photosynthetic apparatus under salt stress. Therefore, CD spectroscopy was used to observe changes in the macro-organization of thylakoid membranes after salt treatment. In *C. reinhardtii*, the bands with highest intensity in the CD spectra of intact cells (Figure 11), at (+) 510, (−) 676 and (+) 690 nm, referred to as "psi-type" CD, originate from long-range interactions between many chromophores in chirally ordered macrodomains. The major psi-type bands are decreased by 50–70% in all strains, even at moderate salt concentrations (50 mM NaCl), suggesting that salinity induces significant changes in the macroorganization of thylakoid membranes (Figure 11). The magnitude of the salt effect on psi-type CD was approximately the same for *pgrl1* and *stt7* as for WT (Figure 11 A–C). Significance of the changes in psi-type CD bands at different salt concentrations in all the strains is represented in Table 5.

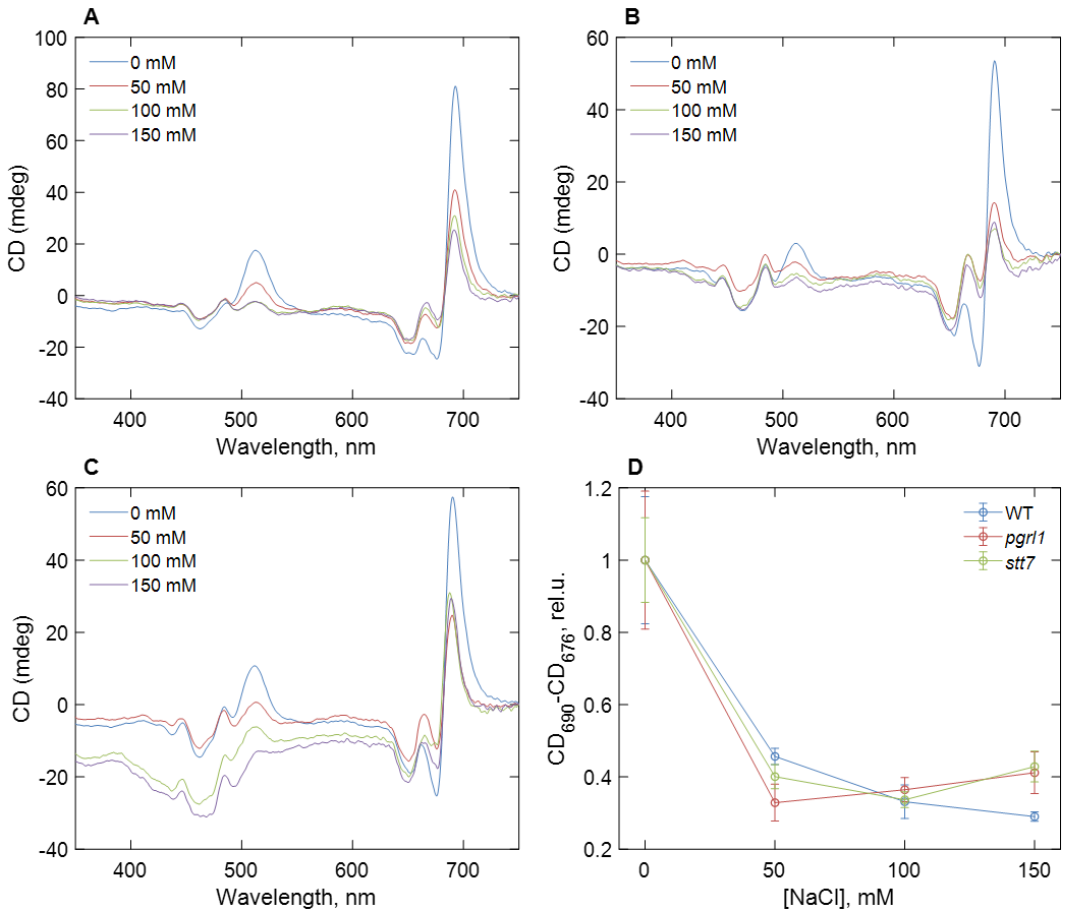

Figure 11. Circular dichroism spectra of (A) wild type (WT), (B) *pgrl1*, and (C) *stt7 C. reinhardtii* cells grown under different salinity concentrations, as indicated, and (D) dependence of the total amplitude of the psi-type CD bands in the red spectral region (CD690-CD676) on the salinity of the growth medium (Devadasu *et al*. in preparation).

Table 5. One-way ANOVA of the dependence of the psi-type CD on salt concentration.

NaCl	WT	*stt7*	*pgrl1*
50 mM		+	
100 mM	+	+	+
150 mM	+	+	

At severe salt stress (150 mM NaCl), changes in psi-type bands were also accompanied by distortions of some excitonic bands in the Soret region (430–490 nm) suggesting changes in the composition or molecular architecture of the pigment-protein complexes. Thus, it can be interpreted that even moderate salt stress had a significant effect on the macro-organization of protein complexes in the thylakoid membranes and severe salt stress has also resulted in changes in the composition of the pigment-protein complexes. As a part of acclimation responses to the changing environmental conditions, photosynthetic supercomplexes undergo supramolecular reorganizations like state transitions and non-

photochemical quenching (Minagawa, 2013). Phosphorylation of LHCII can disrupt protein packing, particularly with the ordered arrangement of PSII-LHCII supercomplexes in the membrane (Boekema *et al.*, 2000; Allen and Forsberg, 2001), and interrupt the close packing of grana stacks – both these phenomena are sensed by the psi-type CD (Garab and van Amerongen, 2009). Our results suggested that the observed changes in psi-type CD might be due to the salt-induced phosphorylation of the LHCII in WT and *pgrl1* cells. However, the observed decrease in psi-type CD signal in *stt7* mutant appears to be a direct effect of NaCl treatment, regardless of LHCII phosphorylation.

4.1.4. 77 K fluorescence spectroscopy

To evaluate the distribution of excitation energy and changes in the absorption cross-section of the two photosystems during salt stress, fluorescence emission spectra were recorded at 77 K in the case of *C. reinhardtii* cells (WT, *stt7*, and *pgrl1*) grown at different salt concentrations (0, 50, 100, 150 mM NaCl) (Figure 12).

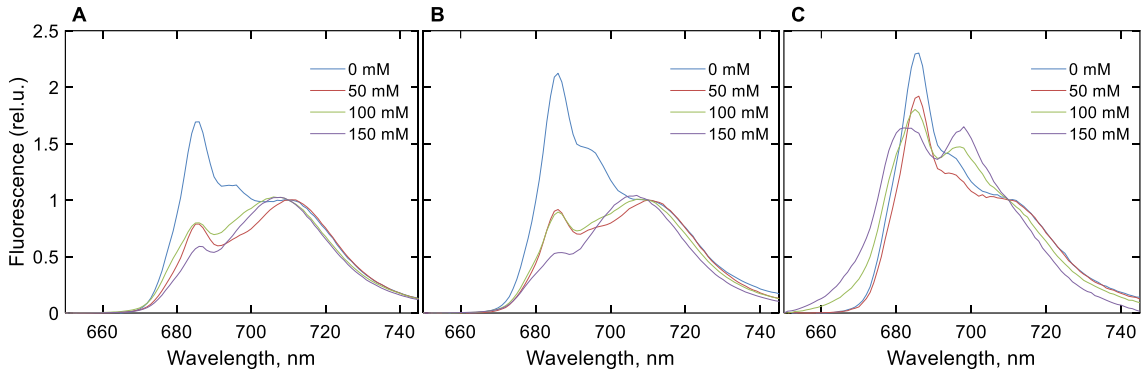

Figure 12. 77 K fluorescence emission spectra of (**A**) wild type, (**B**) *pgrl1*, and (**C**) *stt7* strains of *C. reinhardtii* cells grown in media containing different concentrations of NaCl as indicated. The spectra are averages from at least three measurements on different batches and are normalized at 710 nm (Devadasu *et al.* in preparation).

The averaged spectra normalized to their intensity at 710 nm are shown in Figure 12. The emission bands at 685 nm and 694 nm arise from the PSII reaction centre (RC) and PSII core antenna (CP43 and CP47), respectively, while the band at 715 nm comes from PSI (Murata *et al.*, 1966). In all *C. reinhardtii* strains grown in high-salinity media, we observed a significant reduction in the relative intensity of PSII emission bands. Similar observations were reported in the 77 K spectra of the thylakoids of salt stressed *C. reinhardtii* cells (Neelam and Subramanyam, 2013). Moreover, our results revealed that the spectra at 100 mM NaCl or more showed an obvious blue shift of the far-red maximum, which could be attributed to a relative decrease of the PSI emission band and the appearance of an additional band around 700 nm. The latter could be interpreted as originating from aggregated LHCII trimers (Andreeva *et al.*,

2003; Kirchhoff *et al.*, 2003). In parallel, a shoulder in the 670–680 nm range indicated the presence of uncoupled LHCs and, in some cases, increased emission below 670 nm signified the presence of Chls that were not bound to the protein complexes. These effects were more evident in *stt7* cells grown under 150 mM NaCl conditions (Figure 12).

The relative areas of the fluorescence components associated with PSII (F685 + F694) and with PSI and aggregates (F700 + F710) are plotted in Figures 13 A and B, respectively, as means and standard errors from independent experiments. Figure 13 also shows the ratios of fluorescence intensity F676/F686, reflecting the set of free LHCs (Figure 13 C), and F700/F710, reflecting aggregated LHCs (Figure 13 D).

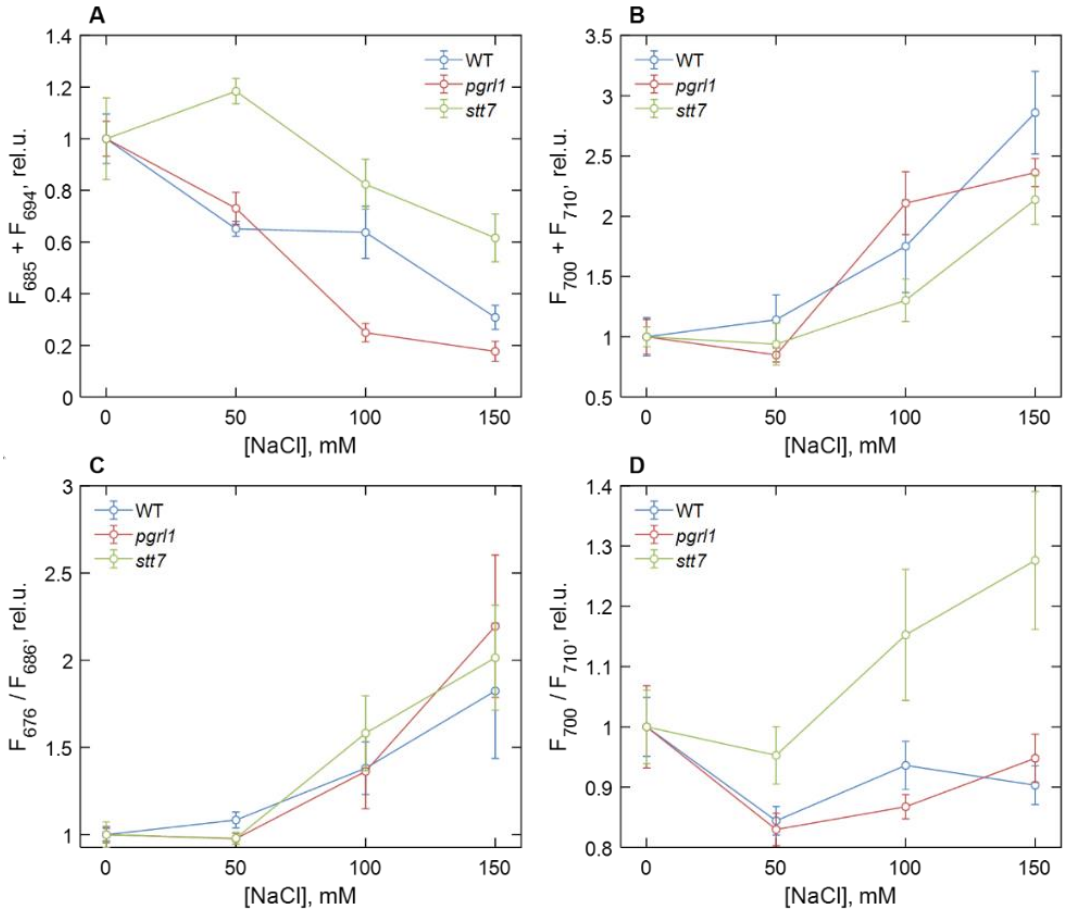

Figure 13. Dependence of different 77 K fluorescence emission parameters of wild type (WT), *pgrl1* and *stt7* cells on the NaCl concentration of growth medium, relative to the salt-free control group. (A) Sum of F685 and F694; (B) sum of F700 and F710; (C) F676 relative to F686; (D) F700 relative to F710. The values are calculated from the areas of the corresponding Gaussian components normalized to the total area under the fluorescence curves (except for F676, which is normalized to F685) and plotted relative to the corresponding value in the control. Symbols and bars indicate mean and standard error, n = 3–6. Closed symbols represent statistically significant differences ($p < 0.05$) with the respective control (0 mM), based on multiple comparison ANOVA (Devadasu *et al*. in preparation).

For a quantitative description of the observed spectral changes, the fluorescence spectra were subjected to Gaussian decomposition by nonlinear least-squares fitting. The

spectra of WT cells grown in the control medium were modelled with four Gaussian bands, centered at 678, 685, 694, and 710 nm (Figure 14 A). The additional band peaking at 700 nm, assigned to aggregated LHCII, was present in salt-treated cells (Figure 14 B). Analysis of variance (one-way ANOVA) showed that high salinity significantly affected all four fluorescence parameters (Table 6).

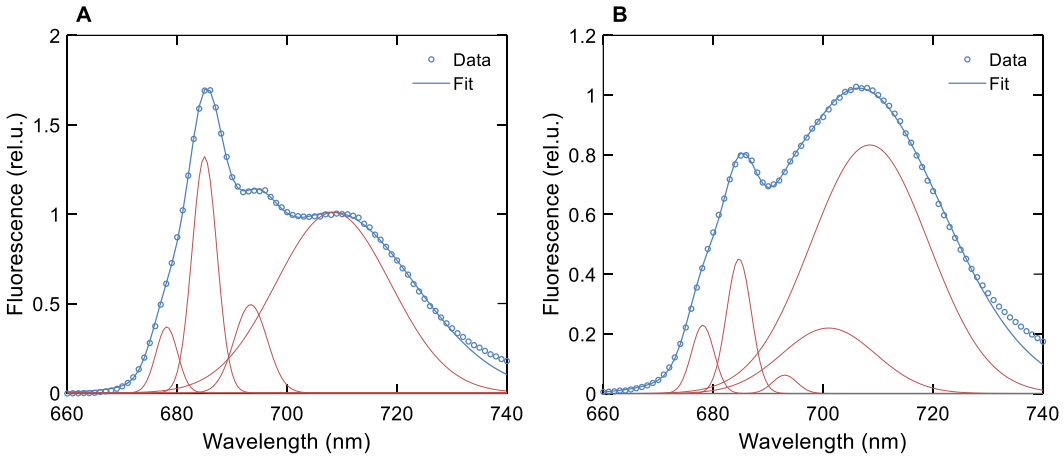

Figure 14. Gaussian-component decomposition of the 77 K fluorescence emission spectra. (A) Control wild type cells and (B) cells grown in a medium containing 100 mM NaCl (Devadasu *et al*. in preparation).

Table 6. One-way ANOVA of the dependence of the fluorescence emission components on salt concentration (given in mM NaCl).

Component	**WT**			***stt7***			***pgrl1***		
	50	100	150	50	100	150	50	100	150
F676			+			+			+
F685 + F694	+	+	+			+	+	+	+
F700			+			+		+	+
F710						+			

In WT cells, the relative PSII emission intensity gradually decreased with increasing salinity, and a significant decrease was observed even at moderate NaCl concentrations (50 mM). Conversely, the relative emission from PSI increased, and emission from uncoupled LHCs appeared under high-salt (≥100 mM NaCl) conditions. The behaviour of *pgrl1* mutant was very similar to that of WT. In the case of *stt7* cells, PSII emission was not reduced to the same extent as in WT or *pgrl1*, but rather showed higher amounts of LHCII aggregates in high-salt media. It has been earlier reported that the stress factors like light and temperature can trigger the activation of STN7 kinase in *A. thaliana* (Nellaepalli *et al.*, 2011; Nellaepalli *et al.*, 2012; Ghysels *et al.*, 2013). Previously, state transitions were considered as a short-

term response to balance the energy between photosystems, PSII and PSI (Minagawa, 2011). Several reports have described that the PQ pool decreases for a short time at low light exposure for short duration (Finazzi, 2005; Ebenhöh *et al.*, 2014; Erickson *et al.*, 2015; Minagawa and Tokutsu, 2015; Cariti *et al.*, 2020), LHCII is phosphorylated in *C. reinhardtii* by the enzyme Stt7 kinase. Moreover, the P-LHCII migrates to PSI and forms PSI-LHCI-LHCII complexes. It was shown that the energy transfer kinetics has been interrupted due to salt stress in cyanobacteria (Schubert and Hagemann, 1990; Schubert *et al.*, 1993; Lu *et al.*, 1999; Lu and Vonshak, 2002). Therefore, based on the earlier reports, it has been understood that salt stress could result in an alteration in the energy transfer kinetics of the photosynthetic organisms. From our observations, it appears that NaCl triggers LHCII phosphorylation in the cells of *C. reinhardtii* grown at high salt concentration. Thus, it can be interpreted that the phosphorylation of LHCII could be involved in reorganization of supercomplexes to protect against salt stress. Moreover, the results suggest that (1) LHCII phosphorylation was the main cause of the reduced PSII antenna size under salt stress, and (2) the phosphorylation-induced changes had a photoprotective effect.

4.1.5. Time-resolved fluorescence emission spectroscopy

Time-resolved fluorescence spectroscopy measures the decay of fluorescence intensity over time after a short excitation pulse. It has an advantage over the steady state fluorescence in that it is an absolute measurement of the fluorescence lifetime, independent on fluorophore concentration and instrumental factors, whereas steady state fluorescence is always a relative measurement. It can reveal quenching mechanisms, excitation energy transfer kinetics (Lakowicz, 1999).

Fluorescence decays of dark-adapted WT and stt7 cell suspensions were recorded with picosecond time resolution at emission wavelengths from 670 nm to 740 nm. The fluorescence decay kinetics can be described with several lifetimes – 60 ps, mainly associated with PSI, and 0.2–1 ns which can be attributed to PSII (Figure 15). The longest lifetime component (1.5–2 ns) reflects a small number of closed PSII RCs (Unlu et al., 2014). The PSII decay lifetimes in salt-grown cells were compared to the control and a decay component with a lifetime of 3–4 ns can be associated with the presence of energetically uncoupled pigments – in agreement with the emission spectra at 77 K. As a result of these changes, the average fluorescence lifetimes increased in the salt-treated cells (Figure 16), indicating a decreased photochemical quantum yield of PSII. Based on this parameter, the *stt7* mutant also appeared to be more sensitive to high salt than WT.

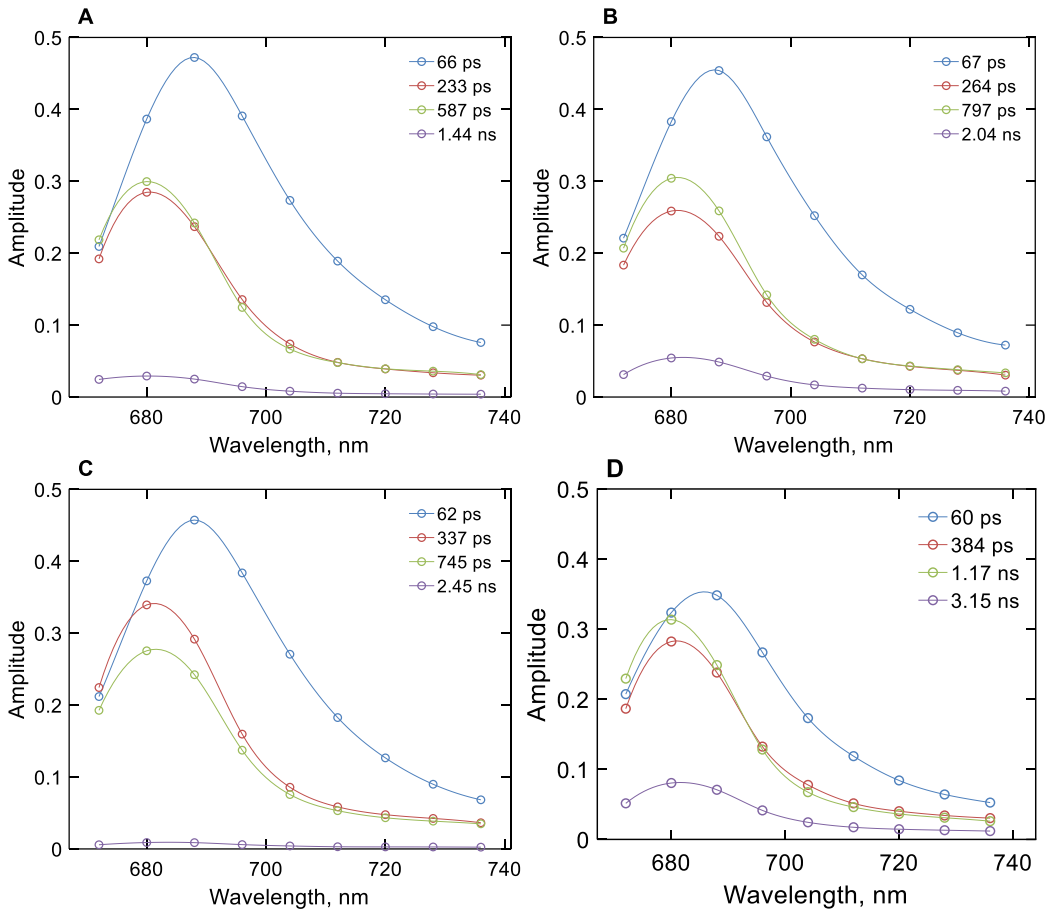

Figure 15. Decay-associated spectra of (A), (B) wild-type and (C), (D) *stt7* cells of *C. reinhardtii*, under (A), (C) control condition and (B), (D) 100 mM NaCl treatment (Devadasu *et al*. in preparation).

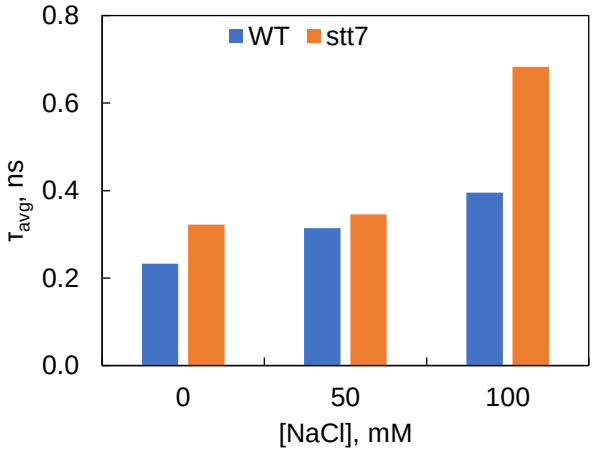

Figure 16. Average fluorescence decay lifetimes at 680 nm determined from the fluorescence kinetics of *C. reinhardtii* WT and *stt7* cells grown in media of different salinity (Devadasu *et al*. in preparation).

In reminiscence of light-induced state transitions, the fluorescence emission spectra of salt-treated *C. reinhardtii* cells showed pronounced decrease in PSII emission in favour of PSI emission even at moderate NaCl concentrations (50 mM). This effect was not observed in the *stt7* mutant unable to phosphorylate LHCII. However, in high-salt conditions, the

emission spectra indicated the formation of LHCII aggregates in salt-stressed cells (Figure 14). Moreover, the increased intensity at 678 nm in the emission spectra at low temperatures and the appearance of long (nanoseconds) decay components in the fluorescence decay at high salinity likely originate from a small fraction of energetically detached LHCs. We observed increase in the relative amplitudes and fluorescence intensities of fluorescence lifetime component of free LHCs in Figure 17. These results further provide evidence that even moderate salt treatment (50 mM NaCl) causes the separation of LHCs thus reducing the photochemical efficiency. Uncoupling of LHCs occurs also in the absence of phosphorylation (in the *stt7* mutant) – even more so than in WT at high salt concentration. The more severe salt induced effects on the fluorescence kinetics and 77 K emission spectra (Figure 15 and 12) hint that LHCII phosphorylation in this case is an acclimatory stress response stabilizing the photosynthetic apparatus.

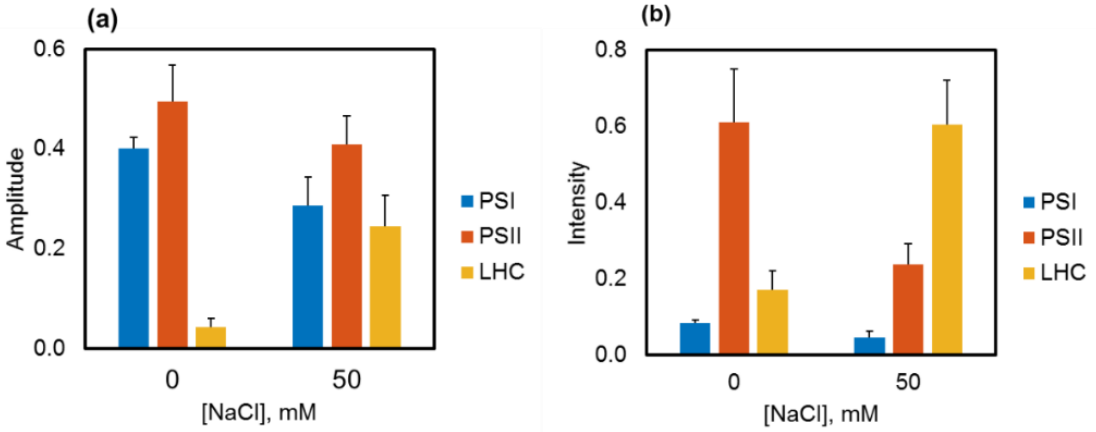

Figure 17. (A) Relative amplitudes and (B) relative fluorescence intensities (amplitude * lifetime) of the fluorescence lifetime components associated with PSI (60-70 ps lifetime), PSII (200-700 ps lifetimes) and free LHC (lifetimes > 1 ns). The values are average from 4 independent experiments; error bars show standard errors (Devadasu *et al*. in preparation).

4.2. Salt stress acclimation of *E. gracilis*

4.2.1. Effect on growth rate and chlorophyll content

E. gracilis is known to tolerate variations of different abiotic factors, such as pH, temperature, oxygen concentration, and salinity (Richter et al., 2003). To evaluate the effects of salt stress on the *E. gracilis* growth, optical density and Chl content of *E. gracilis* batch culture were followed. First, the time course of the salt stress-induced changes in growth rate and total Chl content of *E. gracilis* cells was determined spectrophotometrically. Optical density values at 750 nm of the salt-treated cells compared with the control showed a reduction in growth rate as shown in Figure 18 A (Kanna *et al.*, 2021). We observed a decrease in the total Chl content with increasing salt concentration as shown in Figure 18 B (Kanna *et al.*, 2021).

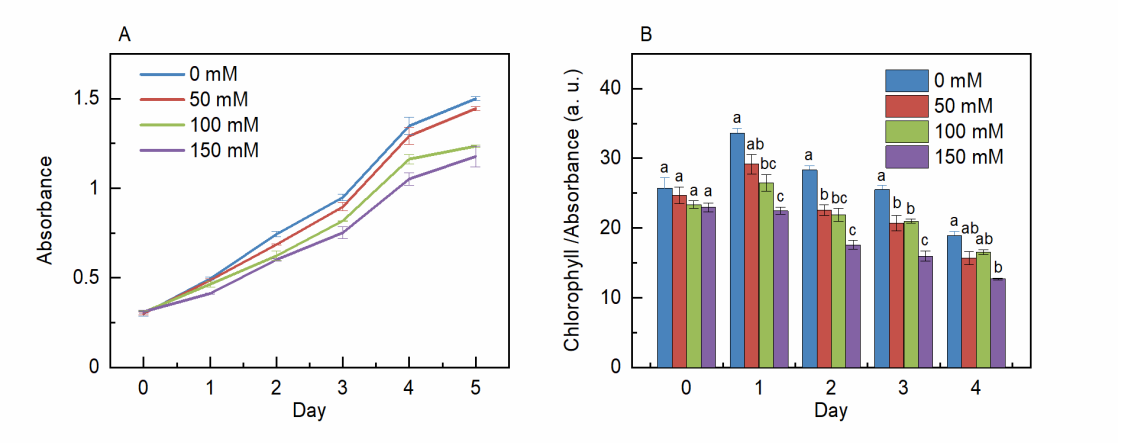

Figure 18. Effect of salt on the growth rate and Chl content of *E. gracilis* cells subjected to 50 mM, 100 mM and 150 mM NaCl salt treatments monitored over a time period of five days. (A) Representative growth curves; (B) Chlorophyll content normalized to the optical density. The data represent mean ± SE of 3 independent experimental batches. Different letters on the bars indicate significant differences compared to control (ANOVA with Tukey test). a = $p < 0.05$; b = $p < 0.01$ (Kanna *et al.*, 2021).

These results are consistent with previous observations on salt-treated cells of *E. gracilis* and *C. reinhardtii* (González-Moreno *et al.*, 1997; Subramanyam *et al.*, 2010; Neelam and Subramanyam, 2013). Our results, hinderance of growth and reduction of the Chl content in the meantime are in line with observations made in plant and other algal cultures under salt stress (Zakery-Asl *et al.*, 2014; Forieri *et al.*, 2016; Ji *et al.*, 2018). It has been suggested that salt stress can lead to delayed transitions between the different growth stages of *Scenedesmus obliquus* (El-Katony and El-Adl, 2020). All the cultures reached stationary phase within fifth day, although we observed a slower growth rate in the salt-treated *E. gracilis* cells. Previous reports showed that salt stress could increase oxidative stress, leading to degradation of Chls in *Scenedesmus* species (El-Katony and El-Adl, 2020;

Elloumi *et al.,* 2020). It has also been suggested that Chl degradation is due to enhanced enzymatic activity induced by the salt stress in *Scendesmus obliquus* (Ji *et al.,* 2018). Interestingly, it has been previously reported that *E. gracilis* cells exhibit enhanced Chl accumulation and reduced photosynthetic efficiency, when grown in an acidic organotrophic medium containing glutamate and malate as carbon sources supplemented with 200 mM NaCl (González-Moreno *et al.,* 1997). It should be noted that, when 100 mM NaCl was applied alone as a stress factor the Chl content was reduced. This might suggest that the adaptation of mixotrophic *E. gracilis* cells to moderate salt stress depends on the pre-treatment of the cells and the composition of the culture media. Moreover, in addition to photosynthesis, salt stress could also affect aerobic respiration and thus cell growth, since biomass accumulation depends on the balance between photosynthesis and respiration (Jacoby *et al.*, 2011). Photosynthetic performance also depends on the function of RuBisCO, which can switch between releasing or absorbing CO_2 (Wingler *et al.*, 2000). Salt stress can also affect the activity of RuBisCO, thus influencing biomass production (Wingler *et al.*, 2000; He *et al.,* 2014). Further studies are required to determine exactly how salt stress affects respiration or RuBisCO activity in *E. gracilis*.

4.2.2. Morphological and ultrastructural changes

Under stress conditions, *E. gracilis* cells often change morphologically and round cells can be frequently observed (Azizullah *et al.*, 2012; Peng *et al.*, 2015). However, we could not detect round cells even at the highest salt concentration we have applied (150 mM) as it could be seen on the SEM pictures (Figure 19 B). The cells showed no significant change in their shape and external morphology (Figure 19 B). Earlier reports showed that *E. gracilis* is able to tolerate relatively high salt concentration for a couple of days, but NaCl concentrations greater than 10 g/L result in a marked loss of motility and velocity (Richter *et al.*, 2003). Examination of salt stress on detergent pre-treated *E. gracilis* and isolated pellicular structures indicates that the microtubules of the pellicular strips are disrupted above a NaCl concentration of 150 mM, which in turn affect cell movement (Murata and Suzaki, 1998). However, we did not observe any remarkable effect on the cell movement due to moderate salt stress (150 mM NaCl). Our TEM observations showed that cells contained 4–5 disc-shaped chloroplasts located near the periphery of the cells, parallel to the plasma membranes (Figure 19 C). The chloroplasts consisted of elongated lamellae, each formed by 2–4 (rarely 5) closely appressed thylakoids (Figure 19 C). After salt treatment, we observed shrinkage of thylakoid membranes and increased number of paramylon grains (Figure 19 D).

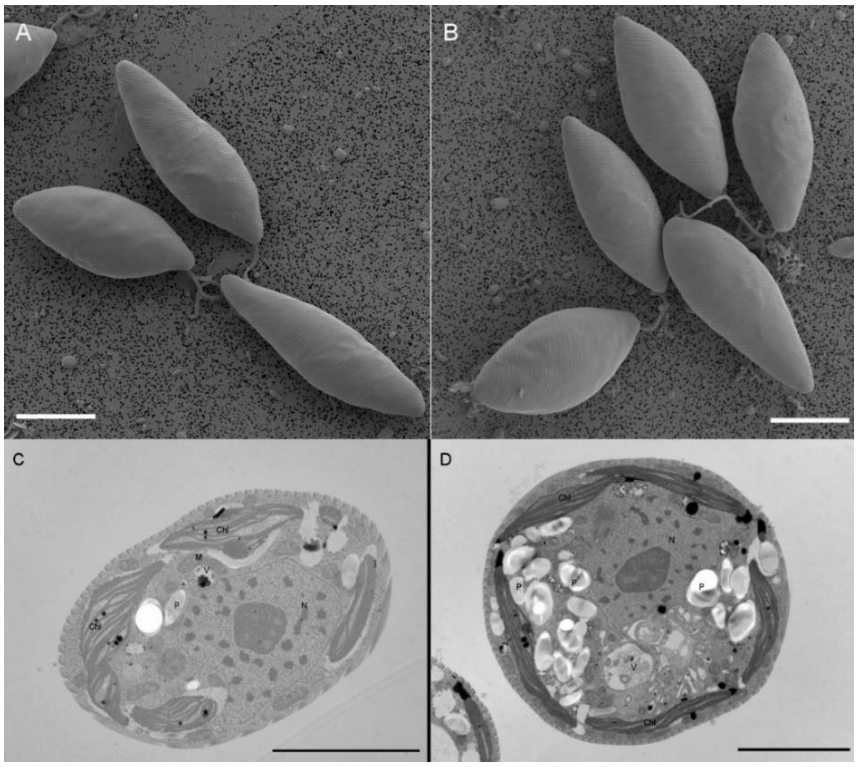

Figure 19. Scanning electron micrographs of (A) control and (B) 150 mM NaCl treated *E. gracilis* cells. Bars 10 µm. Transmission electron micrographs of (C) control and (D) 150 mM NaCl treated *E. gracilis* cells. Bars 5 µm, Chl – chloroplast, P – paramylon, N – nucleus, M – mitochondrion, V- vacuole. Bars: 5 µm (Kanna *et al.*, 2021).

To obtain structural information from photosynthetic organisms under changing conditions, non-destructive techniques have a great potential to study the membrane systems of living cells. SANS is a non-invasive technique which provides statistically and spatially averaged information on the periodic organization of TMs without the need for fixation. In general, SANS can provide valuable information about the structure of mesoscopic systems. SANS measurements illustrate the ability of TM to undergo structural changes that affect its lamellar order and RD (Nagy *et al.*, 2011; Nagy *et al.*, 2013). Under physiologically appropriate conditions, it can be used to detect the rapid and reversible membrane reorganizations on a timescale of minutes and even seconds. The scattering patterns obtained with SANS contain information about the size, shape, and orientation of the scattering particles in the sample. They can provide structural information for length scales between a few angstroms to a few µm. Further, ultrastructural changes induced by salt treatments of the thylakoid membranes of *E. gracilis* cells were studied using SANS. Treatment of cells with increasing concentration of NaCl affected the shape and the position of both characteristic peaks arising from thylakoid membrane of *E. gracilis* cells. The SANS profiles (Figure 20) of the cells show two well defined peaks at around 0.035 and 0.06 $Å^{-1}$; the peak at 0.035 $Å^{-1}$ corresponds to a repeat distance of thylakoid membranes of 179 Å; the peak at higher q value

probably originates from stacked membrane pairs (Nagy *et al.*, 2013). Upon salt treatment, both peaks were shifted towards higher q values (~ 5.5 %) indicating shrinkage of the periodic lamellar order. However, the shrinking effect showed no correlation with the salt concentration – differences between the effects of different salt concentrations appear to be insignificant (Figure 20, Table 7).

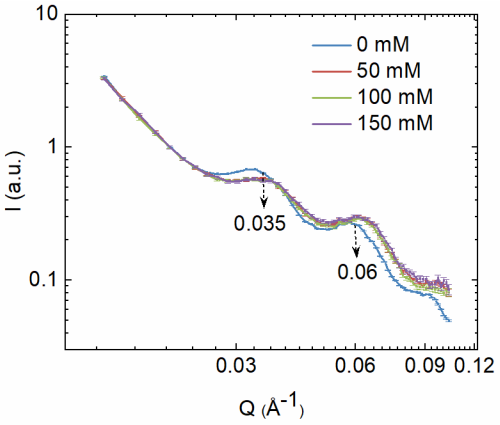

Figure 20. SANS profiles of control and 50 mM, 100 mM and 150 mM NaCl treated *E. gracilis* cells. To facilitate the demonstration of any variation in the intensity of the peaks, scattering curves were normalized to 1 at Q = 0.0204 Å-1, where scattering curves followed well the power law in all investigated samples (Kanna *et al.*, 2021).

Table 7. Calculated repeat distance values for the thylakoid membranes from SANS measurements of different samples. The error calculated from the fitting of the Gaussian peaks is in most of the cases within 2 Å and in all cases within. 2.5 Å.

	Control	**50 mM NaCl**	**100 mM NaCl**	**150 mM NaCl**
RD (Å)	188 187	175 176	181 178	174 175

These data in the real space suggest that the RD of the thylakoid membranes decrease, and the stacked adjacent membrane pairs shrink in a NaCl-concentration dependent manner. Similar changes were observed in diatom *Phaeodactylum tricornutum* (Nagy *et al.*, 2012). RD of thylakoid membranes calculated from electron micrographs showed a decrease in the values of salt-treated cells (18.6 ± 0.2 nm) compared to the control (20.5 ± 0.2 nm); the shrinkage of thylakoid membranes is in good qualitative agreement with the SANS observations (Kanna *et al.*, 2021). Gonzalez-Moreno and co-workers assumed the increased stacking of chloroplasts of *E. gracilis* increases based on the change in the ratio of Chl *a* and *b* (González-Moreno *et al.*, 1997). Now we have evidence of more tightly organised thylakoid system after salt-treatment of *E. gracilis* cells. There was a difference between the RD values of the SANS measurements and those of the TEM images. This difference was also observed

in *Chlorella variabilis* cells treated with Cr (Zsiros *et al.*, 2020). The difference can be explained by the different sample preparation procedures; SANS provided information on the periodic organization of thylakoid membranes obtained *in vivo* without fixation or staining, but in D_2O instead of H_2O (Nagy *et al.*, 2011). The thylakoid membrane systems of photosynthetic organisms are able to respond to rapidly changing environmental conditions (Ünnep *et al.*, 2014b); however, the molecular background of this phenomenon is not well studied in stress acclimation processes. Light induced reversible RD changes have been observed in the study of various photosynthetic organisms (Nagy *et al.*, 2011). It has been suggested that the changes in membrane reorganization observed by SANS can be associated with efficient NPQ (Nagy *et al.*, 2012; Ünnep *et al.*, 2020).

4.2.3. Structural changes in the macroorganization of pigment-protein complexes

The decreased Chl content might indicate changes in the photosynthetic apparatus under salt stress. Therefore, CD spectroscopy was used to observe changes in the macroorganization of thylakoid membranes upon salt treatment. CD spectra recorded from the control and saline-treated cells on different days are shown in Figure 21. The CD spectrum of *E. gracilis* cells differed from that of plant or *C. reinhardtii* thylakoids (Tóth *et al.*, 2016; Lambrev and Akhtar, 2019), this might be related to differences in the composition of light-harvesting antenna and pigments. In the Chl Q_y region (red maximum ~ 696 nm), the spectra showed characteristic psi-type CD signatures, which resemble the thylakoid membranes of higher plants and result from the long-range chiral dipole-dipole interactions of the Chls of PSII and LHCII embedded in the membranes (Lambrev and Akhtar, 2019). However, unlike higher plants, there was no psi-type CD in the blue-green region. The CD in the blue-green region was also slightly different from that in the green alga *C. reinhardtii* (Tóth *et al.*, 2016) but similar to the diatom *Cyclotella meneghiniana* (Ghazaryan *et al.*, 2016). The CD signal in the Soret region contains contributions from short-range, excitonic interactions between Chls and Cars; therefore, different carotenoid compositions may result in different CD signals. The psi-type CD is associated with the presence of grana stacking (Lambrev and Akhtar, 2019) and it disappears when membrane stacking is abolished by removing cations from the medium (Murakami and Packer, 1971). *E. gracilis* cells lack typical granal organization, but still exhibited a psi-type CD signature similar to some other algae, such as diatoms (Szabó *et al.*, 2008). CD spectra of the cells showed detectable changes in the macro-organization of the protein complexes in the thylakoid membranes under salt stress (Figure 21).

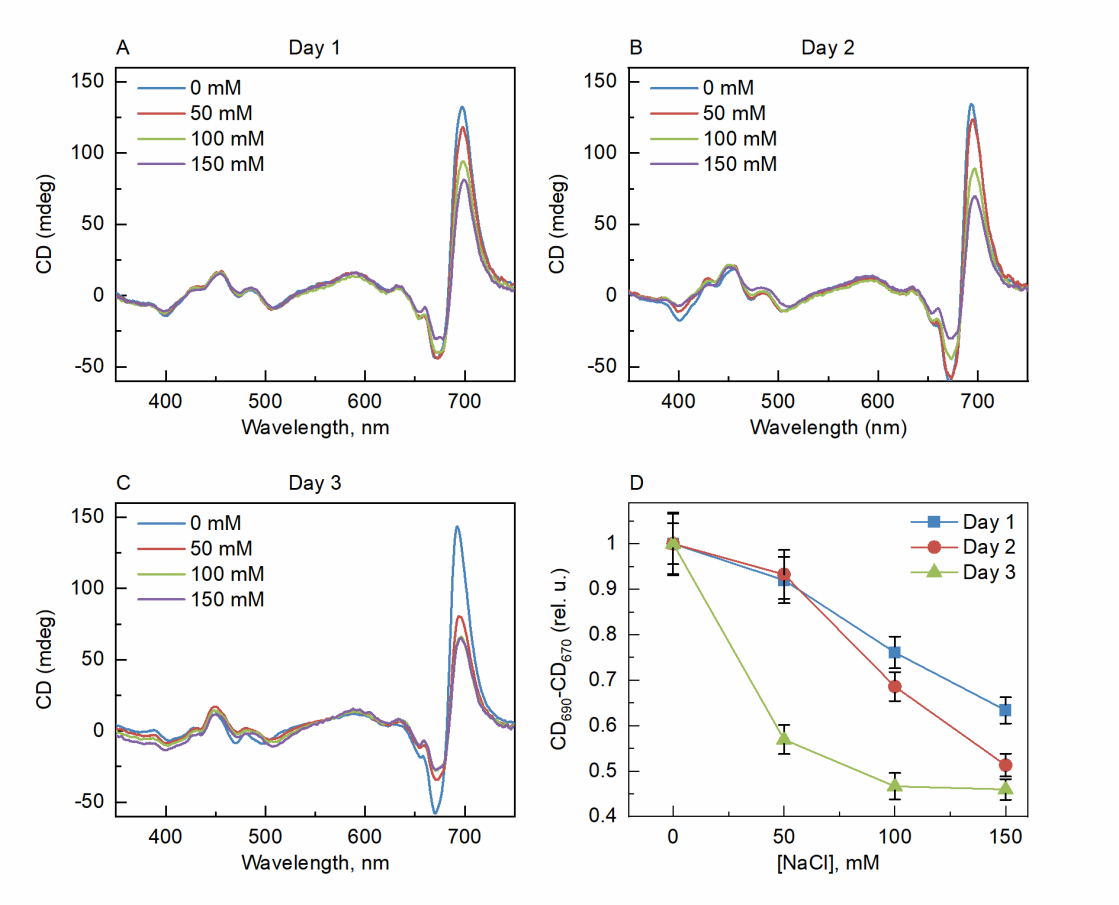

Figure 21. Circular dichroism spectra of *E. gracilis* cells grown in 50 mM, 100 mM and 150 mM NaCl concentrations on (A) day 1, (B) day 2 and (C) day 3, as indicated, and (D) dependence of the total amplitude of the psi-type CD bands in the red spectral region (CD690 – CD670) on the salinity of the growth medium. The spectra are normalized to the red absorption maxima. The data represent mean ± SE of 3 independent experimental batches in panel D, the 3rd day salt-treated data significantly differed from the control (ANOVA with Tukey test, $p < 0.05$) (Kanna *et al.*, 2021).

After salt treatment, the effects were visible only on the main psi-type CD band, on the other hand no significant change was observed in the blue region of the spectrum. The amplitude of the psi-type CD band, which is generally related to grana stacking and its intensity depends on the extent of long-range chiral order, the domain size and the direction of the chiral order (Keller and Bustamante, 1986; Kim *et al.*, 1986), decreased with increased salt concentration. The amplitude of psi-type CD, plotted in the Figure 21 as a function of salt concentration, showed a significant decrease on the third day of treatment. It is well known that chirally organized macrodomains in photosynthetic membranes exhibit structural flexibility that appear to provide photoprotective capability at the supramolecular level (Garab *et al.*, 1988; Barzda *et al.*, 1996; Ünnep *et al.*, 2020). Thylakoids of the diatom *Phaeodactylum tricornutum* have been shown to be arranged in a loosely stacked multilamellar membrane system without strictly distinguishing between granal and stromal regions, yet exhibiting intense psi-type CD signals (Szabó *et al.*, 2008) with sensitivity to

light, temperature, and osmolarity. We observed similar structure in *E. gracilis* cells. The changes in the RD values and in the psi-type CD signals indicate changes in the supramolecular arrangement of the complexes associated with changes in the ultrastructure of membrane. Because the composition of the photosynthetic complexes and membrane organization of the thylakoid membrane of the *E. gracilis* cells differ from higher plants and other well-studied microalgae, more detailed studies of the molecular mechanisms behind the observed changes are needed (Kanna *et al.*, 2021).

4.2.4. 77 K fluorescence emission spectroscopy

The contributions of the two photosystems to the fluorescence can be estimated from emission spectra. Representative fluorescence emission spectra at 77 K of control and salt-treated cells of *E. gracilis* after Chl *a* (436 nm) excitation are shown in the Figure 22. The emission spectra are very similar to previously published data (Doege *et al.*, 2000) on the same species dominated only by emission from PSI – with a peak at 727 nm. The small shoulder at 685 nm indicates negligible fluorescence from PSII. Based on the previous studies, emission spectra of the cells indicate specific antenna composition typically with a visible maximum around 722 nm (Tschiersch *et al.*, 2002). It was shown that this characteristic PSII fluorescence band became visible when the cells were treated with norflurazon which caused reduction in the carotenoid content resulting in the drastic decrease of the amount of common antenna (Tschiersch *et al.*, 2002). We observed that the emission spectra at 480 nm excitation (with Chl *b* preferentially excited) were similar to the spectra at 436 nm excitation (Figure 23). These emission spectra are very different from those of thylakoid membranes of higher plants (Walters and Horton, 1995) and other green algae (Kramer *et al.*, 1985), where the two photosystems showed different peaks. A major difference in *E. gracilis* from higher plants is that both photosystems use a common antenna system comprised of LHCI and LHCII proteins; and, unlike higher plants, the energy-dependent quenching (qE) in *E. gracilis* is independent of the xanthophyll cycle and the aggregation of LHCII (Doege *et al.*, 2000). Upon salt treatment, no significant changes were observed in the 77 K emission spectra of *E. gracilis* cells suggesting that salt did not induce significant changes in the photosynthetic energy transfer. Contrary to this, remarkable differences were found in the 77 K fluorescence spectra of the salt stressed cells of *Synechocystis* sp. PCC 6803 (Schubert and Hagemann, 1990). This study claimed that the changes suggested alterations in the light reaction in salt adapted cells (Schubert and Hagemann, 1990). It was shown that enhanced Na^+ concentration causes a decrease in energy transfer from PBS to PSII in *Spirulina platensis* (Verma and Mohanty, 2000). It seems that the regulatory mechanism in case of *E. gracilis* is different,

our results indicate that salt stress did not affect the photosynthetic light reactions of the *E. gracilis* cells.

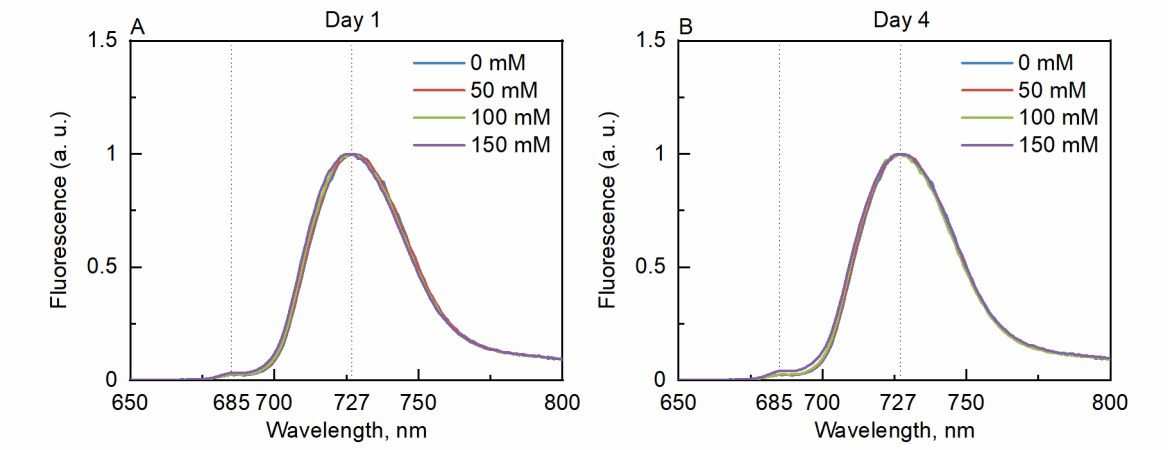

Figure 22. 77 K fluorescence emission spectra of control and 50 mM, 100 mM and 150 mM NaCl treated *E. gracilis* cells with 436 nm excitation measured on (A) day 1 and (B) day 4. The spectra are normalized to their maxima (Kanna *et al.*, 2021).

4.2.5. Assessment of the carotenoid content upon salt treatment

Pigment extracts from control and salt-treated cells were analysed by HPLC to determine the effects of salt on pigment composition. Typical HPLC profiles show peaks for Chl *a*, Chl *b*, β-carotene, Nx, and Ddx. Ddx is found in the antenna of many diatom species (Lavaud *et al.*, 2003), while the antenna of green algae (Goss and Jakob, 2010) and higher plants are known to contain lutein instead (Liu *et al.*, 2004). However, diatoxanthin which is a component of classical Ddx-cycle in diatoms, was not detected in either the control or the salt stressed cells. We observed no change in the relative composition of carotenoids due to salt stress, but each carotenoid increased individually and thus the ratio of total carotenoid content to Chl increased significantly. (Figure 23). Similarly, increase in the content of total carotenoids has been described in *Synechocystis* sp. PCC 6803 (Schubert *et al.*, 1993). Cars in photosynthetic organisms are known to be involved in light harvesting while playing an important role in photoprotective mechanisms and could serve as antioxidants. In addition, carotenoids modulate membrane microviscosity and are involved in the maintaining proper cell architecture (Domonkos *et al.*, 2013). It has been reported that high salinity stress (1.026 M NaCl) led to an increased Car content which was described to decline the photodamage in *Synechococcus* sp. PCC 6803 (Schubert *et al.*, 1993). Thus, it could be inferred that increased content of Cars under salt stress in *E. gracilis* cells could protect the cells from oxidative stress thereby ensuring the function of photosynthetic complexes.

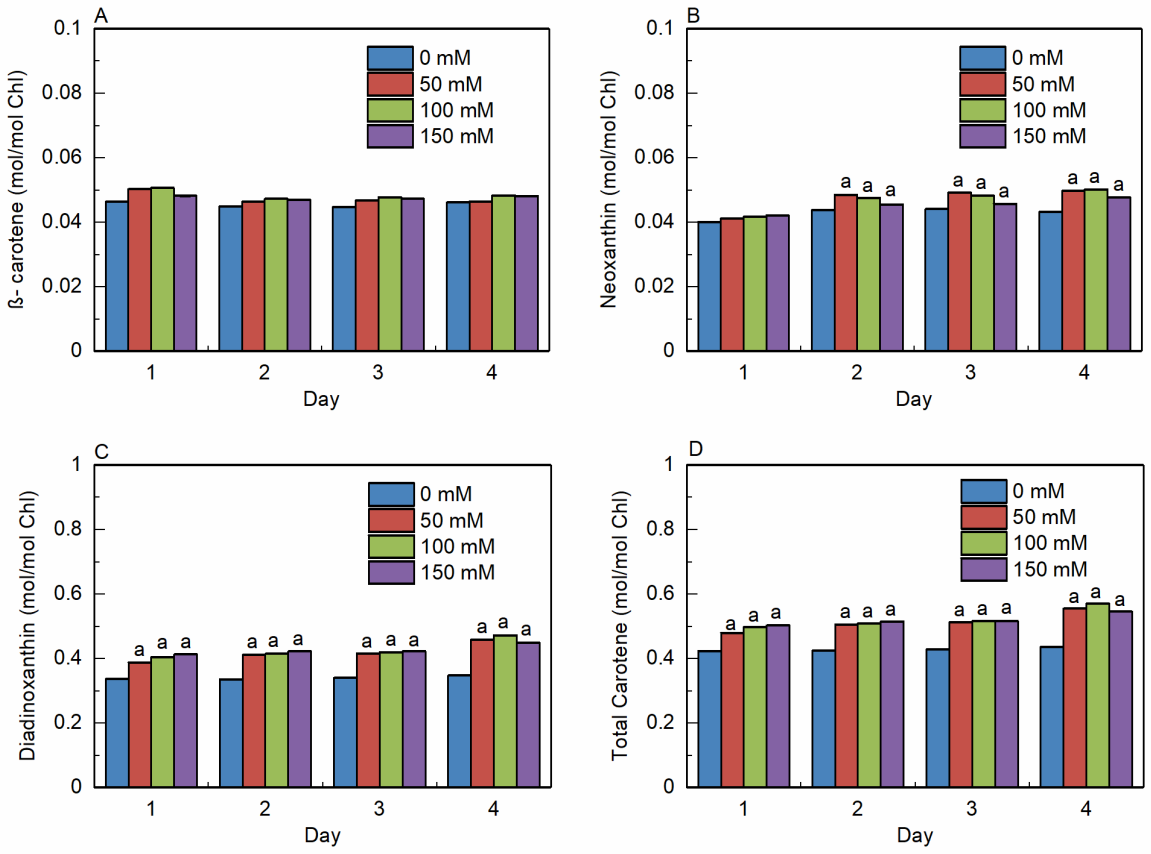

Figure 23. Effect of salt-treatment on the content of photosynthetic pigments in *E. gracilis* cells. Cellular content of (A) β-carotene (B) Neoxanthin (C) Diadinoxanthin and (D) Total carotenoid relative to the total content of chlorophyll in the algal cells subjected to 50 mM, 100 mM and 150 mM NaCl salt treatments for 4 days. The data represent mean ± SE of 3 different batches. Letters indicate significant differences between means relative to control (ANOVA with Tukey test; $p<0.05$) (Kanna *et al.*, 2021).

4.2.6. Chl *a* fluorescence induction kinetics

During the transition from darkness to light, the fluorescence intensity of a photosynthetic sample increases from a low value (F_0 or O) through two intermediate stages (F_j or J and F_i or I) in 200–300 ms to a maximum value (F_m or P) during the application of a saturating light pulse. The different phases of the fluorescence rise (OJ, JI and IP) can be associated with different steps in the reduction of the ETC electron transport chain. OJ parallels the reduction of the acceptor side of PSII ($Q_A + Q_B$); JI parallels the reduction of the PQ pool; and IP parallels the reduction of electron transport acceptors in and around PSI. This means that the OJIP transients provide information about the state of the ETC. OJIP fluorescence curve analysis is routinely used to study the effect of various climatic stresses, that alter the structure, architecture, and function of the photosynthetic apparatus (Strasser *et al.*, 2004).

To evaluate the effects of salt stress on the functionality of the photosynthetic electron transport chain, polyphasic OJIP fluorescence transient was used. The fast Chl *a* fluorescence induction transients, measured by exposing dark-adapted samples to high light, show a complex multistep rise curve, which represents a fingerprint of the species and the physiological status of the cells (Srivastava and Strasser, 1995). The shape of the transient is sensitive to many photosynthetic processes – the flow of excitation energy from the antenna to the reaction centres, the structural plasticity of the reaction centre complexes and electron transfer on the donor and acceptor sides of PSII, the availability and redox state of intersystem electron carriers and downstream electron transfer to PSI. According to the theory of energy flux, any change in any of these processes results in a change in the shape of the induction curve. The fluorescence induction curves recorded from *E. gracilis* cells have an unusual shape, with no clearly visible J and I steps (Figure 24).

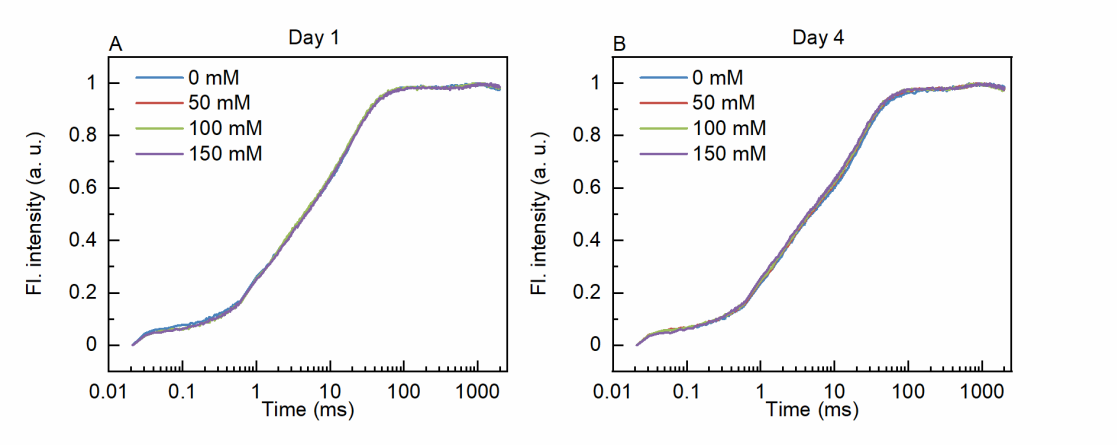

Figure 24. Variable Chl *a* fluorescence induction curves of control and 50 mM, 100 mM and 150 mM NaCl treated; dark-adapted *E. gracilis* cells (20 min) recorded on (A) day 1 and (B) day 4 using 650 nm saturating light (Kanna *et al.*, 2021).

In higher plants (Stirbet *et al.*, 2018) and green alga *C. reinhardtii* (Kodru *et al.*, 2015), after 100 ms, there is fast drop in the transient fluorescence which usually assigned to state transitions, non-photochemical quenching or redox state of P700 (Strasser *et al.*, 2004). The OJIP curve differ in the cases of *E. gracilis* and in higher plants, which may be due to the differences of their antenna systems. In the case of *E. gracilis*, the induction curve remains flat up to 1000 ms. This could very well be explained by the common antenna system of PSI and PSII or the absence of the classical violaxanthin cycle. When comparing the transients for different salt-treatments, no remarkable difference could be observed (Figure 25). Very similar F_v/F_m values – 0.6 were recorded for both salt-treated and control cells, thus the functional state of PSII is not affected by the salt treatment. However, it is known that high

salt stress can lead to the most significant differences in the kinetics of Chl fluorescence in higher plants, *Oryza sativa* (Hu *et al.,* 2012). It has been reported that the donor side of PSII is damaged in response to salt stress in *Triticum aestivum* (Mehta *et al.,* 2010). Earlier reports on OJIP kinetic analysis revealed increase in the number of non-reducing Q_B sites as a result of salt stress in *Spirulina platensis* (Lu *et al.,* 1999; Lu and Vonshak, 2002). Earlier reports showed that *E. gracilis* cells grown in the presence of 200 mM NaCl resulted in significant reduction of F_v/F_m value to 0.49 from 0.71 (González-Moreno *et al.,* 1997). From our results, it can be interpreted that moderate salt stress could not cause any damage to the PSII activity and electron transfer processes in *E. gracilis* cells unlike higher plants.

4.2.7. PSII photochemical efficiency, PSI absorbance changes and quenching analysis

Simultaneous measurements of variable Chl fluorescence and P700 absorbance changes represent a powerful tool to monitor PSI and PSII functions in parallel. P700 provides analogous information on PSI electron transport as Chl fluorescence provides on PSII. Based on a highly innovative pulse-modulation technique, absorbance changes of P700 (reaction centre Chl of PSI) can be measured with a similar signal/noise ratio as Chl fluorescence. Saturation pulses were applied for assessment of energy conversion efficiency in PSI and PSII. Differences between quantum yields, Y(I) and Y(II) and between apparent electron transport rates, ETR(I) and ETR(II), may be related to cyclic electron flow, differences in energy distribution and/or PSI/ PSII ratio. Non-photochemical quenching of chlorophyll fluorescence is an indicator of the extent of non-radiative energy dissipation in LHCII of PSII, which is attributed to prevent over-reduction of the electron transfer chain and thus provide protection against photodamage. NPQ is a measure of heat dissipation and is the sum of photoprotection, state transition quenching and photoinhibition (Muller *et al.*, 2001).

To understand how salt stress affects photosynthesis in *E. gracilis* cells, light curves were also recorded. Photochemical quantum yield of PSI and PSII was measured in both control and salt-treated *E. gracilis* cells on different days (Figure 25). In good agreement with the previous observations that NaCl treatment has no significant effect on the functional state of PSII (F_v/F_m) of the cells, we also found that the activity of PSI was not affected. Similarly, some studies have shown that salt stress had no effect on PSII activity (Robinson *et al.,* 1983; Morales *et al.*, 1992). In higher plants, salt stress is known to inhibit PSII activity (Mishra *et al.*, 1991; Parida *et al.,* 2003). Upon irradiation with high-light intensity, both the control and salt-treated *E. gracilis* cells showed significant induction of non-photochemical quenching

(Table 8). NPQ of 0.4 was observed which is similar to the results published by (González-Moreno *et al.*, 1997). However, the NPQ of the salt treated cells was not significantly different from that of the control cells as shown in Table 8.

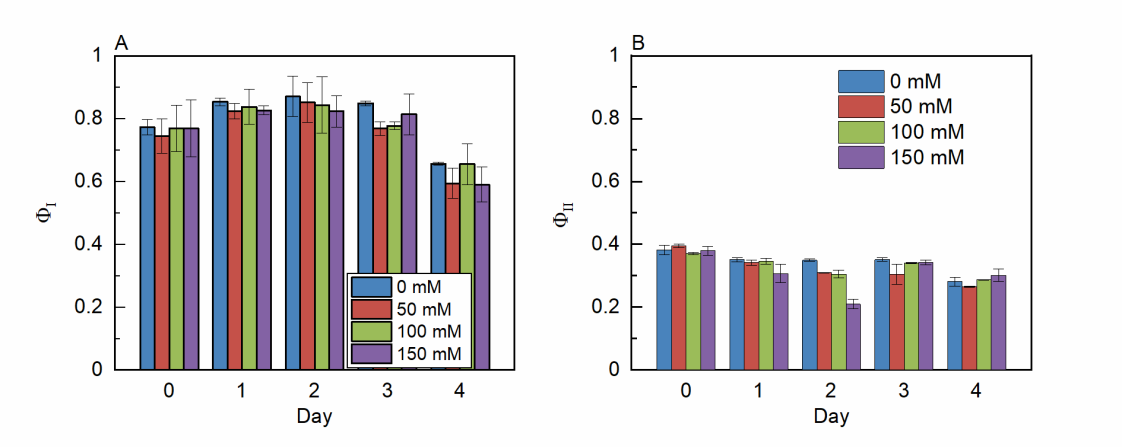

Figure 25. The photosynthetic fluorescence parameters of *E. gracilis* cells subjected to 50 mM, 100 mM and 150 mM NaCl salt treatments for 4 days. (A) PSI yield and (B) PSII yield of the cells subjected to 0 mM (control) 50 mM, 100 mM and 150 mM NaCl salt treatments at 220 µmol photon m^{-2} s^{-1} of the light response curve. Data represent mean ±SE of 3 independent cultures and shows no significant differences in the means (Kanna *et al.*, 2021).

Table 8. Chlorophyll fluorescence parameters of *E. gracilis* cells grown under salt stress. Cells were grown in the presence of the indicated NaCl concentrations. The data represent mean ± SE of 3 different batches of cultures.

Day	NaCl (mM)	F_o	F_m	F_v/F_m	NPQ
1	0	0.031 ± 0.005	0.087 ± 0.007	0.67 ± 0.03	0.43 ± 0.12
	50	0.030 ± 0.003	0.083 ± 0.001	0.67 ± 0.03	0.41 ± 0.14
	100	0.026 ± 0.001	0.079 ± 0.003	0.67 ± 0.02	0.44 ± 0.10
	150	0.028 ± 0.004	0.087 ± 0.005	0.67 ± 0.03	0.48 ± 0.03
4	0	0.027 ± 0.002	0.088 ± 0.007	0.68 ± 0.01	0.50 ± 0.04
	50	0.027 ± 0.004	0.093 ± 0.012	0.69 ± 0.01	0.55 ± 0.10
	100	0.030 ± 0.002	0.096 ± 0.008	0.69 ± 0.01	0.54 ± 0.13
	150	0.030 ± 0.004	0.097 ± 0.011	0.69 ± 0.01	0.51 ± 0.06

Interestingly, it has been described that higher concentration of NaCl (200 mM) induced a significant reduction in the NPQ from 0.41 to 0.02 of *E. gracilis* cells (González-Moreno *et al.*, 1997). Previous reports have described that high salinity (above 27 g/L) can lead to an increase in NPQ in *Nannochloropsis* species (Martínez-Roldán *et al.*, 2014). At higher salt concentrations, the osmotic stress and the toxic ionic stress of salt can reduce the photosynthetic efficiency. The effect on the photosynthetic efficiency is often related to the

damage of PSII through the production of reactive oxygen species. It has been reported that NaCl stress can damage the oxygen evolving complex and the PSII reaction centre, leading to the suppression of the electron transport on the donor and acceptor sides affecting the use of the light energy in *Scenedesmus obliquus* (Ji *et al.*, 2018). However, our observations regarding the functional state of PSII (F_v/F_m), and the activity of PSI, all of which were not affected by the NaCl treatments (Figure 25 and 26, Table 8). Moreover, these results corroborated the OJIP curve measurements which also indicated no effect of salt treatment (Figure 25). It has to be noted that prior to the measurements, the samples were adjusted to the same Chl concentration, but the Chl content in the salt treated cultures was slightly reduced to cell mass, so the results reflect the functionality of the photosynthetic pigment protein complexes, which were not affected by the salt treatment.

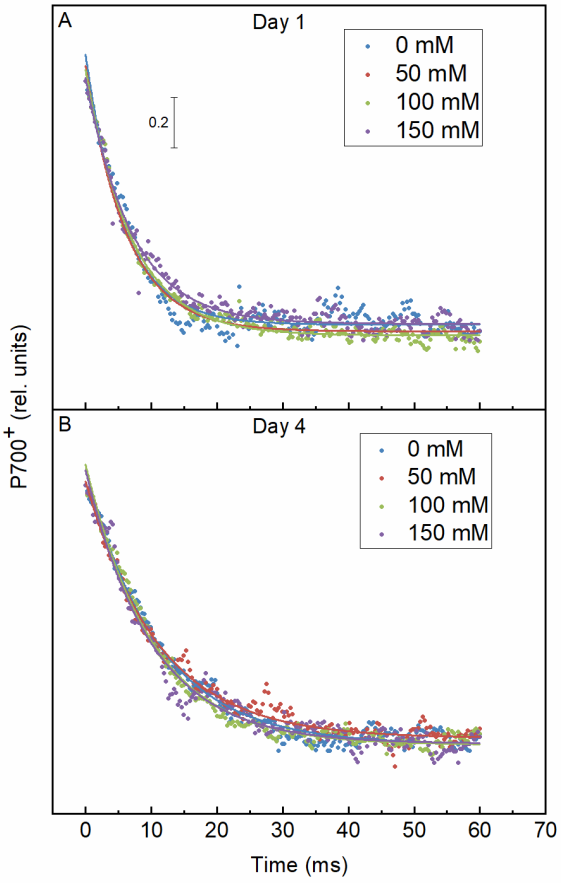

Figure 26. Effect of salt treatment on the re-reduction kinetics of P700. Samples were pre-illuminated for 20 minutes with 530 µmol photon m^{-2} s^{-1} and re-reduction kinetics of P700 were recorded after cessation of light. Measurements were done with *E. gracilis* cells grown in 50 mM, 100 mM and 150 mM NaCl concentrations on (A) day 1 and (B) day 4 (Kanna *et al.*, 2021).

In addition, P700 absorbance changes were monitored in the salt stressed cells. Reduction kinetics of P700 in both control and salt-treated cells are represented in Figure 26. The activity of PSI was monitored by the change in absorbance at 830 nm due to oxidation

of P700. Decay lifetimes of $P700^+$ reduction kinetics of the cells treated with 50 mM, 100 mM and 150 mM NaCl are 11.05 ± 0.238, 10.12 ± 0.177, and 9.997 ± 0.276 respectively, which is similar to the lifetime of control cells, 10.98 ± 0.227 on day 4 of the treatment as shown in Table 9. Salt treatment induced no significant changes in the PSI activity. In contrast to our study, recent reports suggested severe inhibition of the PSI activity upon the Cr treatment of *Chlorella variabilis* cells (Zsiros *et al.*, 2020).

Table 9. Rate of P700 re-reduction. Life-times obtained by fitting the kinetics of absorbance change at 830 nm and the decay of $P700^+$ reduction was calculated by one exponential function from control and salt-treated cells.

$t_{1/2}$ (ms)	0 mM NaCl	50 mM NaCl	100 mM NaCl	150 mM NaCl
Day 1	5.806 ± 0.196	6.247 ± 0.117	6.957 ± 0.116	7.092 ± 0.178
Day 4	10.98 ± 0.227	11.05 ± 0.238	10.12 ± 0.177	± 0.276

Previous reports showed that electron transport activity of PSI increased with increasing salinity in cyanobacteria and algae (Gilmour *et al.*, 1985; Canaani, 1990; Lu *et al.*, 1999). Since we did not observe any significant change in the photosynthetic parameters of salt stressed *E. gracilis* cells, our results indicated that the photosynthetic activity of the cells is maintained under moderate salt stress.

4.2.8. Analysis of photosynthetic pigment-protein complexes using BN-PAGE

Useful information about the composition and interactions of the protein complexes in the thylakoid membrane can be obtained by solubilizing the membrane by treatment with mild detergents and then separating it on a polyacrylamide gel. Blue native polyacrylamide gel electrophoresis (BN-PAGE) is one of the methods used to separate protein complexes in their native and functional forms. In this study, BN-PAGE was used to determine whether salt treatment induced changes in the interactions between protein complexes. The patterns of thylakoid membrane protein complexes, after solubilisation with β-DM and separation by BN-PAGE (Figure 27), showed similarity to that of higher plants (Järvi *et al.*, 2011). No visible changes in the pattern of BN-PAGE were observed when comparing different salt treatments. These results are consistent with the 77 K emission spectral data that indicated no significant effect of salt stress (Figure 22) which further reflect there were no significant changes in the amount of photosynthetic complexes as evidenced by BN-PAGE analyses.

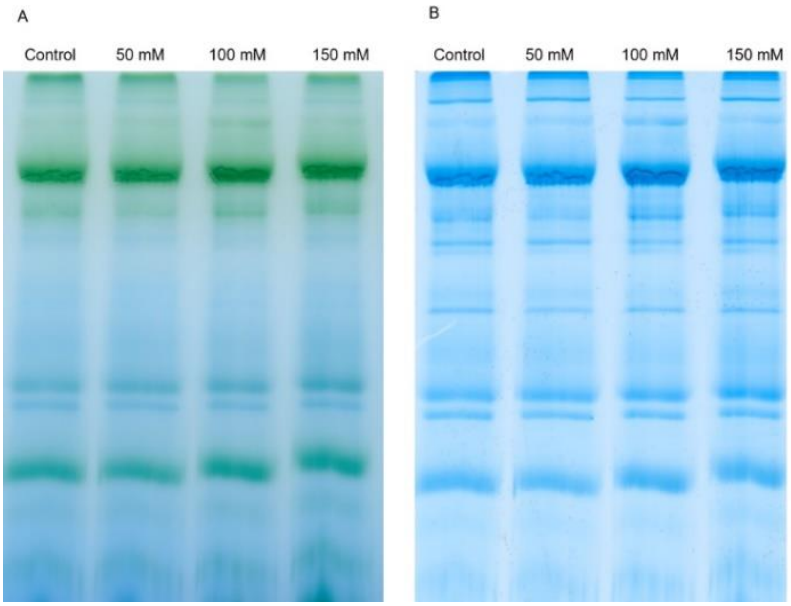

Figure 27. Thylakoid membrane protein complexes in *E. gracilis* separated on a 5-13% BN-PAGE. (A) Blue native pattern of pigment-protein complexes in control and 50 mM, 100 mM and 150 mM NaCl treated cells. (B) The BN gel after Coomassie Brilliant Blue (G-250) staining. The samples loaded onto each gel lane contained 8 mg Chl (Kanna *et al.*, 2021).

4.2.9. Accumulation of paramylon as a stress response

Our ultrastructural analyses indicated the accumulation of paramylon grains in the cytoplasm of salt stressed cells (Figure 19 D). Paramylon was isolated and quantified. The isolated paramylon granules were visualised by SEM (Figure 28). Table 10 shows the changes in paramylon content at the cellular level in the control and the NaCl treated cells of *E. gracilis* after 4 days of treatment. Accumulation of paramylon increased with increasing salt treatment and the highest levels of paramylon was observed in the cells grown in the presence of 150 mM NaCl. The increase was 2.5, 3.5 and 5-fold in cells treated with 50, 100 and 150 mM NaCl respectively.

Figure 28. Scanning electron micrograph of paramylon granules isolated from 150 mM NaCl treated *E. gracilis* cells. Bar 1 µm (Kanna *et al.*, 2021).

Table 10. Effect of salt stress on paramylon accumulation in *E. gracilis*. Cells were cultured in the medium containing different salt concentrations. After 4 days of treatment, cells were harvested, and paramylon content was determined. The experiments were done in triplicate. CDW: cell dry weight. PDW: paramylon dry weight.

NaCl (mM)	PDW/CDW (µg/mg)	Paramylon (%)
0	51.23 ± 6.29	100
50	126.18 ± 20.86	245.46 ± 13.36
100	181.64 ± 20.06	355.02 ± 10.6
150	261.04 ± 20.97	515.04 ± 76.67

In *E. gracilis* cells paramylon serves as a storage form of sugar. Paramylon is a β-1,3-glucan, that has high biotechnological potential and was considered as functional food (Nakashima *et al.*, 2018; Barsanti and Gualtieri, 2019). Several potential biomedical applications of paramylon, such as immunostimulant and anti-inflammatory agent are currently being studied in detail (Nakashima *et al.*, 2017; Okouchi *et al.*, 2019), and it may serve as feed stock for biofuels, as well (Inui *et al.*, 1982; Zimorski *et al.*, 2017; Khatiwada *et al.*, 2020). Earlier studies showed that the paramylon content decreased upon treatment with 200 mM NaCl most probably because of degradation and conversion to soluble sugars, resulting in trehalose accumulation in the cells (Takenaka *et al.*, 1997). Trehalose accumulation was also increased by KCl, NaCl, sugars and sugar alcohols suggesting that osmolarity of the medium induces paramylon degradation (Takenaka *et al.*, 1997). Porchia *et al.* (1999) observed the trehalose accumulation in the late exponential phase of cells during salt stress. In contrast, we observed an accumulation of paramylon during moderate salt stress. We can assume that this storage sugar can play an important role in the adaptative mechanism enabling a rapid response of the cells to osmotic stress.

4.3. Role of GNAT2 in the organization of the thylakoid membrane of *A. thaliana*

4.3.1. CD fingerprints of leaves and thylakoid membranes

In higher plants, photosynthetic protein complexes occupy 70% surface area of the TM of which LHC complexes constitute half of the protein complexes (Kirchhoff *et al.*, 2002). Hence the rearrangement of LHCII proteins is induced by phosphorylation exerts a direct influence on the structure of TM (Rantala *et al.*, 2020). It is well known that sudden changes in the light intensity can result in state transitions which is primarily related to reversible phosphorylation of LHCII catalysed by STN7 kinase (Bellafiore *et al.*, 2005; Pribil *et al.*, 2010). The *stn7* mutant is defective in state transition due to lack of the phosphorylation of LHCII and interaction between PSI and LHCII (Koskela et al., 2020). Recent study demonstrated that the chloroplast acetyl transferase GNAT2 plays a key role in the regulation of photosynthetic light reactions (Koskela *et al.*, 2018). The *gnat2* mutant is unable to form the PSI-LHCII complex specific to the state transition and balance the excitation energy between the two photosystems although there are no defects in the LHCII phosphorylation (Koskela *et al.*, 2018). CD spectroscopy was used to study the macro-organization of TM of *gnat2* and *stn7* with respect to WT from the intact leaves and isolated TMs. We observed that the main characteristics of CD spectrum of *Arabidopsis* leaves (Figure 29 A) are similar to the CD signature of TMs (Figure 29 B) as already reported (Tóth *et al.*, 2016). CD spectrum of TMs is known to be complex due to the superposition of CD signals with different physical origins. It has been demonstrated that the characteristic psi-type CD bands of *Arabidopsis* at (+)690 nm and (−)674 nm and (+)506 nm come from a long-range chiral order of the protein complexes of PSII and LHCII in the grana (Lambrev and Akhtar, 2019). The additional bands at (-)650 nm in the red, and even below 650 nm at around (+)448, (−)460 and (+)484 nm in the Soret region originate short-range excitonic interactions. The intensity of red positive psi-type CD band i.e., (+)690 nm band of WT leaves was significantly higher than in the *gnat2* and *stn7* leaves (Figure 29 A), which holds true in case of the isolated TMs as well (Figure 29 B). These data might indicate detachment of some of LHCIIs from PSII (Kovács *et al.*, 2006; Kiss *et al.*, 2008; Lambrev and Akhtar, 2019). We observed no significant difference in the intensity of (−)674 nm band of WT leaves when compared to the mutant leaves (Figure 29 C). However, the amplitude of the (−)674 nm band in the WT TMs appeared to be higher than that of the mutants, *stn7* and *gnat2* (Figure 29 D). CD spectra of both the leaves and TMs showed the presence of (+)506 nm band, which is generally assigned to β-carotene bound to the PSII core complexes (Tóth *et al.*, 2016). Our results showed that the amplitude

of (+)506 nm band, in case of leaves is similar in all the strains (Figure 29 C). However, it should be noted that the amplitude of the (+)506 nm band is significantly higher in the WT compared to the *gnat2* and *stn7* mutants in the case of TMs (Figure 29 D) (Rantala *et al.*, 2022).

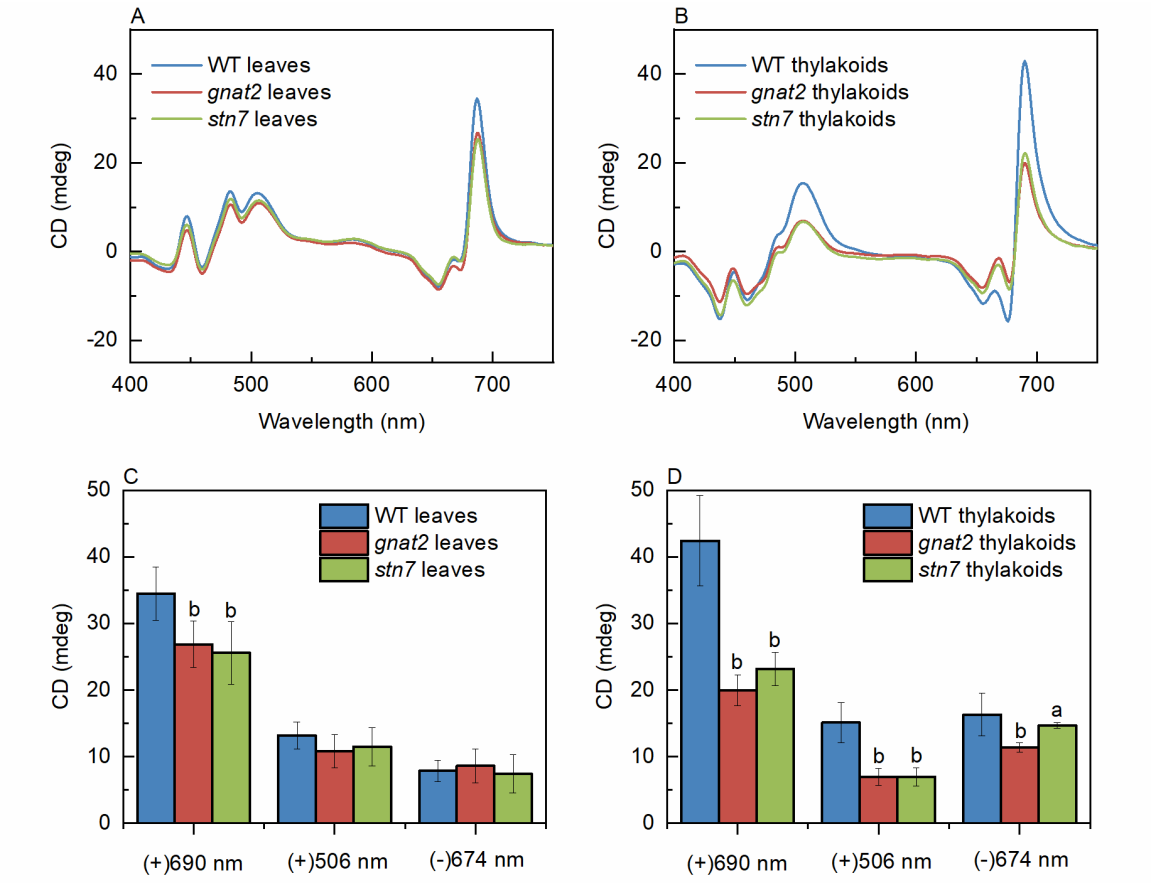

Figure 29. Circular dichroism spectra and amplitudes of the main psi –type CD bands, (+)690 nm, (-)674 nm and (+)506 nm, of *Arabidopsis thaliana* WT and *gnat2* and *stn7* mutant leaves (A, C) and isolated thylakoid membranes (B, D). The spectra were normalized to the red absorption maxima and represent the averages obtained from n ≥ 7 independent samples. Amplitudes of the psi-type CD bands were determined with a reference wavelength at 750 nm; the data represent mean ± SE of 7 biological replicates (one-way ANOVA with TUKEY test). Different letters on the bars indicate significant differences compared to control (ANOVA with Tukey test). a = $p < 0.05$; b = $p < 0.01$ (Rantala *et al.*, 2022).

All these changes can be related to changes in the structure of LHCII and PSII-LHCII supercomplex, as it was previously shown that decreased stability of PSII-LHCII complex, or changes in the LHCII composition and decrease of LHCII trimers, can induce diminishment of the psi-type CD bands (Tóth *et al.*, 2016). Previously published data on the ultrastructure of TM of *A. thaliana* suggested that the grana membranes of *gnat2* mutant are tightly stacked when compared to the WT (Koskela *et al.*, 2018). Changes in TM architecture caused by unstacking of grana upon transition to state 2 during state transitions were reported (Chuartzman *et al.*, 2008). From our observations, GNAT2 protein appears to be involved in the TM membrane organization similar to STN7 kinase.

5. Conclusions

Based on our results, we came to the following conclusions:

1. In *C. reinhardtii*, salt stress induces an increase in the repeat distances of thylakoid membranes in the salt-treated WT cells but not in *stt7* mutant. There is a reduction in the growth rate and chlorophyll content with increasing salinity. This is followed by disturbed macro-organization of PSII:LHCII protein complexes and significant alteration in the distribution of excitation energy between the two photosystems, favoring PSI and an energetic detachment of LHCII from PSII. In the mutant strains *stt7* and *pgrl1*, lacking the ability of state transitions and deficient in PSI CEF, respectively, these effects become more prominent and are accompanied by changes in the excitation energy migration pathways in PSI (in both mutants), and in perturbation of excitonic interactions of antenna complexes and a degradation of light-harvesting antenna complexes in *stt7*. There is an increase in the fluorescence lifetimes of salt-stressed cells indicating a decreased photochemical quantum yield of PSII.

   These results suggest that while diminished efficiency of the cyclic electron flow exerts minor additional effect on salt stress acclimation, the incapability of state transitions causes severe damages in the (macro-)organization of the pigment-protein complexes – suggesting that state transitions play an important role in the acclimatory response of the photosynthetic apparatus of *C. reinhardtii* cells to salinity.

2. In *E. gracilis*, there is a decrease in the chlorophyll content of the cells with increasing salinity. There is a change in the supramolecular arrangement of the pigment-protein complexes associated with a decrease in the repeat distances of thylakoid membranes in salt-treated cells suggesting the shrinkage of thylakoid membranes upon salt stress. We show that the cells accumulate paramylon, the concentration of which increases relative to salt concentration. We demonstrate that there is no effect of salt on the energy transfer kinetics of the cells. However, we also find that there is an increase in the total carotenoid content of the salt-treated cells relative to the chlorophyll.

   From the results, we can conclude that *E. gracilis* cells can maintain the

photosynthetic activity under moderate salt stress with modification of the pigment composition and the reorganization of the thylakoid membranes. Moreover, the increase in paramylon content prepares the cells for a higher osmotic shock. It appears that *E. gracilis* cells can compensate for moderate salt stress, by adjusting metabolism, without extreme effects on other cell functions. These beneficial properties of *E. gracilis* clearly indicate that the alga possesses inherent capabilities including the incredible metabolic and physiological versatility which enables acclimation to the hostile saline environment and make *E. gracilis* an excellent target for commercial use.

3. In *A. thaliana*, CD spectra of *gnat2* mutant showed that intensity of all the psi-type and excitonic CD bands were diminished similar to *stn7* mutant unlike WT which suggested alterations in the structure or arrangement of LHCII and PSII-LHCII supercomplex across the thylakoid membrane.

   From our results, it can be concluded that both phosphorylation and acetylation play key role in macro-organization of thylakoid membranes in addition to the induction of state transitions.

6. References

Abdel-Raouf, N., Al-Homaidan, A., and Ibraheem, I. (2012). Microalgae and Wastewater Treatment. *Saudi journal of biological sciences* 19(3), 257-275.

Abou-Shanab, R.A., El-Dalatony, M.M., El-Sheekh, M.M., Ji, M.-K., Salama, E.-S., Kabra, A.N., and Jeon, B.-H. (2014). Cultivation of a New Microalga, *Micractinium Reisseri*, in Municipal Wastewater for Nutrient Removal, Biomass, Lipid, and Fatty Acid Production. *Biotechnology and Bioprocess Engineering* 19(3), 510-518.

Adl, S.M., Simpson, A.G., Lane, C.E., Lukeš, J., Bass, D., Bowser, S.S., . . . Hampl, V. (2012). The Revised Classification of Eukaryotes. *Journal of Eukaryotic Microbiology* 59(5), 429-514.

Ahmad, I., and Hellebust, J.A. (1984). Osmoregulation in the Extremely Euryhaline Marine Micro-Alga *Chlorella autotrophica*. *Plant Physiology* 74(4), 1010-1015.

Ahmad, M.T., Shariff, M., Md. Yusoff, F., Goh, Y.M., and Banerjee, S. (2020). Applications of Microalga *Chlorella Vulgaris* in Aquaculture. *Reviews in Aquaculture* 12(1), 328-346.

Akhtar, P., Lingvay, M., Kiss, T., Deák, R., Bóta, A., Ughy, B., . . . Lambrev, P.H. (2016). Excitation Energy Transfer between Light-Harvesting Complex II and Photosystem I in Reconstituted Membranes. *Biochim Biophys Acta* 1857(4), 462-472.

Allakhverdiev, S.I., and Murata, N. (2008). Salt Stress Inhibits Photosystems II and I in Cyanobacteria. *Photosynthesis Research* 98(1), 529-539.

Allakhverdiev, S.I., Sakamoto, A., Nishiyama, Y., Inaba, M., and Murata, N. (2000a). Ionic and Osmotic Effects of NaCl-Induced Inactivation of Photosystems I and II in *Synechococcus* Sp. *Plant Physiology* 123(3), 1047-1056.

Allakhverdiev, S.I., Sakamoto, A., Nishiyama, Y., and Murata, N. (2000b). Inactivation of Photosystems I and II in Response to Osmotic Stress in *Synechococcus*. Contribution of Water Channels. *Plant Physiology* 122(4), 1201-1208.

Allen, J.F. (2003). State Transitions--a Question of Balance. *Science* 299(5612), 1530-1532.

Allen, J.F., and Forsberg, J. (2001). Molecular Recognition in Thylakoid Structure and Function. *Trends in plant science* 6(7), 317-326.

Anderson, J.M. (1981). Consequences of Spatial Separation of Photosystem 1 and 2 in Thylakoid Membranes of Higher Plant Chloroplasts. *FEBS Letters* 124(1), 1-10.

Anderson, J.M., Chow, W., and Goodchild, D. (1988). Thylakoid Membrane Organisation in Sun/Shade Acclimation. *Functional Plant Biology* 15(2), 11-26.

Andreeva, A., Stoitchkova, K., Busheva, M., and Apostolova, E. (2003). Changes in the Energy Distribution between Chlorophyll–Protein Complexes of Thylakoid Membranes from Pea Mutants with Modified Pigment Content: I. Changes Due to the Modified Pigment Content. *Journal of Photochemistry and Photobiology B: Biology* 70(3), 153-162.

Annamalai, J., Shanmugam, J., and Nallamuthu, T. (2016). Salt Stress Enhancing the Production of Phytochemicals in *Chlorella Vulgaris* and *Chlamydomonas reinhardtii*. *J Algal Biomass Util* 7, 37-44.

Apte, S.K., and Bhagwat, A.A. (1989). Salinity-Stress-Induced Proteins in Two Nitrogen-Fixing *Anabaena* Strains Differentially Tolerant to Salt. *Journal of Bacteriology* 171(2), 909-915.

Apte, S.K., Reddy, B.R., and Thomas, J. (1987). Relationship between Sodium Influx and Salt Tolerance of Nitrogen-Fixing Cyanobacteria. *Applied and Environmental Microbiology* 53(8), 1934-1939.

Apte, S.K., and Thomas, J. (1986). Membrane Electrogenesis and Sodium Transport in Filamentous Nitrogen-Fixing Cyanobacteria. *European Journal of Biochemistry* 154(2), 395-401.

Armbruster, U., Labs, M., Pribil, M., Viola, S., Xu, W., Scharfenberg, M., . . . Rappaport, F. (2013). *Arabidopsis* Curvature Thylakoid1 Proteins Modify Thylakoid Architecture by Inducing Membrane Curvature. *The Plant Cell* 25(7), 2661-2678.

Arvidsson, P.-O., and Sundby, C. (1999). A Model for the Topology of the Chloroplast Thylakoid Membrane. *Functional Plant Biology* 26(7), 687-694.

Ashraf, M., and Harris, P.J. (2013). Photosynthesis under Stressful Environments: An Overview. *Photosynthetica* 51(2), 163-190.

Avenson, T.J., Cruz, J.A., Kanazawa, A., and Kramer, D.M. (2005). Regulating the Proton Budget of Higher Plant Photosynthesis. *Proceedings of the National Academy of Sciences* 102(27), 9709-9713.

Azizullah, A., Richter, P., and Häder, D.-P. (2012). Responses of Morphological, Physiological, and Biochemical Parameters in *Euglena gracilis* to 7-Days Exposure to Two Commonly Used Fertilizers Dap and Urea. *Journal of Applied Phycology* 24(1), 21-33.

Bag, P. (2021). Light Harvesting in Fluctuating Environments: Evolution and Function of Antenna Proteins across Photosynthetic Lineage. *Plants* 10(6), 1184.

Barros, T., Royant, A., Standfuss, J., Dreuw, A., and Kühlbrandt, W. (2009). Crystal Structure of Plant Light-Harvesting Complex Shows the Active, Energy-Transmitting State. *The EMBO journal* 28(3), 298-306.

Barsanti, L., and Gualtieri, P. (2019). Paramylon, a Potent Immunomodulator from WZSL Mutant of *Euglena gracilis*. *Molecules* 24(17), 3114.

Barsanti, L., Passarelli, V., Evangelista, V., Frassanito, A.M., and Gualtieri, P. (2011). Chemistry, Physico-Chemistry and Applications Linked to Biological Activities of B-Glucans. *Natural product reports* 28(3), 457-466.

Barsanti, L., Vismara, R., Passarelli, V., and Gualtieri, P. (2001). Paramylon (β-1, 3-glucan) Content in Wild Type and WZSL Mutant of *Euglena gracilis*. Effects of Growth Conditions. *Journal of Applied Phycology* 13(1), 59-65.

Barzda, V., Garab, G., Gulbinas, V., and Valkunas, L. (1996). Evidence for Long-Range Excitation Energy Migration in Macroaggregates of the Chlorophyll a/b Light-Harvesting Antenna Complexes. *Biochimica et Biophysica Acta (BBA) - Bioenergetics* 1273(3), 231-236.

Bellafiore, S., Barneche, F., Peltier, G., and Rochaix, J.-D. (2005). State Transitions and Light Adaptation Require Chloroplast Thylakoid Protein Kinase Stn7. *Nature* 433(7028), 892-895.

Bellou, S., Moustogianni, A., Makri, A., and Aggelis, G. (2012). Lipids Containing Polyunsaturated Fatty Acids Synthesized by Zygomycetes Grown on Glycerol. *Applied Biochemistry and Biotechnology* 166(1), 146-158.

Beltagi, M., Ismail, M., and Mohamed, F. (2006). Induced Salt Tolerance in Common Bean (*Phaseolus Vulgaris* L.) by Gamma Irradiation. *Pak J Biol Sci* 6, 1143-1148.

Ben-Amotz, A., and Avron, M. (1973). The Role of Glycerol in the Osmotic Regulation of the Halophilic Alga *Dunaliella parva*. *Plant Physiology* 51(5), 875-878.

Benemann, J.R. (2000). Hydrogen Production by Microalgae. *Journal of Applied Phycology* 12(3), 291-300.

Bennett, J. (1979). Chloroplast Phosphoproteins: Phosphorylation of Polypeptides of the Light-Harvesting Chlorophyll Protein Complex. *European Journal of Biochemistry* 99(1), 133-137.

Bhatti, A.F., Choubeh, R.R., Kirilovsky, D., Wientjes, E., and van Amerongen, H. (2020). State Transitions in Cyanobacteria Studied with Picosecond Fluorescence at Room Temperature. *Biochimica et Biophysica Acta (BBA)-Bioenergetics* 1861(10), 148255.

Blankenship, R.E. (2010). Early Evolution of Photosynthesis. *Plant Physiology* 154(2), 434-438.

Block, M.A., and Albrieux, C. (2018). "Purification of Chloroplasts and Chloroplast Subfractions: Envelope, Thylakoids, and Stroma—from Spinach, Pea, and *Arabidopsis thaliana*," in *Plastids*. Springer), 123-135.

Blumwald, E., Mehlhorn, R.J., and Packer, L. (1983). Ionic Osmoregulation During Salt Adaptation of the Cyanobacterium *Synechococcus* 6311. *Plant Physiology* 73(2), 377-380.

Boekema, E.J., van Breemen, J.F., van Roon, H., and Dekker, J.P. (2000). Arrangement of Photosystem II Supercomplexes in Crystalline Macrodomains within the Thylakoid Membrane of Green Plant Chloroplasts. *Journal of molecular biology* 301(5), 1123-1133.

Borowitzka, L.J., Demmerle, S., Mackay, M.A., and Norton, R.S. (1980). Carbon-13 Nuclear Magnetic Resonance Study of Osmoregulation in a Blue-Green Alga. *Science* 210(4470), 650-651.

Brandt, P., and Wilhelm, C. (1990). The Light-Harvesting System of *Euglena gracilis* During the Cell Cycle. *Planta* 180(2), 293-296.

Brown, L.M., and Hellebust, J.A. (1978). Sorbitol and Proline as Intracellular Osmotic Solutes in the Green Alga *Stichococcus Bacillaris*. *Canadian Journal of Botany* 56(6), 676-679.

Bukhov, N., and Carpentier, R. (2004). Alternative Photosystem I-Driven Electron Transport Routes: Mechanisms and Functions. *Photosynthesis Research* 82(1), 17-33.

Campos, H., Boeing, W.J., Dungan, B.N., and Schaub, T. (2014). Cultivating the Marine Microalga *Nannochloropsis salina* under Various Nitrogen Sources: Effect on Biovolume Yields, Lipid Content and Composition, and Invasive Organisms. *biomass and bioenergy* 66, 301-307.

Canaani, O. (1990). The Role of Cyclic Electron Flow around Photosystem I and Excitation Energy Distribution between the Photosystems Upon Acclimation to High Ionic Stress in *Dunaliella salina*. *Photochemistry and photobiology* 52(3), 591-599.

Cardol, P., Alric, J., Girard-Bascou, J., Franck, F., Wollman, F.-A., and Finazzi, G. (2009). Impaired Respiration Discloses the Physiological Significance of State Transitions in *Chlamydomonas*. *Proceedings of the National Academy of Sciences* 106(37), 15979-15984.

Cariti, F., Chazaux, M., Lefebvre-Legendre, L., Longoni, P., Ghysels, B., Johnson, X., and Goldschmidt-Clermont, M. (2020). Regulation of Light Harvesting in *Chlamydomonas reinhardtii* Two Protein Phosphatases Are Involved in State Transitions. *Plant Physiology* 183(4), 1749-1764.

Chen, T.H., and Murata, N. (2002). Enhancement of Tolerance of Abiotic Stress by Metabolic

Engineering of Betaines and Other Compatible Solutes. *Current opinion in plant biology* 5(3), 250-257.

Chow, W. (1984). The Extent to Which the Spatial Separation between Photosystems I and II Associated with Granal Formation Limits Noncyclic Electron Flow in Isolated Lett. Uce Chloroplasts. *Archives of Biochemistry and Biophysics* 232(1), 162-171.

Chow, W.S., Kim, E.-H., Horton, P., and Anderson, J.M. (2005). Granal Stacking of Thylakoid Membranes in Higher Plant Chloroplasts: The Physicochemical Forces at Work and the Functional Consequences That Ensue. *Photochemical & Photobiological Sciences* 4(12), 1081-1090.

Chuartzman, S.G., Nevo, R., Shimoni, E., Charuvi, D., Kiss, V., Ohad, I., . . . Reich, Z. (2008). Thylakoid Membrane Remodeling During State Transitions in *Arabidopsis*. *The Plant Cell* 20(4), 1029-1039.

Correa-Galvis, V., Redekop, P., Guan, K., Griess, A., Truong, T.B., Wakao, S., . . . Jahns, P. (2016). Photosystem II Subunit Psbs Is Involved in the Induction of Lhcsr Protein-Dependent Energy Dissipation in *Chlamydomonas reinhardtii*. *Journal of Biological Chemistry* 291(33), 17478-17487.

DalCorso, G., Pesaresi, P., Masiero, S., Aseeva, E., Schünemann, D., Finazzi, G., . . . Leister, D. (2008). A Complex Containing Pgrl1 and Pgr5 Is Involved in the Switch between Linear and Cyclic Electron Flow in *Arabidopsis*. *Cell* 132(2), 273-285.

Daum, B., and Kühlbrandt, W. (2011). Electron Tomography of Plant Thylakoid Membranes. *Journal of Experimental Botany* 62(7), 2393-2402.

de Farias Silva, C.E., and Bertucco, A. (2016). Bioethanol from Microalgae and Cyanobacteria: A Review and Technological Outlook. *Process Biochemistry* 51(11), 1833-1842.

del Pilar Bremauntz, M., Torres-Bustillos, L.G., Duran-Paramo, E., and Fernández-Linares, L. (2011). Trehalose and Sucrose Osmolytes Accumulated by Algae as Potential Raw Material for Bioethanol. *Natural Resources* 2(03), 173.

Demmig-Adams, B., and Adams, W.W. (1992). Photoprotection and Other Responses of Plants to High Light Stress. *Annual review of plant physiology and plant molecular biology* 43(1), 599-626.

Depège, N., Bellafiore, S., and Rochaix, J.-D. (2003). Role of Chloroplast Protein Kinase Stt7 in LHCII Phosphorylation and State Transition in *Chlamydomonas*. *Science* 299(5612), 1572-1575.

Devars, S., Torres-Márquez, M.E., González-Halphen, D., Uribe, A., and Moreno-Sánchez, R. (1992). Cyanide-Sensitive and Cyanide-Resistant Respiration of Dark-Grown *Euglena gracilis*. *Plant Science* 82(1), 37-46.

Devi, M.P., and Mohan, S.V. (2012). Co2 Supplementation to Domestic Wastewater Enhances Microalgae Lipid Accumulation under Mixotrophic Microenvironment: Effect of Sparging Period and Interval. *Bioresource Technology* 112, 116-123.

Dietzel, L., Bräutigam, K., Steiner, S., Schüffler, K., Lepetit, B., Grimm, B., . . . Pfannschmidt, T. (2011). Photosystem II Supercomplex Remodeling Serves as an Entry Mechanism for State Transitions in *Arabidopsis*. *The Plant Cell* 23(8), 2964-2977.

Doege, M., Ohmann, E., and Tschiersch, H. (2000). Chlorophyll Fluorescence Quenching in the Alga *Euglena gracilis*. *Photosynthesis Research* 63(2), 159-170.

Domonkos, I., Kis, M., Gombos, Z., and Ughy, B. (2013). Carotenoids, Versatile Components of Oxygenic Photosynthesis. *Progress in lipid research* 52(4), 539-561.

Drexler, I.L., and Yeh, D.H. (2014). Membrane Applications for Microalgae Cultivation and Harvesting: A Review. *Reviews in Environmental Science and Biotechnology* 13(4), 487-504.

Du, W., Liang, F., Duan, Y., Tan, X., and Lu, X. (2013). Exploring the Photosynthetic Production Capacity of Sucrose by Cyanobacteria. *Metabolic engineering* 19, 17-25.

Ducat, D.C., Avelar-Rivas, J.A., Way, J.C., and Silver, P.A. (2012). Rerouting Carbon Flux to Enhance Photosynthetic Productivity. *Applied and Environmental Microbiology* 78(8), 2660-2668.

Ebenhöh, O., Fucile, G., Finazzi, G., Rochaix, J.-D., and Goldschmidt-Clermont, M. (2014). Short-Term Acclimation of the Photosynthetic Electron Transfer Chain to Changing Light: A Mathematical Model. *Philosophical Transactions of the Royal Society B: Biological Sciences* 369(1640), 20130223.

El-Katony, T.M., and El-Adl, M.F. (2020). Salt Response of the Freshwater Microalga *Scenedesmus obliquus* (Turp.) Kutz Is Modulated by the Algal Growth Phase. *Journal of Oceanology and Limnology* 38(3), 802-815.

Elloumi, W., Jebali, A., Maalej, A., Chamkha, M., and Sayadi, S. (2020). Effect of Mild Salinity Stress on the Growth, Fatty Acid and Carotenoid Compositions, and Biological Activities of the Thermal Freshwater Microalgae *Scenedesmus* Sp. *Biomolecules* 10(11), 1515.

Endo, T., Schreiber, U., and Asada, K. (1995). Suppression of Quantum Yield of Photosystem II by Hyperosmotic Stress in *Chlamydomonas reinhardtii*. *Plant and Cell Physiology* 36(7), 1253-1258.

Erickson, E., Wakao, S., and Niyogi, K.K. (2015). Light Stress and Photoprotection in *Chlamydomonas reinhardtii*. *The Plant Journal* 82(3), 449-465.

Fernyhough, P., Foyer, C., and Horton, P. (1983). The Influence of Metabolic State on the Level of Phosphorylation of the Light-Harvesting Chlorophyll-Protein Complex in Chloroplasts Isolated from Maize Mesophyll. *Biochimica et Biophysica Acta (BBA)-Bioenergetics* 725(1), 155-161.

Finazzi, G. (2005). The Central Role of the Green Alga *Chlamydomonas reinhardtii* in Revealing the Mechanism of State Transitions. *Journal of Experimental Botany* 56(411), 383-388.

Forieri, I., Hildebrandt, U., and Rostás, M. (2016). Salinity Stress Effects on Direct and Indirect Defence Metabolites in Maize. *Environmental and Experimental Botany* 122, 68-77.

Fulda, S., Mikkat, S., Huang, F., Huckauf, J., Marin, K., Norling, B., and Hagemann, M. (2006). Proteome Analysis of Salt Stress Response in the Cyanobacterium *Synechocystis* Sp. Strain Pcc 6803. *Proteomics* 6(9), 2733-2745.

Galinski, E.A., and Trüper, H.G. (1994). Microbial Behaviour in Salt-Stressed Ecosystems. *FEMS Microbiology Reviews* 15(2-3), 95-108.

Gan, P., Liu, F., Li, R., Wang, S., and Luo, J. (2019). Chloroplasts—Beyond Energy Capture and Carbon Fixation: Tuning of Photosynthesis in Response to Chilling Stress. *International journal of molecular sciences* 20(20), 5046.

Garab, G., Kieleczawa, J., Sutherland, J., Bustamante, C., and Hind, G. (1991). Organization of Pigment-Protein Complexes into Macrodomains in the Thyalkoid Membranes of Wild-Type and Chlorophyll-Fo-Less Mutant of Barley as Revealed by Circular Dichroism. *Photochemistry and photobiology* 54(2), 273-281.

Garab, G., Leegood, R.C., Walker, D.A., Sutherland, J.C., and Hind, G. (1988). Reversible Changes in Macroorganization of the Light-Harvesting Chlorophyll *a*/*b* Pigment-Protein Complex Detected by Circular Dichroism. *Biochemistry* 27(7), 2430-2434.

Garab, G., and van Amerongen, H. (2009). Linear Dichroism and Circular Dichroism in Photosynthesis Research. *Photosynthesis Research* 101(2), 135-146.

Genty, B., Briantais, J.-M., and Baker, N.R. (1989). The Relationship between the Quantum Yield of Photosynthetic Electron Transport and Quenching of Chlorophyll Fluorescence. *Biochimica et Biophysica Acta (BBA) - General Subjects* 990(1), 87-92.

Ghazaryan, A., Akhtar, P., Garab, G., Lambrev, P.H., and Büchel, C. (2016). Involvement of the Lhcx Protein Fcp6 of the Diatom *Cyclotella meneghiniana* in the Macro-Organisation and Structural Flexibility of Thylakoid Membranes. *Biochimica et Biophysica Acta (BBA) - Bioenergetics* 1857(9), 1373-1379.

Ghysels, B., Godaux, D., Matagne, R.F., Cardol, P., and Franck, F. (2013). Function of the Chloroplast Hydrogenase in the Microalga *Chlamydomonas*: The Role of Hydrogenase and State Transitions During Photosynthetic Activation in Anaerobiosis. *PLoS One* 8(5), e64161.

Gibbs, S.P. (1960). The Fine Structure of *Euglena gracilis* with Special Reference to the Chloroplasts and Pyrenoids. *Journal of Ultrastructure Research* 4(2), 127-148.

Gilmour, D., Hipkins, M., and Boney, A. (1982). The Effect of Salt Stress on the Primary Processes of Photosynthesis in *Dunaliella tertiolecta*. *Plant Science Letters* 26(2-3), 325-330.

Gilmour, D., Hipkins, M., Webber, A., Baker, N., and Boney, A. (1985). The Effect of Ionic Stress on Photosynthesis in *Dunaliella tertiolecta*. *Planta* 163(2), 250-256.

Gissibl, A., Care, A., Parker, L.M., Iqbal, S., Hobba, G., Nevalainen, H., and Sunna, A. (2018). Microwave Pretreatment of Paramylon Enhances the Enzymatic Production of Soluble B-1, 3-Glucans with Immunostimulatory Activity. *Carbohydrate polymers* 196, 339-347.

Gissibl, A., Sun, A., Care, A., Nevalainen, H., and Sunna, A. (2019). Bioproducts from *Euglena gracilis*: Synthesis and Applications. *Frontiers in Bioengineering and Biotechnology* 7, 108.

González-Moreno, S., Gómez-Barrera, J., Perales, H., and Moreno-Sánchez, R. (1997). Multiple Effects of Salinity on Photosynthesis of the Protist *Euglena gracilis*. *Physiologia Plantarum* 101(4), 777-786.

Goodenough, U.W., and Staehelin, L.A. (1971). Structural Differentiation of Stacked and Unstacked Chloroplast Membranes: Freeze-Etch Electron Microscopy of Wild-Type and Mutant Strains of *Chlamydomonas*. *The Journal of cell biology* 48(3), 594-619.

Goss, R., and Jakob, T. (2010). Regulation and Function of Xanthophyll Cycle-Dependent Photoprotection in Algae. *Photosynthesis Research* 106(1-2), 103-122.

Hagemann, M., Techel, D., and Rensing, L. (1991). Comparison of Salt-and Heat-Induced Alterations of Protein Synthesis in the Cyanobacterium *Synechocystis* Sp. Pcc 6803. *Archives of Microbiology* 155(6), 587-592.

Hagemann, M., Wöfel, L., and Krüger, B. (1990). Alterations of Protein Synthesis in the Cyanobacterium *Synechocystis* Sp. Pcc 6803 after a Salt Shock. *Microbiology* 136(7), 1393-1399.

Hasanuzzaman, M., Nahar, K., and Fujita, M. (2013). "Plant Response to Salt Stress and Role of Exogenous Protectants to Mitigate Salt-Induced Damages," in *Ecophysiology and Responses of Plants under Salt Stress*. Springer), 25-87.

Hayashi, H., Sakamoto, A., and Murata, N. (1998). Enhancement of the Tolerance of *Arabidopsis* to High Temperatures by Genetic Engineering of the Synthesis of Glycinebetaine. *The Plant Journal* 16(2), 155-161.

Hayat, M., and Giaquinta, R. (1970). Rapid Fixation and Embedding for Electron Microscopy. *Tissue and cell* 2(2), 191-195.

He, Y., Fu, J., Yu, C., Wang, X., Jiang, Q., Hong, J., . . . James, A. (2015). Increasing Cyclic Electron Flow Is Related to Na+ Sequestration into Vacuoles for Salt Tolerance in Soybean. *Journal of Experimental Botany* 66(21), 6877-6889.

He, Y., Yu, C., Zhou, L., Chen, Y., Liu, A., Jin, J., . . . Jiang, D. (2014). Rubisco Decrease Is Involved in Chloroplast Protrusion and Rubisco-Containing Body Formation in Soybean (*Glycine Max*.) under Salt Stress. *Plant physiology and biochemistry* 74, 118-124.

Herbstová, M., Tietz, S., Kinzel, C., Turkina, M.V., and Kirchhoff, H. (2012). Architectural Switch in Plant Photosynthetic Membranes Induced by Light Stress. *Proceedings of the National Academy of Sciences* 109(49), 20130-20135.

Hertle, A.P., Blunder, T., Wunder, T., Pesaresi, P., Pribil, M., Armbruster, U., and Leister, D. (2013). Pgrl1 Is the Elusive Ferredoxin-Plastoquinone Reductase in Photosynthetic Cyclic Electron Flow. *Molecular cell* 49(3), 511-523.

Hiremath, S., and Mathad, P. (2010). Impact of Salinity on the Physiological and Biochemical Traits of *Chlorella Vulgaris* Beijerinck. *J Algal Biomass Utln* 1(2), 51-59.

Ho, S.-H., Huang, S.-W., Chen, C.-Y., Hasunuma, T., Kondo, A., and Chang, J.-S. (2013). Bioethanol Production Using Carbohydrate-Rich Microalgae Biomass as Feedstock. *Bioresource Technology* 135, 191-198.

Ho, S.-H., Nakanishi, A., Ye, X., Chang, J.-S., Hara, K., Hasunuma, T., and Kondo, A. (2014). Optimizing Biodiesel Production in Marine *Chlamydomonas* Sp. Jsc4 through Metabolic Profiling and an Innovative Salinity-Gradient Strategy. *Biotechnology for Biofuels* 7(1), 1-16.

Hoober, J.K. (1989). All About Some Algae: The *Chlamydomonas* Sourcebook. A Comprehensive Guide to Biology and Laboratory Use. Elizabeth H. Harris. Academic Press, San Diego, Ca, 1989. Xiv, 780 Pp., Illus. $145. *Science* 246(4936), 1503-1504.

Horton, P., Ruban, A.V., and Walters, R.G. (1994). Regulation of Light Harvesting in Green Plants (Indication by Nonphotochemical Quenching of Chlorophyll Fluorescence). *Plant Physiology* 106(2), 415.

Hu, H., Zhang, H., Chu, J., Zhang, X., Zheng, K., Li, S., . . . Zhang, X. (2012). Leaf Chlorophyll Fluorescence Effect of Different Rice (*Oryza Sativa* L.) Genotypes under Salt Stress. *Advanced Science Letters* 11(1), 706-709.

Inui, H., Miyatake, K., Nakano, Y., and Kitaoka, S. (1982). Wax Ester Fermentation in *Euglena gracilis*. *FEBS Letters* 150(1), 89-93.

Iwai, M., Takahashi, Y., and Minagawa, J. (2008). Molecular Remodeling of Photosystem II During State Transitions in *Chlamydomonas reinhardtii*. *The Plant Cell* 20(8), 2177-2189.

Iwai, M., Takizawa, K., Tokutsu, R., Okamuro, A., Takahashi, Y., and Minagawa, J. (2010). Isolation of the Elusive Supercomplex That Drives Cyclic Electron Flow in Photosynthesis. *Nature* 464(7292), 1210-1213.

Jacoby, R.P., Taylor, N.L., and Millar, A.H. (2011). The Role of Mitochondrial Respiration in Salinity Tolerance. *Trends in plant science* 16(11), 614-623.

Järvi, S., Suorsa, M., Paakkarinen, V., and Aro, E.-M. (2011). Optimized Native Gel Systems for Separation of Thylakoid Protein Complexes: Novel Super-and Mega-Complexes. *Biochemical Journal* 439(2), 207-214.

Jensen, P.E., Rosgaard, L., Knoetzel, J.r., and Scheller, H.V. (2002). Photosystem I Activity Is Increased in the Absence of the PSI-G Subunit. *Journal of Biological Chemistry* 277(4), 2798-2803.

Ji, X., Cheng, J., Gong, D., Zhao, X., Qi, Y., Su, Y., and Ma, W. (2018). The Effect of NaCl Stress on Photosynthetic Efficiency and Lipid Production in Freshwater Microalga—*Scenedesmus obliquus* XJ002. *Science of the total environment* 633, 593-599.

Joliot, P., and Johnson, G.N. (2011). Regulation of Cyclic and Linear Electron Flow in Higher Plants. *Proceedings of the National Academy of Sciences* 108(32), 13317-13322.

Kaçka, A., and Dönmez, G. (2008). Isolation of *Dunaliella* Spp. From a Hypersaline Lake and Their Ability to Accumulate Glycerol. *Bioresource Technology* 99(17), 8348-8352.

Kalra, I., Wang, X., Cvetkovska, M., Jeong, J., McHargue, W., Zhang, R., . . . Morgan-Kiss, R. (2020). *Chlamydomonas* Sp. Uwo 241 Exhibits High Cyclic Electron Flow and Rewired Metabolism under High Salinity. *Plant Physiology* 183(2), 588-601.

Kanna, S.D., Domonkos, I., Kóbori, T.O., Dergez, Á., Böde, K., Nagyapáti, S., . . . Garab, G. (2021). Salt Stress Induces Paramylon Accumulation and Fine-Tuning of the Macro-Organization of Thylakoid Membranes in *Euglena gracilis* Cells. *Frontiers in Plant Science* 12.

Kato, S., Soshino, M., Takaichi, S., Ishikawa, T., Nagata, N., Asahina, M., and Shinomura, T. (2017). Suppression of the Phytoene Synthase Gene (Egcrtb) Alters Carotenoid Content and Intracellular Structure of *Euglena gracilis*. *BMC plant biology* 17(1), 1-10.

Keeling, P.J. (2009). Chromalveolates and the Evolution of Plastids by Secondary Endosymbiosis 1. *Journal of Eukaryotic Microbiology* 56(1), 1-8.

Keller, D., and Bustamante, C. (1986). Theory of the Interaction of Light with Large Inhomogeneous Molecular Aggregates. II. Psi-Type Circular Dichroism. *The Journal of chemical physics* 84(6), 2972-2980.

Khan, S.A., Hussain, M.Z., Prasad, S., and Banerjee, U. (2009). Prospects of Biodiesel Production from Microalgae in India. *Renewable and sustainable energy reviews* 13(9), 2361-2372.

Khatiwada, B., Sunna, A., and Nevalainen, H. (2020). Molecular Tools and Applications of *Euglena gracilis*: From Biorefineries to Bioremediation. *Biotechnology and Bioengineering*.

Khona, D.K., Shirolikar, S.M., Gawde, K.K., Hom, E., Deodhar, M.A., and D'Souza, J.S. (2016). Characterization of Salt Stress-Induced Palmelloids in the Green Alga, *Chlamydomonas reinhardtii*. *Algal Research* 16, 434-448.

Kim, M.H., Ulibarri, L., Keller, D., Maestre, M.F., and Bustamante, C. (1986). The Psi-Type Circular Dichroism of Large Molecular Aggregates. III. Calculations. *The Journal of chemical physics* 84(6), 2981-2989.

Kirchhoff, H., Hall, C., Wood, M., Herbstová, M., Tsabari, O., Nevo, R., . . . Reich, Z. (2011). Dynamic Control of Protein Diffusion within the Granal Thylakoid Lumen. *Proceedings of the National Academy of Sciences* 108(50), 20248-20253.

Kirchhoff, H., Hinz, H.-J., and Rösgen, J. (2003). Aggregation and Fluorescence Quenching of Chlorophyll *a* of the Light-Harvesting Complex II from Spinach in Vitro. *Biochimica et Biophysica Acta (BBA)-Bioenergetics* 1606(1-3), 105-116.

Kirchhoff, H., Mukherjee, U., and Galla, H.-J. (2002). Molecular Architecture of the Thylakoid Membrane: Lipid Diffusion Space for Plastoquinone. *Biochemistry* 41(15), 4872-4882.

Kirsch, F., Luo, Q., Lu, X., and Hagemann, M. (2018). Inactivation of Invertase Enhances Sucrose Production in the Cyanobacterium *Synechocystis* Sp. Pcc 6803. *Microbiology* 164(10), 1220-1228.

Kiss, A.Z., Ruban, A.V., and Horton, P. (2008). The Psbs Protein Controls the Organization of the Photosystem II Antenna in Higher Plant Thylakoid Membranes. *Journal of Biological Chemistry* 283(7), 3972-3978.

Klughammer, C., and Schreiber, U. (1994). Saturation Pulse Method for Assessment of Energy Conversion in PSI. *Planta* 192, 261-268.

Kodru, S., Malavath, T., Devadasu, E., Nellaepalli, S., Stirbet, A., and Subramanyam, R. (2015). The Slow S to M Rise of Chlorophyll *a* Fluorescence Reflects Transition from State 2 to State 1 in the Green Alga *Chlamydomonas reinhardtii*. *Photosynthesis Research* 125(1-2), 219-231.

Kono, M., Noguchi, K., and Terashima, I. (2014). Roles of the Cyclic Electron Flow around PSI (Cef-PSI) and O2-Dependent Alternative Pathways in Regulation of the Photosynthetic Electron Flow in Short-Term Fluctuating Light in *Arabidopsis thaliana*. *Plant and Cell Physiology* 55(5), 990-1004.

Koskela, M.M., Brünje, A., Ivanauskaite, A., Grabsztunowicz, M., Lassowskat, I., Neumann, U., . . . Wirtz, M. (2018). Chloroplast Acetyltransferase Nsi Is Required for State Transitions in *Arabidopsis thaliana*. *The Plant Cell* 30(8), 1695-1709.

Kouřil, R., Wientjes, E., Bultema, J.B., Croce, R., and Boekema, E.J. (2013). High-Light Vs. Low-Light: Effect of Light Acclimation on Photosystem II Composition and Organization in *Arabidopsis thaliana*. *Biochimica et Biophysica Acta (BBA)-Bioenergetics* 1827(3), 411-419.

Kovács, L., Damkjær, J., Kereïche, S., Ilioaia, C., Ruban, A.V., Boekema, E.J., . . . Horton, P. (2006). Lack of the Light-Harvesting Complex Cp24 Affects the Structure and Function of the Grana Membranes of Higher Plant Chloroplasts. *The Plant Cell* 18(11), 3106-3120.

Kramer, D.M., Johnson, G., Kiirats, O., and Edwards, G.E. (2004). New Fluorescence Parameters for the Determination of QA Redox State and Excitation Energy Fluxes. *Photosynthesis Research* 79(2), 209-218.

Kramer, H., Westerhuis, W., and Amesz, J. (1985). Low Temperature Spectroscopy of Intact Algae. *Physiologie végétale (Paris)* 23(5), 535-543.

Krämer, U. (2015). Planting Molecular Functions in an Ecological Context with *Arabidopsis thaliana*. *Elife* 4.

Kukwa, D.T., and Chetty, M. (2021). Microalgae: The Multifaceted Biomass of the 21st Century. *Biotechnological Applications of Biomass*, 355.

Kumar Rai, A. (1990). Biochemical Characteristics of Photosynthetic Response to Various External Salinities in Halotolerant and Fresh Water Cyanobacteria. *FEMS Microbiology Letters* 69(1-2), 177-180.

Lakowicz, R.J. (1999). "Lakowicz:" Principles of Fluorescence Spectroscopy"". KLUWER

ACADEMIC/PLENUM PUBLISHERS).

Lambrev, P.H., and Akhtar, P. (2019). Macroorganisation and Flexibility of Thylakoid Membranes. *Biochemical Journal* 476(20), 2981-3018.

Lambrev, P.H., Várkonyi, Z., Krumova, S., Kovács, L., Miloslavina, Y., Holzwarth, A.R., and Garab, G. (2007). Importance of Trimer–Trimer Interactions for the Native State of the Plant Light-Harvesting Complex II. *Biochimica et Biophysica Acta (BBA)-Bioenergetics* 1767(6), 847-853.

Lapashina, A., and Feniouk, B. (2018). Adp-Inhibition of H+-Fof1-Atp Synthase. *Biochemistry (Moscow)* 83(10), 1141-1160.

Lavaud, J. (2007). Fast Regulation of Photosynthesis in Diatoms: Mechanisms, Evolution and Ecophysiology. *Functional Plant Science and Biotechonology* 1, 267-287.

Lavaud, J., and Kroth, P.G. (2006). In Diatoms, the Transthylakoid Proton Gradient Regulates the Photoprotective Non-Photochemical Fluorescence Quenching Beyond Its Control on the Xanthophyll Cycle. *Plant and Cell Physiology* 47(7), 1010-1016.

Lavaud, J., Rousseau, B., and Etienne, A.-L. (2003). Enrichment of the Light-Harvesting Complex in Diadinoxanthin and Implications for the Nonphotochemical Fluorescence Quenching in Diatoms. *Biochemistry* 42(19), 5802-5808.

Lefort-Tran, M., Pouphile, M., Freyssinet, G., and Pineau, B. (1980). Structural and Functional Significance of the Chloroplast Envelope of *Euglena*: Immunocytological and Freeze Fracture Study. *Journal of Ultrastructure Research* 73(1), 44-63.

León, R., and Galván, F. (1994). Halotolerance Studies on *Chlamydomonas reinhardtii*: Glycerol Excretion by Free and Immobilized Cells. *Journal of Applied Phycology* 6(1), 13-20.

Li, K., Liu, Q., Fang, F., Luo, R., Lu, Q., Zhou, W., . . . Addy, M. (2019). Microalgae-Based Wastewater Treatment for Nutrients Recovery: A Review. *Bioresource Technology* 291, 121934.

Liang, Y., Sarkany, N., and Cui, Y. (2009). Biomass and Lipid Productivities of *Chlorella Vulgaris* under Autotrophic, Heterotrophic and Mixotrophic Growth Conditions. *Biotechnology letters* 31(7), 1043-1049.

Liberton, M., Collins, A.M., Page, L.E., O'Dell, W.B., O'Neill, H., Urban, V.S., . . . Pakrasi, H.B. (2013a). Probing the Consequences of Antenna Modification in Cyanobacteria. *Photosynthesis Research* 118(1), 17-24.

Liberton, M., Page, L.E., O'Dell, W.B., O'Neill, H., Mamontov, E., Urban, V.S., and Pakrasi, H.B.

(2013b). Organization and Flexibility of Cyanobacterial Thylakoid Membranes Examined by Neutron Scattering. *Journal of Biological Chemistry* 288(5), 3632-3640.

Lichtenthaler, H., Buschmann, C., Döll, M., Fietz, H.-J., Bach, T., Kozel, U., . . . Rahmsdorf, U. (1981). Photosynthetic Activity, Chloroplast Ultrastructure, and Leaf Characteristics of High-Light and Low-Light Plants and of Sun and Shade Leaves. *Photosynthesis Research* 2(2), 115-141.

Lichtenthaler, H.K., and Wellburn, A.R. (1983). Determinations of Total Carotenoids and Chlorophylls *a* and *b* of Leaf Extracts in Different Solvents. *Biochemical Society Transactions* 11(5), 591-592.

Liguori, N., Croce, R., Marrink, S.J., and Thallmair, S. (2020). Molecular Dynamics Simulations in Photosynthesis. *Photosynthesis Research* 144(2), 273-295.

Lim, K.C., Yusoff, F.M., Shariff, M., and Kamarudin, M.S. (2018). Astaxanthin as Feed Supplement in Aquatic Animals. *Reviews in Aquaculture* 10(3), 738-773.

Liu, J., and Zhu, J.-K. (1997). Proline Accumulation and Salt-Stress-Induced Gene Expression in a Salt-Hypersensitive Mutant of *Arabidopsis*. *Plant Physiology* 114(2), 591-596.

Liu, W., Ming, Y., Li, P., and Huang, Z. (2012). Inhibitory Effects of Hypo-Osmotic Stress on Extracellular Carbonic Anhydrase and Photosynthetic Efficiency of Green Alga *Dunaliella salina* Possibly through Reactive Oxygen Species Formation. *Plant physiology and biochemistry* 54, 43-48.

Liu, Z., Yan, H., Wang, K., Kuang, T., Zhang, J., Gui, L., . . . Chang, W. (2004). Crystal Structure of Spinach Major Light-Harvesting Complex at 2.72 Å Resolution. *Nature* 428(6980), 287-292.

Lu, C., Torzillo, G., and Vonshak, A. (1999). Kinetic Response of Photosystem II Photochemistry in the Cyanobacterium *Spirulina platensis* to High Salinity Is Characterized by Two Distinct Phases. *Functional Plant Biology* 26(3), 283-292.

Lu, C., and Vonshak, A. (2002). Effects of Salinity Stress on Photosystem II Function in Cyanobacterial *Spirulina platensis* Cells. *Physiologia Plantarum* 114(3), 405-413.

Lu, J., Yin, Z., Lu, T., Yang, X., Wang, F., Qi, M., . . . Liu, Y. (2020). Cyclic Electron Flow Modulate the Linear Electron Flow and Reactive Oxygen Species in Tomato Leaves under High Temperature. *Plant Science* 292, 110387.

Lu, Q., Li, H., Zou, Y., Liu, H., and Yang, L. (2021). Astaxanthin as a Microalgal Metabolite for Aquaculture: A Review on the Synthetic Mechanisms, Production Techniques, and Practical Application. *Algal Research* 54, 102178.

Lu, Q., Zhou, W., Min, M., Ma, X., Ma, Y., Chen, P., . . . Chen, C. (2016). Mitigating Ammonia Nitrogen Deficiency in Dairy Wastewaters for Algae Cultivation. *Bioresource Sechnology* 201, 33-40.

Ma, M., Liu, Y., Bai, C., Yang, Y., Sun, Z., Liu, X., . . . Yong, J.W.H. (2021). The Physiological Functionality of Pgr5/Pgrl1-Dependent Cyclic Electron Transport in Sustaining Photosynthesis. *Frontiers in Plant Science*, 1313.

Madeira, M.S., Cardoso, C., Lopes, P.A., Coelho, D., Afonso, C., Bandarra, N.M., and Prates, J.A. (2017). Microalgae as Feed Ingredients for Livestock Production and Meat Quality: A Review. *Livestock Science* 205, 111-121.

Mager, W.H., and Siderius, M. (2002). Novel Insights into the Osmotic Stress Response of Yeast. *FEMS yeast research* 2(3), 251-257.

Martínez-Roldán, A., Perales-Vela, H.V., Cañizares-Villanueva, R.O., and Torzillo, G. (2014). Physiological Response of *Nannochloropsis* Sp. To Saline Stress in Laboratory Batch Cultures. *Journal of Applied Phycology* 26(1), 115-121.

Masson, P. (2001). Gravitropism in *Arabidopsis thaliana*.

Mehta, P., Jajoo, A., Mathur, S., and Bharti, S. (2010). Chlorophyll *a* Fluorescence Study Revealing Effects of High Salt Stress on Photosystem II in Wheat Leaves. *Plant physiology and biochemistry* 48(1), 16-20.

Meloni, D.A., Gulotta, M.R., Martínez, C.A., and Oliva, M.A. (2004). The Effects of Salt Stress on Growth, Nitrate Reduction and Proline and Glycinebetaine Accumulation in *Prosopis Alba*. *Brazilian Journal of Plant Physiology* 16(1), 39-46.

Meng, X., Yang, J., Xu, X., Zhang, L., Nie, Q., and Xian, M. (2009). Biodiesel Production from Oleaginous Microorganisms. *Renewable energy* 34(1), 1-5.

Menke, W. (1960). Das Allgemeine Bauprinzip Des Lamellarsystems Der Chloroplasten. *Experientia* 16(12), 537-538.

Miller, C., Arvan, P., Telford, J.N., and Racker, E. (1976). Ca++-Induced Fusion of Proteoliposomes: Dependence on Transmembrane Osmotic Gradient. *The Journal of Membrane Biology* 30(1), 271-282.

Minagawa, J. (2011). State Transitions—the Molecular Remodeling of Photosynthetic Supercomplexes That Controls Energy Flow in the Chloroplast. *Biochimica et Biophysica Acta (BBA)-Bioenergetics* 1807(8), 897-905.

Minagawa, J. (2013). Dynamic Reorganization of Photosynthetic Supercomplexes During Environmental Acclimation of Photosynthesis. *Frontiers in Plant Science* 4, 513.

Minagawa, J., and Tokutsu, R. (2015). Dynamic Regulation of Photosynthesis in *Chlamydomonas reinhardtii*. *The Plant Journal* 82(3), 413-428.

Mishra, A., Mandoli, A., and Jha, B. (2008). Physiological Characterization and Stress-Induced Metabolic Responses of *Dunaliella salina* Isolated from Salt Pan. *Journal of Industrial Microbiology and Biotechnology* 35(10), 1093.

Mishra, S.K., Subrahmanyam, D., and Singhal, G.S. (1991). Interrelationship between Salt and Light Stress on Primary Processes of Photosynthesis. *Journal of plant physiology* 138(1), 92-96.

Moradi, F., and Ismail, A.M. (2007). Responses of Photosynthesis, Chlorophyll Fluorescence and Ros-Scavenging Systems to Salt Stress During Seedling and Reproductive Stages in Rice. *Annals of botany* 99(6), 1161-1173.

Morales, F., Abadía, A., Gómez-Aparisi, J., and Abadía, J. (1992). Effects of Combined NaCl and Cacl2 Salinity on Photosynthetic Parameters of Barley Grown in Nutrient Solution. *Physiologia Plantarum* 86(3), 419-426.

Moreno-Garcia, L., Adjallé, K., Barnabé, S., and Raghavan, G. (2017). Microalgae Biomass Production for a Biorefinery System: Recent Advances and the Way Towards Sustainability. *Renewable and sustainable energy reviews* 76, 493-506.

Msanne, J., Lin, J., Stone, J.M., and Awada, T. (2011). Characterization of Abiotic Stress-Responsive *Arabidopsis thaliana* Rd29a and Rd29b Genes and Evaluation of Transgenes. *Planta* 234(1), 97-107.

Muller, P., Li, X.-P., and Niyogi, K.K. (2001). Non-Photochemical Quenching. A Response to Excess Light Energy. *Plant Physiology* 125(4), 1558-1566.

Munekage, Y., Hojo, M., Meurer, J., Endo, T., Tasaka, M., and Shikanai, T. (2002). Pgr5 Is Involved in Cyclic Electron Flow around Photosystem I and Is Essential for Photoprotection in *Arabidopsis*. *Cell* 110(3), 361-371.

Murakami, S., and Packer, L. (1971). The Role of Cations in the Organization of Chloroplast Membranes. *Archives of Biochemistry and Biophysics* 146(1), 337-347.

Murata, K., and Suzaki, T. (1998). High-Salt Solutions Prevent Reactivation of Euglenoid Movement in Detergent-Treated Cell Models of *Euglena gracilis*. *Protoplasma* 203(3-4), 125-129.

Murata, N. (2009). The Discovery of State Transitions in Photosynthesis 40 Years Ago. *Photosynthesis Research* 99(3), 155-160.

Murata, N., Nishimura, M., and Takamiya, A. (1966). Fluorescence of Chlorophyll in Photosynthetic Systems III. Emission and Action Spectra of Fluorescence—Three Emission Bands of Chlorophyll *a* and the Energy Transfer between Two Pigment Systems. *Biochimica et Biophysica Acta (BBA)-Biophysics including Photosynthesis* 126(2), 234-243.

Mustárdy, L., and Garab, G. (2003). Granum Revisited. A Three-Dimensional Model–Where Things Fall into Place. *Trends in plant science* 8(3), 117-122.

Nagy, G., Kovács, L., Ünnep, R., Zsiros, O., Almásy, L., Rosta, L., . . . Garab, G. (2013). Kinetics of Structural Reorganizations in Multilamellar Photosynthetic Membranes Monitored by Small-Angle Neutron Scattering. *The European Physical Journal E* 36(7), 1-12.

Nagy, G., Posselt, D., Kovács, L., Holm, J.K., Szabó, M., Ughy, B., . . . Garab, G. (2011). Reversible Membrane Reorganizations During Photosynthesis in Vivo: Revealed by Small-Angle Neutron Scattering. *Biochemical Journal* 436(2), 225-230.

Nagy, G., Szabó, M., Ünnep, R., Káli, G., Miloslavina, Y., Lambrev, P.H., . . . Rosta, L. (2012). Modulation of the Multilamellar Membrane Organization and of the Chiral Macrodomains in the Diatom *Phaeodactylum tricornutum* Revealed by Small-Angle Neutron Scattering and Circular Dichroism Spectroscopy. *Photosynthesis Research* 111(1), 71-79.

Nagy, G., Ünnep, R., Zsiros, O., Tokutsu, R., Takizawa, K., Porcar, L., . . . Finazzi, G. (2014). Chloroplast Remodeling During State Transitions in *Chlamydomonas reinhardtii* as Revealed by Noninvasive Techniques in Vivo. *Proceedings of the National Academy of Sciences* 111(13), 5042-5047.

Nakashima, A., Suzuki, K., Asayama, Y., Konno, M., Saito, K., Yamazaki, N., and Takimoto, H. (2017). Oral Administration of *Euglena gracilis* Z and Its Carbohydrate Storage Substance Provides Survival Protection against Influenza Virus Infection in Mice. *Biochemical and biophysical research communications* 494(1-2), 379-383.

Nakashima, A., Yamada, K., Iwata, O., Sugimoto, R., Atsuji, K., Ogawa, T., . . . Suzuki, K. (2018). β-Glucan in Foods and Its Physiological Functions. *Journal of nutritional science and vitaminology* 64(1), 8-17.

Nawrocki, W.J., Bailleul, B., Picot, D., Cardol, P., Rappaport, F., Wollman, F.-A., and Joliot, P. (2019). The Mechanism of Cyclic Electron Flow. *Biochimica et Biophysica Acta (BBA)-Bioenergetics* 1860(5), 433-438.

Neelam, S., and Subramanyam, R. (2013). Alteration of Photochemistry and Protein Degradation of Photosystem II from *Chlamydomonas reinhardtii* under High Salt Grown Cells. *Journal of Photochemistry and Photobiology B: Biology* 124, 63-70.

Nellaepalli, S., Kodru, S., Tirupathi, M., and Subramanyam, R. (2012). Anaerobiosis Induced State Transition: A Non Photochemical Reduction of Pq Pool Mediated by Ndh in *Arabidopsis thaliana*. *PLoS One* 7(11), e49839.

Nellaepalli, S., Mekala, N.R., Zsiros, O., Mohanty, P., and Subramanyam, R. (2011). Moderate Heat Stress Induces State Transitions in *Arabidopsis thaliana*. *Biochimica et Biophysica Acta (BBA)-Bioenergetics* 1807(9), 1177-1184.

Nelson, N., and Yocum, C.F. (2006). Structure and Function of Photosystems I and II. *Annu. Rev. Plant Biol.* 57, 521-565.

Nishiyama, Y., Yamamoto, H., Allakhverdiev, S.I., Inaba, M., Yokota, A., and Murata, N. (2001). Oxidative Stress Inhibits the Repair of Photodamage to the Photosynthetic Machinery. *The EMBO journal* 20(20), 5587-5594.

Nixon, P.J. (2000). Chlororespiration. *Philosophical Transactions of the Royal Society of London. Series B: Biological Sciences* 355(1402), 1541-1547.

O'neill, E.C., Trick, M., Hill, L., Rejzek, M., Dusi, R.G., Hamilton, C.J., . . . Field, R.A. (2015). The Transcriptome of *Euglena gracilis* Reveals Unexpected Metabolic Capabilities for Carbohydrate and Natural Product Biochemistry. *Molecular BioSystems* 11(10), 2808-2820.

Okouchi, R., Yamamoto, K., Ota, T., Seki, K., Imai, M., Ota, R., . . . Tsuduki, T. (2019). Simultaneous Intake of *Euglena gracilis* and Vegetables Exerts Synergistic Anti-Obesity and Anti-Inflammatory Effects by Modulating the Gut Microbiota in Diet-Induced Obese Mice. *Nutrients* 11(1), 204.

Ooi, V.E., and Liu, F. (2000). Immunomodulation and Anti-Cancer Activity of Polysaccharide-Protein Complexes. *Current medicinal chemistry* 7(7), 715-729.

Ozturk, A., Unlukara, A., Ipek, A., and Gurbuz, B. (2004). Effects of Salt Stress and Water Deficit on Plant Growth and Essential Oil Content of Lemon Balm (*Melissa Officinalis* L.). *Pak. J. Bot* 36(4), 787-792.

Papageorgiou, G.C. (2004). *Chlorophyll a Fluorescence: A Signature of Photosynthesis.* Springer.

Papageorgiou, G.C. (2014). "The Non-Photochemical Quenching of the Electronically Excited State of Chlorophyll *a* in Plants: Definitions, Timelines, Viewpoints, Open Questions," in *Non-*

Photochemical Quenching and Energy Dissipation in Plants, Algae and Cyanobacteria. Springer), 1-44.

Papageorgiou, G.C., and Murata, N. (1995). The Unusually Strong Stabilizing Effects of Glycine Betaine on the Structure and Function of the Oxygen-Evolving Photosystem II Complex. *Photosynthesis Research* 44(3), 243-252.

Parida, A., Das, A., and Mittra, B. (2003). Effects of NaCl Stress on the Structure, Pigment Complex Composition, and Photosynthetic Activity of Mangrove *Bruguiera parviflora* Chloroplasts. *Photosynthetica* 41(2), 191.

Parida, A., Das, A.B., and Das, P. (2002). NaCl Stress Causes Changes in Photosynthetic Pigments, Proteins, and Other Metabolic Components in the Leaves of a True Mangrove, *Bruguiera parviflora*, in Hydroponic Cultures. *Journal of Plant Biology* 45(1), 28-36.

Parvaneh, R., Shahrokh, T., and Meysam, H.S. (2012). Studying of Salinity Stress Effect on Germination, Proline, Sugar, Protein, Lipid and Chlorophyll Content in Purslane (*Portulaca Oleracea* L.) Leaves. *Journal of Stress Physiology & Biochemistry* 8(1), 182-193.

Peltier, G., Aro, E.-M., and Shikanai, T. (2016). Ndh-1 and Ndh-2 Plastoquinone Reductases in Oxygenic Photosynthesis. *Annual review of plant biology* 67, 55-80.

Peng, C., Lee, J.-W., Sichani, H.T., and Ng, J.C. (2015). Toxic Effects of Individual and Combined Effects of BTEX on *Euglena gracilis*. *Journal of hazardous materials* 284, 10-18.

Pesaresi, P., Hertle, A., Pribil, M., Schneider, A., Kleine, T., and Leister, D. (2010). Optimizing Photosynthesis under Fluctuating Light: The Role of the *Arabidopsis* Stn7 Kinase. *Plant signaling & behavior* 5(1), 21-25.

Petroutsos, D., Terauchi, A.M., Busch, A., Hirschmann, I., Merchant, S.S., Finazzi, G., and Hippler, M. (2009). Pgrl1 Participates in Iron-Induced Remodeling of the Photosynthetic Apparatus and in Energy Metabolism in *Chlamydomonas reinhardtii*. *Journal of Biological Chemistry* 284(47), 32770-32781.

Pignolet, O., Jubeau, S., Vaca-Garcia, C., and Michaud, P. (2013). Highly Valuable Microalgae: Biochemical and Topological Aspects. *Journal of Industrial Microbiology and Biotechnology* 40(8), 781-796.

Pisal, D.S., and Lele, S. (2005). Carotenoid Production from Microalga, *Dunaliella salina*. *Indian Journal of Biotechnology*.

Polívka, T.s., and Frank, H.A. (2010). Molecular Factors Controlling Photosynthetic Light

Harvesting by Carotenoids. *Accounts of chemical research* 43(8), 1125-1134.

Porchia, A.C., Fiol, D.F., and Salerno, G.L. (1999). Differential Synthesis of Sucrose and Trehalose in *Euglena gracilis* Cells During Growth and Salt Stress. *Plant Science* 149(1), 43-49.

Porra, R., Thompson, W., and Kriedemann, P. (1989). Determination of Accurate Extinction Coefficients and Simultaneous Equations for Assaying Chlorophylls a and b Extracted with Four Different Solvents: Verification of the Concentration of Chlorophyll Standards by Atomic Absorption Spectroscopy. *Biochimica et Biophysica Acta (BBA)-Bioenergetics* 975(3), 384-394.

Posselt, D., Nagy, G., Kirkensgaard, J.J., Holm, J.K., Aagaard, T.H., Timmins, P., . . . Garab, G. (2012). Small-Angle Neutron Scattering Study of the Ultrastructure of Chloroplast Thylakoid Membranes—Periodicity and Structural Flexibility of the Stroma Lamellae. *Biochimica et Biophysica Acta (BBA)-Bioenergetics* 1817(8), 1220-1228.

Pribil, M., Pesaresi, P., Hertle, A., Barbato, R., and Leister, D. (2010). Role of Plastid Protein Phosphatase Tap38 in LHCII Dephosphorylation and Thylakoid Electron Flow. *PLoS biology* 8(1), e1000288.

Rai, A.K., and Abraham, G. (1993). Salinity Tolerance and Growth Analysis of the Cyanobacterium *Anabaena Doliolum*. *Bulletin of Environmental contamination and Toxicology* 51(5), 724-731.

Raja, R., Coelho, A., Hemaiswarya, S., Kumar, P., Carvalho, I.S., and Alagarsamy, A. (2018). Applications of Microalgal Paste and Powder as Food and Feed: An Update Using Text Mining Tool. *Beni-Suef University journal of basic and applied sciences* 7(4), 740-747.

Raja, R., Hemaiswarya, S., and Rengasamy, R. (2007). Exploitation of *Dunaliella* for B-Carotene Production. *Applied Microbiology and Biotechnology* 74(3), 517-523.

Rantala, M., Ivanauskaite, A., Laihonen, L., Kanna, S.D., Ughy, B., and Mulo, P. (2022). Chloroplast Acetyltransferase Gnat2 Is Involved in the Organization and Dynamics of Thylakoid Structure. *Plant and Cell Physiology*.

Rantala, M., Rantala, S., and Aro, E.-M. (2020). Composition, Phosphorylation and Dynamic Organization of Photosynthetic Protein Complexes in Plant Thylakoid Membrane. *Photochemical & Photobiological Sciences* 19(5), 604-619.

Reed, R., Chudek, J., Foster, R., and Stewart, W. (1984). Osmotic Adjustment in Cyanobacteria from Hypersaline Environments. *Archives of Microbiology* 138(4), 333-337.

Reed, R., and Stewart, W. (1985). Osmotic Adjustment and Organic Solute Accumulation in Unicellular Cyanobacteria from Freshwater and Marine Habitats. *Marine Biology* 88(1), 1-9.

Reynolds, E.S. (1963). The Use of Lead Citrate at High Ph as an Electron-Opaque Stain in Electron Microscopy. *The Journal of cell biology* 17(1), 208.

Rhoades, J. (1990). Salinity in Irrigated Agriculture. *American Society of Civil Engineers, Irrigation of Agricultural Crops*, 1089-1142.

Richter, P., Börnig, A., Streb, C., Ntefidou, M., Lebert, M., and Häder, D.-P. (2003). Effects of Increased Salinity on Gravitaxis in *Euglena gracilis*. *Journal of plant physiology* 160(6), 651-656.

Rizwan, M., Mujtaba, G., Memon, S.A., Lee, K., and Rashid, N. (2018). Exploring the Potential of Microalgae for New Biotechnology Applications and Beyond: A Review. *Renewable and sustainable energy reviews* 92, 394-404.

Robinson, S.P., Downton, W.J.S., and Millhouse, J.A. (1983). Photosynthesis and Ion Content of Leaves and Isolated Chloroplasts of Salt-Stressed Spinach. *Plant Physiology* 73(2), 238-242.

Rochaix, J.-D. (2014). Regulation and Dynamics of the Light-Harvesting System. *Annual review of plant biology* 65, 287-309.

Rodjaroen, S., Juntawong, N., Mahakhant, A., and Miyamoto, K. (2007). High Biomass Production and Starch Accumulation in Native Green Algal Strains and Cyanobacterial Strains of Thailand. *Agriculture and Natural Resources* 41(3), 570-575.

Round, F.E. (1984). *The Ecology of Algae*. CUP Archive.

Ruban, A.V. (2016). Nonphotochemical Chlorophyll Fluorescence Quenching: Mechanism and Effectiveness in Protecting Plants from Photodamage. *Plant Physiology* 170(4), 1903-1916.

Ruban, A.V. (2018). Light Harvesting Control in Plants. *FEBS Letters* 592(18), 3030-3039.

Russo, R., Barsanti, L., Evangelista, V., Frassanito, A.M., Longo, V., Pucci, L., . . . Gualtieri, P. (2017). *Euglena gracilis* Paramylon Activates Human Lymphocytes by Upregulating Pro-Inflammatory Factors. *Food Science & Nutrition* 5(2), 205-214.

Sadler, D., and Worcester, D. (1982). Neutron Diffraction Studies of Oriented Photosynthetic Membranes. *Journal of molecular biology* 159(3), 467-482.

Satoh, K., Smith, C.M., and Fork, D.C. (1983). Effects of Salinity on Primary Processes of Photosynthesis in the Red Alga *Porphyra Perforata*. *Plant Physiology* 73(3), 643-647.

Schagger, H., Cramer, W., and Vonjagow, G. (1994). Analysis of Molecular Masses and Oligomeric States of Protein Complexes by Blue Native Electrophoresis and Isolation of Membrane

Protein Complexes by Two-Dimensional Native Electrophoresis. *Analytical Biochemistry* 217(2), 220-230.

Schubert, H., Fulda, S., and Hagemann, M. (1993). Effects of Adaptation to Different Salt Concentrations on Photosynthesis and Pigmentation of the Cyanobacterium *Synechocystis* Sp. Pcc 6803. *Journal of plant physiology* 142(3), 291-295.

Schubert, H., and Hagemann, M. (1990). Salt Effects on 77k Fluorescence and Photosynthesis in the Cyanobacterium *Synechocystis* Sp. Pcc 6803. *FEMS Microbiology Letters* 71(1-2), 169-172.

Shapiguzov, A., Ingelsson, B., Samol, I., Andres, C., Kessler, F., Rochaix, J.-D., . . . Goldschmidt-Clermont, M. (2010). The Pph1 Phosphatase Is Specifically Involved in LHCII Dephosphorylation and State Transitions in *Arabidopsis*. *Proceedings of the National Academy of Sciences* 107(10), 4782-4787.

Shetty, P., Gitau, M.M., and Maróti, G. (2019). Salinity Stress Responses and Adaptation Mechanisms in Eukaryotic Green Microalgae. *Cells* 8(12), 1657.

Shimoni, E., Rav-Hon, O., Ohad, I., Brumfeld, V., and Reich, Z. (2005). Three-Dimensional Organization of Higher-Plant Chloroplast Thylakoid Membranes Revealed by Electron Tomography. *The Plant Cell* 17(9), 2580-2586.

Srivastava, A., and Strasser, R.J. (1995). Polyphasic Rise of Chlorophyll *a* Fluorescence in Herbicide-Resistant D1 Mutants of *Chlamydomonas reinhardtii*. *Photosynthesis Research* 43(2), 131-141.

Staehelin, L.A. (2003). Chloroplast Structure: From Chlorophyll Granules to Supra-Molecular Architecture of Thylakoid Membranes. *Photosynthesis Research* 76(1), 185-196.

Staehelin, L.A., and van der Staay, G.W. (1996). "Structure, Composition, Functional Organization and Dynamic Properties of Thylakoid Membranes," in *Oxygenic Photosynthesis: The Light Reactions*. Springer), 11-30.

Stahl-Rommel, S., Kalra, I., D'Silva, S., Hahn, M.M., Popson, D., Cvetkovska, M., and Morgan-Kiss, R.M. (2022). Cyclic Electron Flow (Cef) and Ascorbate Pathway Activity Provide Constitutive Photoprotection for the Photopsychrophile, *Chlamydomonas* Sp. Uwo 241 (Renamed *Chlamydomonas Priscuii*). *Photosynthesis Research* 151(3), 235-250.

Stingaciu, L., O'Neill, H., Liberton, M., Urban, V., Pakrasi, H., and Ohl, M. (2016). "Revealing the Dynamics of Thylakoid Membranes in Living Cyanobacterial Cells. Sci. Rep. 6, 19627".).

Stirbet, A., Lazár, D., and Kromdijk, J. (2018). Chlorophyll *a* Fluorescence Induction: Can Just a

One-Second Measurement be Used to Quantify Abiotic Stress Responses? *Photosynthetica* 56(1), 86-104.

Strand, D.D., Fisher, N., and Kramer, D.M. (2017). The Higher Plant Plastid Nad (P) H Dehydrogenase-Like Complex (Ndh) Is a High Efficiency Proton Pump That Increases Atp Production by Cyclic Electron Flow. *Journal of Biological Chemistry* 292(28), 11850-11860.

Strasser, R.J., Tsimilli-Michael, M., and Srivastava, A. (2004). "Analysis of the Chlorophyll *a* Fluorescence Transient," in *Chlorophyll a Fluorescence*. Springer), 321-362.

Strauch, S.M., Becker, I., Pölloth, L., Richter, P.R., Haag, F.W., Hauslage, J., and Lebert, M. (2018). Restart Capability of Resting-States of *Euglena gracilis* after 9 Months of Dormancy: Preparation for Autonomous Space Flight Experiments. *International Journal of Astrobiology* 17(2), 101-111.

Subramanyam, R., Jolley, C., Thangaraj, B., Nellaepalli, S., Webber, A.N., and Fromme, P. (2010). Structural and Functional Changes of PSI-LHCI Supercomplexes of *Chlamydomonas reinhardtii* Cells Grown under High Salt Conditions. *Planta* 231(4), 913-922.

Szabó, I., Bergantino, E., and Giacometti, G.M. (2005). Light and Oxygenic Photosynthesis: Energy Dissipation as a Protection Mechanism against Photo-Oxidation. *EMBO reports* 6(7), 629-634.

Szabó, M., Lepetit, B., Goss, R., Wilhelm, C., Mustárdy, L., and Garab, G. (2008). Structurally Flexible Macro-Organization of the Pigment–Protein Complexes of the Diatom *Phaeodactylum tricornutum*. *Photosynthesis Research* 95(2-3), 237-245.

Takahashi, H., Clowez, S., Wollman, F.-A., Vallon, O., and Rappaport, F. (2013). Cyclic Electron Flow Is Redox-Controlled but Independent of State Transition. *Nature communications* 4(1), 1-8.

Takenaka, S., Kondo, T., Nazeri, S., Tamura, Y., Tokunaga, M., Tsuyama, S., . . . Nakano, Y. (1997). Accumulation of Trehalose as a Compatible Solute under Osmotic Stress in *Euglena gracilis* Z. *Journal of Eukaryotic Microbiology* 44(6), 609-613.

Talebi, A.F., Tabatabaei, M., Mohtashami, S.K., Tohidfar, M., and Moradi, F. (2013). Comparative Salt Stress Study on Intracellular Ion Concentration in Marine and Salt-Adapted Freshwater Strains of Microalgae. *Notulae Scientia Biologicae* 5(3), 309-315.

Tamaki, S., Mochida, K., and Suzuki, K. (2021). Diverse Biosynthetic Pathways and Protective Functions against Environmental Stress of Antioxidants in Microalgae. *Plants* 10(6), 1250.

Taylor, N.L., Tan, Y.-F., Jacoby, R.P., and Millar, A.H. (2009). Abiotic Environmental Stress Induced Changes in the *Arabidopsis thaliana* Chloroplast, Mitochondria and Peroxisome

Proteomes. *Journal of proteomics* 72(3), 367-378.

Thomas, J., and Apte, S.K. (1984). Sodium Requirement and Metabolism in Nitrogen-Fixing Cyanobacteria. *Journal of Biosciences* 6(5), 771-794.

Tikkanen, M., Suorsa, M., Gollan, P.J., and Aro, E.-M. (2012). Post-Genomic Insight into Thylakoid Membrane Lateral Heterogeneity and Redox Balance. *FEBS Letters* 586(18), 2911-2916.

Tiwari, B., Bose, A., and Ghosh, B. (1998). Photosynthesis in Rice under a Salt Stress. *Photosynthetica* 34(2), 303-306.

Tolleter, D., Ghysels, B., Alric, J., Petroutsos, D., Tolstygina, I., Krawietz, D., . . . Beyly, A. (2011). Control of Hydrogen Photoproduction by the Proton Gradient Generated by Cyclic Electron Flow in *Chlamydomonas reinhardtii*. *The Plant Cell* 23(7), 2619-2630.

Torzillo, G., Scoma, A., Faraloni, C., and Giannelli, L. (2015). Advances in the Biotechnology of Hydrogen Production with the Microalga *Chlamydomonas reinhardtii*. *Critical reviews in biotechnology* 35(4), 485-496.

Tóth, T.N., Rai, N., Solymosi, K., Zsiros, O., Schröder, W.P., Garab, G., . . . Kovács, L. (2016). Fingerprinting the Macro-Organisation of Pigment–Protein Complexes in Plant Thylakoid Membranes in Vivo by Circular-Dichroism Spectroscopy. *Biochimica et Biophysica Acta (BBA) - Bioenergetics* 1857(9), 1479-1489.

Trissl, H.-W., and Wilhelm, C. (1993). Why Do Thylakoid Membranes from Higher Plants Form Grana Stacks? *Trends in Biochemical Sciences* 18(11), 415-419.

Tschiersch, H., Ohmann, E., and Doege, M. (2002). Modification of the Thylakoid Structure of *Euglena gracilis* by Norflurazon-Treatment: Consequences for Fluorescence Quenching. *Environmental and Experimental Botany* 47(3), 259-270.

Turan, M.A., Elkarim, A.H.A., Taban, N., and Taban, S. (2009). Effect of Salt Stress on Growth, Stomatal Resistance, Proline and Chlorophyll Concentrations on Maize Plant. *African Journal of Agricultural Research* 4(9), 893-897.

Unlu, C., Drop, B., Croce, R., and van Amerongen, H. (2014). State Transitions in *Chlamydomonas reinhardtii* Strongly Modulate the Functional Size of Photosystem II but Not of Photosystem I. *Proc. Natl. Acad. Sci.* 111(9), 3460-3465.

Ünnep, R., Nagy, G., Markó, M., and Garab, G. (2014a). Monitoring Thylakoid Ultrastructural Changes in Vivo Using Small-Angle Neutron Scattering. *Plant physiology and biochemistry* 81, 197-207.

Ünnep, R., Paul, S., Zsiros, O., Kovács, L., Székely, N.K., Steinbach, G., . . . Garab, G. (2020). Thylakoid Membrane Reorganizations Revealed by Small-Angle Neutron Scattering of *Monstera deliciosa* Leaves Associated with Non-Photochemical Quenching. *Open biology* 10(9), 200144.

Ünnep, R., Zsiros, O., Solymosi, K., Kovacs, L., Lambrev, P.H., Toth, T., . . . Rosta, L. (2014b). The Ultrastructure and Flexibility of Thylakoid Membranes in Leaves and Isolated Chloroplasts as Revealed by Small-Angle Neutron Scattering. *Biochimica et Biophysica Acta (BBA) - Bioenergetics* 1837(9), 1572-1580.

Várkonyi, Z., Nagy, G., Lambrev, P., Kiss, A.Z., Székely, N., Rosta, L., and Garab, G. (2009). Effect of Phosphorylation on the Thermal and Light Stability of the Thylakoid Membranes. *Photosynthesis Research* 99(3), 161-171.

Verma, K., and Mohanty, P. (2000). Changes of the Photosynthetic Apparatus in *Spirulina* Cyanobacterium by Sodium Stress. *Zeitschrift fuer Naturforschung. Section C* 55(1-2), 16-22.

Vicente, G., Bautista, L.F., Rodríguez, R., Gutiérrez, F.J., Sádaba, I., Ruiz-Vázquez, R.M., . . . Garre, V. (2009). Biodiesel Production from Biomass of an Oleaginous Fungus. *Biochemical Engineering Journal* 48(1), 22-27.

Vonshak, A., Kancharaksa, N., Bunnag, B., and Tanticharoen, M. (1996). Role of Light and Photosynthesis on the Acclimation Process of the Cyanobacterium *Spirulina platensis* to Salinity Stress. *Journal of Applied Phycology* 8(2), 119-124.

Walters, R.G., and Horton, P. (1995). Acclimation of *Arabidopsis thaliana* to the Light Environment: Changes in Photosynthetic Function. *Planta* 197(2), 306-312.

Wang, N., Qian, Z., Luo, M., Fan, S., Zhang, X., and Zhang, L. (2018a). Identification of Salt Stress Responding Genes Using Transcriptome Analysis in Green Alga *Chlamydomonas reinhardtii*. *International journal of molecular sciences* 19(11), 3359.

Wang, Y., Seppänen-Laakso, T., Rischer, H., and Wiebe, M.G. (2018b). *Euglena gracilis* Growth and Cell Composition under Different Temperature, Light and Trophic Conditions. *PLoS One* 13(4), e0195329.

Wang, Y., Tibbetts, S.M., and McGinn, P.J. (2021). Microalgae as Sources of High-Quality Protein for Human Food and Protein Supplements. *Foods* 10(12), 3002.

Wehrmeyer, W. (1964). Über Membranbildungsprozesse Im Chloroplasten: II. Mitteilung: Zur Entstehung Der Grana Durch Membranüberschiebung. *Planta* 63(1. H), 13-30.

Wilhelm, C., Büchel, C., Fisahn, J., Goss, R., Jakob, T., LaRoche, J., . . . Stehfest, K. (2006). The

Regulation of Carbon and Nutrient Assimilation in Diatoms Is Significantly Different from Green Algae. *Protist* 157, 91-124.

Wingler, A., Lea, P.J., Quick, W.P., and Leegood, R.C. (2000). Photorespiration: Metabolic Pathways and Their Role in Stress Protection. *Philosophical Transactions of the Royal Society of London. Series B: Biological Sciences* 355(1402), 1517-1529.

Wood, W.H., and Johnson, M.P. (2020). Modeling the Role of LHCII-LHCII, PSII-LHCII, and PSI-LHCII Interactions in State Transitions. *Biophysical Journal* 119(2), 287-299.

Wood, W.H., MacGregor-Chatwin, C., Barnett, S.F., Mayneord, G.E., Huang, X., Hobbs, J.K., . . . Johnson, M.P. (2018). Dynamic Thylakoid Stacking Regulates the Balance between Linear and Cyclic Photosynthetic Electron Transfer. *Nature plants* 4(2), 116-127.

Wright, S., Jeffrey, S., and Mantoura, R. (2005). *Phytoplankton Pigments in Oceanography: Guidelines to Modern Methods.* Unesco Pub.

Wu, X., Shu, S., Wang, Y., Yuan, R., and Guo, S. (2019). Exogenous Putrescine Alleviates Photoinhibition Caused by Salt Stress through Cooperation with Cyclic Electron Flow in Cucumber. *Photosynthesis Research* 141(3), 303-314.

Yamamoto, H., Peng, L., Fukao, Y., and Shikanai, T. (2011). An Src Homology 3 Domain-Like Fold Protein Forms a Ferredoxin Binding Site for the Chloroplast Nadh Dehydrogenase-Like Complex in *Arabidopsis*. *The Plant Cell* 23(4), 1480-1493.

Yamamoto, H.Y., Bugos, R.C., and David Hieber, A. (1999). "Biochemistry and Molecular Biology of the Xanthophyll Cycle," in *The Photochemistry of Carotenoids*. Springer), 293-303.

Yancey, P.H. (2005). Organic Osmolytes as Compatible, Metabolic and Counteracting Cytoprotectants in High Osmolarity and Other Stresses. *Journal of experimental biology* 208(15), 2819-2830.

Ye, Z.-W., Jiang, J.-G., and Wu, G.-H. (2008). Biosynthesis and Regulation of Carotenoids in *Dunaliella*: Progresses and Prospects. *Biotechnology advances* 26(4), 352-360.

Zakery-Asl, M.A., Bolandnazar, S., and Oustan, S. (2014). Effect of Salinity and Nitrogen on Growth, Sodium, Potassium Accumulation, and Osmotic Adjustment of Halophyte *Suaeda aegyptiaca* (Hasselq.) Zoh. *Archives of Agronomy and Soil Science* 60(6), 785-792.

Zeid, I. (2009). Trehalose as Osmoprotectant for Maize under Salinity-Induced Stress. *Res. J. Agric. Biol. Sci.* 5(5), 613-622.

Zhu, J.-K. (2002). Salt and Drought Stress Signal Transduction in Plants. *Annual review of plant biology* 53(1), 247-273.

Zimorski, V., Rauch, C., van Hellemond, J.J., Tielens, A.G., and Martin, W.F. (2017). "The Mitochondrion of *Euglena gracilis*," in *Euglena: Biochemistry, Cell and Molecular Biology*. Springer), 19-37.

Zsiros, O., Nagy, G., Patai, R., Solymosi, K., Gasser, U., Polgár, T.F., . . . Hörcsik, Z.T. (2020). Similarities and Differences in the Effects of Toxic Concentrations of Cadmium and Chromium on the Structure and Functions of Thylakoid Membranes in *Chlorella variabilis*. *Frontiers in Plant Science* 11, 1006.

7. Acknowledgements

First and foremost, I would like to express my sincere gratitude to my supervisor Dr. Bettina Ughy who believed and encouraged me. I thank her for cordially accepting me as a PhD student after welcoming me into the group as an ITC fellow. I appreciate her constant support, guidance, and patience both professionally and personally during all these years.

Besides my supervisor, I am very thankful to Dr. László Szilák for his friendly and persistent guidance specially in writing; Dr. Ildikó Domonkos for technical support and guidance with the electron microscopy and BN-PAGE experiments.

I thank Dr. László Kovács for all the guidance in the fluorescence measurements and HPLC; Dr. Parveen Akhtar for the guidance in time-resolved fluorescence spectroscopy measurements.

I am thankful to Dr. Katalin Solymosi and Tamás Polgár for the technical support with transmission electron microscopy experiments of *Euglena gracilis* and *Chlamydomonas reinhardtii* respectively.

I would like to thank Dr. Gergely Nagy and Dr. Renáta Ünnep for the technical support with small-angle neutron scattering measurements.

I would like to thank Tímea Ottília Kóbori and Ágnes Dergez for supporting my work at Bay Zoltan Research Institute.

I also extend my deepest gratitude to Dr. S. Rajagopal Subramanyam for all his support, advises; I acknowledge him and his research group from the Department of Plant Sciences, University of Hyderabad, India for the contribution of our collaborative research project on salt stress acclimation of *Chlamydomonas reinhardtii*. I am also thankful to Dr. Paula Mulo and her research group from University of Turku, Finland for the collaborative research project on the role of GNAT2 in the thylakoid membrane organization of *Arabidopsis thaliana*.

It has been a great pleasure to carry out my PhD degree in the Photosynthetic Membranes Group in the Institute of Plant Biology, BRC. My sincere thanks to Prof. Győző Garab and Dr. Petar Lambrev for letting me join the group and supporting all through these years.

I specially thank Dr. Parveen Akhtar and Mónika Lingvay for always being so supportive from sharing their knowledge, helping me with experiments, data analysis all the time of research and writing to being good friends in my life.

Many thanks go to all the present and former group members (Dr. Melinda Magyar, Dr. Gábor Sipka, Dr. Ottó Zsiros, Dr. Márta Dorogi, Dr. Lucas Patty, Kinga Böde, Sarolta

Nagyápati, Izabella Leitner, Gergő Gyarmathy, Avratanu Biswas, Fanny Balog–Vig, Fanni Görföl, Annamária Kócsó and Míra Sass) who have been friendly and helpful during these years and for creating a nice atmosphere at work.

I am much obliged to Dr. Milán Szabó for his criticism and suggestions to improve my thesis.

I acknowledge Dr. Imre Vass, Director of the Institute of Plant Biology, BRC for all the support.

I would like to thank Judit Fábián-Barna, Mariann Károlyi, Kiss Anita and other BRC administration staff for their assistance throughout my stay and thesis work.

Finally, I express my deepest and unlimited gratitude, love and respect to my dearest family – my mother Kavitha Kumari, father Srinivasa Rao and brother Sai Ravi Teja for all the sacrifices, love, and endless encouragement throughout the different phases of my academic journey and tolerating my absence in the family that I caused by moving abroad; my grandmothers, Vijaya Lakshmi, Tulasi and my late grandfather Narayana for showering so much love and blessing me always: To them I dedicate my thesis; my uncle Ranjit Kumar for the continuous support and positive influence; my aunt Madhavi, sister Prashanti and cousins Sai Tarun, Vinyan and Ananya for the wonderful moral support and love; To all my friends Dr. Sudheer Babu Sangeetham, Dr. Dondapati Divyateja, Dr. Soujanya Kuntam, Dr. Nia Petrova and Dr. André Vidal Miereles for all the wonderful time and making my stay in Szeged so memorable; specially, Niharika and Vamsy for all the emotional support, for always staying on myside and for helping me to be a better person.

8. Funding

I am grateful to BRC Institute of Plant Biology for the funding during the International Training Course in 2015/2016 and for supporting my PhD research.

The project was supported by the Hungarian National Research, Development and Innovation Office grant GINOP-2.3.2-15-2016-00058.

SUMMARY

Photosynthetic organisms are always exposed to transient changes in various environment. Salinity stress is an important environmental abiotic stress that poses a serious threat to photosynthetic organisms. To cope with this challenge, they have developed sophisticated adaptive mechanisms leading to acclimatory responses through morphological and physiological changes. They have evolved efficient mechanisms to adjust their photosynthetic apparatus to maintain photosynthetic efficiency and adequate photoprotection.

The photosynthetic membranes, so called thylakoid membranes (TM), are assembled into highly organized multilamellar systems with striking variations among different photosynthetic organisms and in the same organisms under varying environmental conditions. This implies the ability of thylakoid membranes to remodel and suggests structural flexibility, they can actively participate in different photosynthetic regulatory mechanisms. Accumulating evidences indicate that the photosynthetic supercomplexes, embedded into the TM, undergo supramolecular reorganization during acclimation to abiotic stresses. Our knowledge of the structure and function of the major protein complexes of photosynthesis has progressed significantly in recent decades, however our understanding of the mechanisms responsible for the fine-tuning of photosynthesis in various organisms and in a wide range of environmental conditions and in relation to the structural flexibility of thylakoid membranes, specifically, is far from complete.

It is well known that the main advantage of the TM organization into grana is to separate both photosystems to prevent energy spillover, to enable controlled distribution of the excitation energy between the photosystems through state transitions. Other important advantage is to regulate the thermal dissipation of the excess energy (non-photochemical quenching), and the balancing of the linear and the cyclic electron flows, so that of the ATP synthesis. Dynamic organization of the TMs is a prerequisite for the regulatory processes of photosynthetic light reactions. Protein phosphorylation is a key regulatory mechanism mediated by STN7 kinase in plants and STT7 kinase in algae causing state transitions. During state transitions the PSII is associated with LHCII in state 1, upon LHCII phosphorylation LHCII leaves the PSII-enriched stacked region and migrates to PSI-containing unstacked stromal region, then it interacts with PSI forming PSI-LHCII supercomplexes in state 2. Thylakoid membranes of green algae contain well-differentiated appressed and non-appressed regions and are able to undergo state transitions.

It is important to understand the dynamics and flexibility of the photosynthetic

apparatus of microalgae in response to salt stress, which is integral to further fundamental research in algal biology and biotechnology. Several lines of evidence were gathered on the adverse effect of salinity on photosynthetic activity and chloroplast structure. However, the real macro-organization of thylakoid membranes in *Chlamydomonas reinhardtii* (*C. reinhardtii*) and *Euglena gracilis* (*E. gracilis*) cells under salt stress has not been fully investigated.

During my PhD work I aimed i) to reveal the changes in the structure and function of photosynthetic apparatus of *C. reinhardtii* under salt stress ii) to gain insight on the acclimation responses of *E. gracilis* to moderate salt stress by examining the morphological changes and pigment composition in addition to the macro-organization of photosynthetic apparatus iii) to clarify the role of acetylation in the membrane dynamics of photosynthetic apparatus of *Arabidopsis thaliana* (*A. thaliana*).

We studied the effect of salt stress on *C. reinhardtii*, green algae wild-type (WT) and on two mutant strains: *stt7* – deficient in stt7 kinase that is involved in state transitions and *pgrl1* - deficient in Pgrl1 protein that is involved in the regulation of in cyclic electron flow around PSI. TEM (transmission electron microscopy) studies revealed that the repeat distances of the thylakoid membranes were increased in salt stressed WT cells contrary to *stt7* that showed no change upon salt treatment. Our data showed that salt stress perturbed the long-range chiral order of the pigment-protein complexes revealed by CD (circular dichroism) spectroscopy. Time-resolved fluorescence spectroscopy data showed an increase in the fluorescence lifetimes of salt-stressed cells suggesting a decreased photochemical quantum yield of PSII. Data of 77 K fluorescence spectroscopy showed changes in the distribution of excitation energy between the two photosystems in WT and *pgrl1* mutants, whereas *stt7* mutant cells were incapable of undergoing state transitions. They seemed to suffer severe damages in their antenna system. Since *stt7* mutant was vulnerable to salt stress we concluded that state transitions play pivotal role in the accommodation to salt stress.

The effect of moderate salt stress on the growth, morphology and photosynthetic performance were studied in the mixotrophic, unicellular, flagellate *E. gracilis*. We found that salt stress had a negative impact on the cell growth, and a reduction of the chlorophyll content. Changes in the macro-organization of pigment-protein complexes as a result of salt treatment are revealed by CD spectroscopy, whereas SANS (small-angle neutron scattering) showed a reduction in the thylakoid stacking, an effect further confirmed by TEM. BN-PAGE (blue native polyacrylamide gel electrophoresis) analysis of the thylakoid membrane complexes didn’t reveal any significant change in the composition of supercomplexes of the

photosynthetic apparatus. Salt stress had no noticeable effect on the photosynthetic activity, as evidenced by the facts that chlorophyll fluorescence yield, electron transport rate and energy transfer between the photosystems did not change considerably in the salt-grown cells. HPLC analyses showed significant increase in carotenoid-chlorophyll ratio. Importantly, paramylon accumulation was observed in salt-treated cells. Accumulation of storage polysaccharide, changes in the pigment composition and in the TM organization can help the *E. gracilis* cells in the adaptation to salt stress and contribute to the maintenance of cellular processes under stress conditions. Production of bioactive compounds by microalgal cell is of high interest for biotechnological applications. Since *E. gracilis* can tolerate salinity stress that in turn induces the production of paramylon, which is known to have immunostimulatory properties; can be used for biotechnological applications.

The role of *A. thaliana* chloroplast acetyl transferase (GNAT2) along with STN7 kinase was studied in the thylakoid membrane organization. The analysis of the CD spectroscopy revealed changes in the structure and arrangement of PSII-LHCII supercomplex and/or that of LHCII across the thylakoid membrane in both the *gnat2* and *stn7* mutants with reference to WT. These results corroborated that GNAT2 was involved in the thylakoid membrane macro-organization (Koskela *et al.*, 2018) similarly to STN7 kinase.

In general, we can conclude that membrane reorganization plays a pivotal role in the stress adaptation of photosynthetic organism that is controlled by several signalling pathways involving post translational modification of proteins. The detailed mechanisms and involvement of different factors still needs to be further elucidated.

ÖSSZEFOGLALÓ

A fotoszintetikus organizmusok ki vannak téve a környezeti körülmények változásainak. A sóstressz egy fontos környezeti stressz faktor, amely komoly veszélyt jelent a fotoszintetikus szervezetekre, melynek leküzdésére összetett válaszfolyamatokat fejlesztettek ki, amelyek morfológiai és fiziológiai változásokon keresztül segítik az élőlények alkalmazkodását.

A fotoszintetikus membránok, az úgynevezett tilakoid membránok (TM) szervezett multilamelláris rendszerekbe állnak össze. A membránok különbözően szerveződnek a különböző fotoszintetikus szervezetekben, valamint eltérhetnek egy adott organizmusban is a változó környezeti körülmények miatt. A TM átrendeződése és szerkezeti rugalmassága fontos szerepet játszhat a különböző fotoszintetikus mechanizmusok szabályozásában. Egyre több bizonyíték mutat arra, hogy a TM-be ágyazott fotoszintetikus komplexek szupramolekuláris átrendeződésen mennek keresztül az abiotikus stresszhez való akklimatizáció során. A fotoszintetikus fehérjekomplexek felépítésével és működésével kapcsolatos ismereteink az elmúlt évtizedekben jelentősen fejlődtek, azonban a fotoszintetikus folyamatok finomhangolásáért felelős mechanizmusok ismerete a különböző organizmusokban és a változó környezeti körülményekre adott válaszok miatt a TM szerkezeti rugalmasságából adódó változások, és azok szerepe részletesen még nem ismert.

A TM gránumokba történő szervezésének fő előnye az, a két fő fotoszintetikus komplex szét van választva az energia átterjedés szabályozásának érdekében, valamint lehetővé válik a gerjesztési energia a fotoszintetikus komplexet közötti szabályozott elosztása. További fontos előny, hogy elősegíti a többletenergia elvezetését hőleadás formájában (nem fotokémiai kioltás), valamint a lineáris és ciklikus elektrontranszport arányának, és ezáltal az ATP szintézis szabályozását. A TM-ok dinamikus szerveződése fontos a fotoszintetikus fényreakcióinak szabályozásában. A növényekben az STN7 kináz, valamint az algákban az STT7 kináz általi fehérje foszforiláció kulcsfontosságú szabályozó mechanizmus, amely fotoszintetikus állapot-átmenetet indukál. Az úgynevezett 1-es állapotban az LHCII a PSII -höz kapcsolódik, majd az állapot-átmenet során az LHCII foszforilálódik és elhagyja a PSII-ben gazdag régiót és a PSI-t tartalmazó sztrómatilakoid régióba vándorol, majd ott kölcsönhatásba lép a PSI-el, PSI-LHCII szuperkomplexeket képezve (2-es állapot). A zöldalgákban a TM rendszer jól megkülönböztethető szervezettebb és lazább régiókat tartalmaz, és képes fotoszintetikus állapotátmenetre.

A mikroalgák fotoszintetikus apparátusának sóstresszre adott válaszát fontos megérteni az alga biológiai és biotechnológiai kutatások szempontjából is. Számos kutatás

vizsgálja a sóstressz fotoszintetikus aktivitásra és a kloroplasztisz szerkezetére gyakorolt hatását. A *Chlamydomonas reinhardtii* (*C. reinhardtii*) és *Euglena gracili*s (*E. gracilis*) sejtekben azonban a tilakoid membránok makroszerveződésének sóstresszre adott változásai nincsenek részletesen feltárva.

Doktori munkám során célom volt i) tanulmányozni a *C. reinhardtii* fotoszintetikus apparátusának szerkezetében és működésében bekövetkezett változásokat sóstressz hatására ii) betekintést nyerni az *E. gracilis* mérsékelt sóstresszre adott akklimatizációs reakcióiba a morfológiai változások, a pigment összetétel és a fotoszintetikus apparátus makro-szerveződésének vizsgálatain keresztül, továbbá iii) feltárni a proteinek acetilezésének szerepét az *Arabidopsis thaliana* (*A. thaliana*) fotoszintetikus apparátusának membrándinamikájában.

Vizsgáltuk a sóstressz hatását a *C. reinhardtii* zöld alga vad típusú (WT) és két mutáns törzsére: *stt7* – az állapotátmenetekben részt vevő Stt7 kináz inaktivált mutáns; és a *pgrl1* – a PSI körüli ciklikus elektronáramlásban résztvevő Pgrl1 fehérjében hiányos mutáns. A TEM (transzmissziós elektronmikroszkópos) vizsgálatok kimutatták, hogy a TM-ok ismétlődési távolsága megnőtt a sóstressz hatására a WT sejtekben, ellentétben az *stt7*-tel, amely nem mutatott változást a sókezelés hatására. CD (cirkuláris dikroizmus) spektroszkópiás vizsgálataink azt mutatták, hogy a sóstressz kihat a pigment-fehérje komplexek szerveződésére. Az időfelbontásos fluoreszcencia spektroszkópiai adatok szerint a sóstressznek kitett sejtek fluoreszcencia élettartama megnő, ami a PSII fotokémiai kvantumhozamának csökkenésére utal. A 77 K fluoreszcencia spektroszkópia rámutatott, hogy a két fotoszisztéma között a gerjesztési energia eloszlásában változás következett be a stressz hatására a WT és a *pgrl1* mutáns sejtekben, míg az *stt7* mutánsban ilyen változás nem volt megfigyelhető. Úgy tűnt, a sóstressz kihatott az antennarendszerre. Mivel az *stt7* mutáns érzékenyebb volt a sóstresszre, így arra a következtetésre jutottunk, hogy a fotoszintetikus állapotátmenetek kulcsszerepet játszanak a sóstresszhez való alkalmazkodásban.

Vizsgáltuk a mérsékelt sóstressz mixotróf, egysejtű *E. gracilis* mikroalga sejtek növekedésre, morfológiájára és fotoszintetikus teljesítményre gyakorolt hatását. Megállapítottuk, hogy a sóstressz negatív hatással volt a sejtek növekedésére, és csökkentette a klorofill tartalmat. A pigment-fehérje komplexek makro-szerveződésében sókezelés hatására bekövetkezett változásait CD spektroszkópiával tártuk fel. A SANS (kisszögű neutronszórás) vizsgálatok a TM-ok ismétlődési távolságának csökkenését mutatta, amit a TEM képek analízise is megerősített. A BN-PAGE (kék natív poliakrilamid gélelektroforézis) analízis stressz hatásra nem mutatott ki jelentős változást a fotoszintetikus

apparátus szuperkomplexeinek összetételében. A sóstressznek nem volt észrevehető hatása a fotoszintetikus folyamatokra. Ugyanakkor a HPLC vizsgálatok a karotinoid-klorofill arány szignifikáns növekedését mutatták. Fontos, hogy a sóval kezelt sejtekben paramilon felhalmozódást figyeltünk meg. A raktározott poliszacharid felhalmozódása, a pigment összetételben és a TM szerveződésében bekövetkező változások segíthetik az *E. gracilis* sejtek sóstresszhez történő alkalmazkodását és hozzájárulnak a sejtfolyamatok fenntartásához stressz körülmények között. A bioaktív vegyületek mikroalgasejtek általi előállítása nagy érdeklődésre tart számot a biotechnológiai iparban. Mivel az *E. gracilis* elviseli a sóstresszt, ami viszont indukálja a paramilon termelést, amelyről pedig ismert, hogy immunstimuláló tulajdonságokkal rendelkezik; így ezen eredmények fontosak lehetnek a biotechnológiai szempontból is.

Vizsgáltuk a kloroplaszt acetil-transzferáz (GNAT2) és az STN7 kináz szerepét *A. thaliana* TM szerveződésében. A CD spektroszkópiai vizsgálatok eltérésre utaltak a PSII-LHCII szuperkomplex és/vagy az LHCII szerkezetében és elrendezésében mind a *gnat2,* és az *stn7* mutánsokban a WT-hoz képest. Ezek az eredmények megerősítették, hogy a GNAT2 az STN7 kinázhoz hasonlóan részt vesz a TM makroszervezésének alakításában (Koskela *et al.*, 2018).

Általánosságban elmondható, hogy a membrán dinamikus szerveződése kulcsszerepet játszik a fotoszintetikus organizmusok stressz-adaptációjában, amelyet számos jelátviteli útvonal szabályoz, beleértve a fehérjék poszttranszlációs módosítását. A részletes mechanizmusok és a különböző tényezők szerepének feltárása még további vizsgálatokat igényelnek.

APPENDICES

List of publications (MTMT: 10056662)

Publications related to the PhD thesis

1. **Sai Divya Kanna**, Ildikó Domonkos, Tímea Ottília Kóbori, Ágnes Dergez, Kinga Böde, Sarolta Nagyapáti, Ottó Zsiros, Renáta Ünnep, Gergely Nagy, Gyözö Garab, László Szilák, Katalin Solymosi, László Kovács, Bettina Ughy (2021) Salt stress induces paramylon accumulation and fine-tuning of the macro-organization of thylakoid membranes in *Euglena gracilis* cells. ***Frontiers in Plant Science***, (IF_{2021}: 6.627)

2. Marjaana Rantala, Aiste Ivanauskaite, Laura Laihonen, **Sai Divya Kanna**, Bettina Ughy, Paula Mulo (2022) Chloroplast acetyl transferase GNAT2 is involved in the organization and dynamics of the thylakoid structure. ***Plant and Cell Physiology***, (IF_{2022}: 4.927)

3. Elsinraju Devadasu, **Sai Divya Kanna**, Satyabala Neelam, Srilatha Nama, Parveen Akhtar, Tamás F. Polgár, Bettina Ughy, Győző Garab, Petar H. Lambrev, Rajagopal Subramanyam. Long- and short-term acclimation of the photosynthetic apparatus to salinity in *Chlamydomonas reinhardtii*: The role of Stt7 protein kinase. (MS under preparation)

Other Publications

4. Ondřej Dlouhý, Václav Karlický, Uroš Javornik, Irena Kurasová, Ottó Zsiros, Primož Šket, **Sai Divya Kanna**, Kinga Böde, Kristýna Večeřová, Otmar Urban, Edward S. Gasanoff, Janez Plavec, Vladimír Špunda, Bettina Ughy, Győző Garab (2022) Structural entities associated with different lipid phases of plant thylakoid membranes – selective susceptibilities to different lipases and proteases. ***Cells MDPI,*** (IF_{2022}: 7.66)